

**Separation from self explains failure of circulating T-cells  
to respond to the CD28 superagonist TGN1412**

**Verlust der "Selbst"-Erkennung erklärt die fehlende Reaktion  
zirkulierender T-Zellen auf den CD28-Superagonisten TGN1412**



Dissertation towards a Doctoral Degree  
at the Graduate School of Life Sciences  
Julius-Maximilians-Universität Würzburg  
Section: Infection and Immunity

Submitted by

**Paula Sofia Romer Roche**

from

Caracas, Venezuela

Würzburg, 2012



Submitted on:

Members of the thesis committee:

Chairperson: Thomas Müller

Primary Supervisor: Thomas Hünig

Supervisor (Second): Thomas Herrmann

Supervisor (Third): Roy Gross

Date of Public Defense: .....

Date of Receipt of Certificates: .....

## Affidavit

I hereby declare that my thesis entitled "Separation from self explains failure of circulating T-cells to respond to the CD28 superagonist TGN1412" is the result of my own work. I did not receive help or support from commercial consultants. All sources and/or materials applied are listed and specified in the thesis.

Furthermore, I verify that this thesis has not yet been submitted as part of another examination process neither in identical nor in similar form.

---

Place, date

---

Signature

## Acknowledgements

Pursuing and completing this project was possible thanks to the help and support of several people. I would like to express my sincere gratitude to all of them.

First and foremost I would like to thank Prof. Thomas Hünig, my thesis supervisor and mentor, for accepting me in his working group and giving me the opportunity to continue my studies in Germany. His valuable guidance, scholarly inputs, and his genuine interest and passion for immunology kept me motivated. His wise advice on "how to become a full-blown scientist" and positive attitude always kept me grounded.

To my thesis committee members Prof. Thomas Herrmann and Prof. Roy Gross for their timely support and encouragement as well as fruitful discussions during seminars and committee meetings.

To the co-authors of our paper, especially Elita Avota, Ineke ten Berge and Manuela Battaglia, for their help in experiments and during the review process.

The Graduate School of Life Sciences (GSLs) of the University of Würzburg for the support, training and guidance throughout my time as a PhD student.

My colleagues in Prof. Hünig's laboratory: Shin-Young, Tea, Monika, Daniela, Madeleine, Julia, Christian and Peter for their help and support during my time in the lab. Special thanks go to Susanne Berr, who from day one trained me and taught me the lab techniques, as well as helping me improve my German, eventually learning and growing together, and through the process, becoming a lifetime friend. Her work is a big part of this thesis. Susi, thanks for everything.

I will forever be thankful to Paula Tabares, who received me in Germany with open arms and helped me settle in this new life. Her constant support, advice and just being there when you most needed her has made her a friend for life. Thanks for being both a great colleague and my partner in crime.

Eliana, Lisa and Elisa who were always willing to help, for their support, fruitful discussions, hallway chats as well as good times in the coffee room.

To my group of friends outside the lab: Iris, Lucas, Marie, Uriel, Simon, Cata, Juan Carlos, and many others. Without you my life in Würzburg would not have been the same! Thanks for the great times, the adventures, and for offering me a friendship that will overcome distance and time.

To my friends from back home whose friendship has remained untouched through it all. Especially to Andrea, your unconditional friendship has made me a better person, thank you for always being there. Tomás, my lab lifeline from afar, thanks for the long chats, jokes, witty comments, advice and kind words that washed away stress during and after lab hours. Mario for a friendship that overcomes it all, through ups and downs, I know I can count on you. Having you three in my life, your faith in me, and your support made everything easier.

To Bastian, whose presence in my life made the second half of my doctorate run smoother, for being a role model of perseverance by not giving up on your goals and dreams. Thank you for your love and unconditional support and for sharing this whole process with me.

Lastly, to my family, for all their love and encouragement. My uncle Bobby for teaching the value of Kartoffelsalat, and showing me that life can be a blast if you put a little bit of humor in everything you do. My dad for believing in me and encouraging me to always pursue my dreams. My brother Gonzalo whom I miss so much, and my sister and friend Isabella, with whom I shared this journey, giving each other continuous support. Thanks for making this process easier by sharing my guilty pleasures. I especially thank my mom, Noëlle Roche, whose example of a strong, independent, hard-working woman helped forge who I am today, and who gave her all to raise my sister, my brother and myself. Thanks for all your love and support. Finally to my beloved grandmother Coca, a friend and a role model, whose wise advice, love and support throughout my life I will carry forever.

## Table of contents

<b>Summary .....</b>	<b>10</b>
<b>Zusammenfassung.....</b>	<b>11</b>
<b>1. Introduction.....</b>	<b>13</b>
1.1. Immune system.....	13
1.1.1. T cells.....	14
1.1.1.1. Structure of the T cell receptor and T cell receptor complex.....	14
1.1.1.2. T cell activation and costimulation .....	14
1.1.1.2.a. T cell receptor signaling .....	15
1.1.1.2.b. CD28 costimulation .....	15
1.2. Immune pathologies.....	16
1.2.1. Classic therapies to control autoimmune diseases .....	17
1.2.2. Biologics.....	17
1.3. Immunomodulatory monoclonal antibodies .....	18
1.3.1. Muronomab (Orthoclone OKT3).....	18
1.4. Regulatory T cells as a target for therapy .....	18
1.4.1. Conventional and superagonistic anti-CD28 mAbs.....	19
1.4.1.1. Signaling pathways of CD28 superagonistic mAbs.....	20
1.4.2. In vitro regulatory T cell expansion by $\alpha$ CD28 conventional and superagonistic mAbs.....	21
1.5. CD28SA preclinical rodent models .....	22
1.5.1. Studies in mice and rats .....	22
1.5.2. CD28SA in autoimmune and inflammatory disease models .....	23
1.6. TGN1412 – a human anti-CD28 superagonistic monoclonal antibody .....	25
1.6.1. TGN1412 preclinical studies – Animal models.....	25

1.6.2.	TGN1412 first-in-man clinical trial .....	25
1.6.3.	Current knowledge on CD28 superagonists – After the CRS .....	26
<b>2.</b>	<b>Introductory statement on contributions and previous publication.....</b>	<b>27</b>
<b>3.</b>	<b>Methods .....</b>	<b>28</b>
3.1.	Cell isolation and preparation .....	28
3.1.1.	Human PBMC isolation .....	28
3.1.2.	Human lymph node cells .....	28
3.1.3.	Cell culture .....	28
3.1.4.	Freezing and thawing .....	28
3.1.5.	Depletion and isolation of cell subsets .....	29
3.2.	Stimulation assays – RESTORE protocol .....	29
3.3.	Western blotting .....	29
3.3.1.	Cell lysis .....	29
3.3.2.	Pre-clearing of cell lysate .....	30
3.3.3.	SDS-polyacrylamide gel electrophoresis.....	30
3.3.4.	Western Blot.....	30
3.4.	Cell proliferation assays.....	30
3.4.1.	<sup>3</sup> H-thymidine incorporation .....	30
3.4.2.	Ki67 staining .....	30
3.5.	Cell dissociation experiment .....	31
3.6.	Transwell assay .....	31
3.7.	Flow cytometry (phenotyping).....	31
3.8.	Cytokine release quantification .....	31
3.8.1.	Intracellular cytokine staining .....	32
3.8.2.	Responding cell subset determination .....	32
3.9.	CFSE labeling .....	32

3.10. Confocal microscopy.....	32
3.11. Statistical analysis.....	33
<b>4. Results .....</b>	<b>34</b>
4.1. PBMC response to soluble TGN1412.....	34
4.2. Optimization of the RESTORE protocol.....	36
4.3. Loss of suppression vs. gain of function after high-density preculture .....	37
4.4. Properties of the RESTORE response of PBMC to soluble TGN1412 .....	39
4.5. Cellular interactions during high-density preculture .....	41
4.6. Human lymph node T cell response to TGN1412.....	52
4.1. Pharmacologic inhibition of the precultured-T-cells response .....	53
4.2. Response to T-cell mitogens .....	56
4.3. Response of precultured PBMC to bacterial antigens .....	58
4.4. Role of the Fc portion of CD28 superagonists on T- cell stimulation .....	59
<b>5. Discussion.....</b>	<b>69</b>
<b>List of figures.....</b>	<b>80</b>
<b>Annex.....</b>	<b>83</b>
Materials .....	83
Chemicals and reagents .....	83
Enzymes and inhibitors.....	84
Commercial kits.....	84
Magnetic beads for cell isolation or depletion .....	84
Radioactive materials.....	84
Antibodies and secondary reagents.....	85
Cell stimulation-related reagents.....	87
Buffers, media and solutions.....	88
Human cells .....	90

Equipment and supplies.....	90
Software.....	91
<b>List of abbreviations and acronyms.....</b>	<b>93</b>
<b>References.....</b>	<b>96</b>
<b>Publications.....</b>	<b>107</b>
<b><i>Curriculum vitae</i>.....</b>	<b>108</b>

## Summary

Stimulatory or superagonistic (SA) CD28-specific monoclonal antibodies (mAbs) are potent polyclonal activators of regulatory T cells and have proven highly effective as treatment in a wide range of rodent models for autoimmune and inflammatory diseases. In these models, a preferential activation of regulatory T cells was observed by *in vivo* administration of CD28SA. In stark contrast, human volunteers receiving TGN1412, a humanized CD28-specific mAb, experienced a life-threatening cytokine release syndrome during the first-in-man trial. Preclinical tests employing human peripheral blood mononuclear cells (PBMC) failed to announce the rapid cytokine release measured in the human volunteers in response to TGN1412.

The aim of this thesis project was to find an explanation of why standard PBMC assays failed to predict the unexpected TGN1412-induced "cytokine storm" observed in human volunteers. CD28 superagonists can activate T cells without T cell receptor (TCR) ligation. They do depend, however, on "tonic" TCR signals received by MHC scanning, signals that they amplify. PBMC do not receive these signals in the circulation. Short-term *in vitro* preculture of human PBMC at a high cell density (HDC) resulted in massive cytokine release during subsequent TGN1412 stimulation. Restoration of reactivity was cell-contact dependent, associated with TCR polarization and tyrosine-phosphorylation, and blocked by HLA-specific mAb. In HDC, both CD4 T cells and monocytes functionally mature in a mutually dependent fashion. However, only CD4 memory T-cells proliferate upon TGN1412 stimulation, and were identified as the main source of pro-inflammatory cytokines. Importantly, responses to other T-cell activating agents were also enhanced if PBMC were first allowed to interact under tissue-like conditions.

A new *in vitro* protocol is provided that returns circulating T-cells to a tissue-like status where they respond to TGN1412 stimulation, and it might represent a more reliable preclinical *in vitro* test for both activating and inhibitory immunomodulatory drugs.

Finally, the surprising observation was made that the IgG1 "sibling" of TGN1412, which is of the poorly Fc receptor-binding IgG4 isotype, has a much lower stimulatory activity. We could exclude steric hindrance as an explanation and provide evidence for removal of TGN1112 from the T-cell surface by trans-endocytosis.

## Zusammenfassung

Stimulatorische oder superagonistische (SA) CD28-spezifische monoklonale Antikörper (mAbs) (CD28SA) haben sich in diversen Nagetiermodellen für Autoimmunerkrankungen sowie für inflammatorische Erkrankungen als effektive Behandlungsmöglichkeit erwiesen. In diesen Modellen konnte nachgewiesen werden, dass CD28SA-Injektionen zu einer verstärkten Aktivierung regulatorischer T-Zellen in führen. Entgegen diesen Beobachtungen im Tiermodell reagierten die Teilnehmer einer ersten klinischen Studie auf die Administration des humanisierten CD28SA TGN1412 mit einer akut lebensbedrohlichen systemischen Zytokinausschüttung. Vorklinische Studien an humanen mononukleären Zellen des Blutes (PBMC) hatten keinen Hinweis auf eine mögliche plötzliche Zytokinausschüttungen als Reaktion auf TGN1412 gegeben.

In der vorliegenden Arbeit wurde versucht eine Erklärung zu finden, warum PBMC-basierte Tests, wie sie vorklinischen Studien als Standard eingesetzt werden, nicht auf den unerwarteten TGN1412-induzierten „Zytokinsturm“ der Probanden hinwies. CD28SA aktivieren T-Zellen ohne Ligation des T-Zell Rezeptors (TCR). Jedoch werden zur CD28SA-abhängigen Aktivierung von T-Zellen „tonische“ TCR Signale benötigt, die durch MHC Scanning der T-Zellen an der Oberfläche anderer Zellen erzeugt werden. PBMC, welche sich in der Zirkulation befinden, erhalten diese „tonischen“ TCR Signale nicht. Kurzzeitige Vorkultur humaner PBMC bei hoher Zelldichte (high-density culture, HDC) führte zu einer starken Zytokinantwort bei nachfolgender TGN1412 Stimulation. Diese wiedererlangte Reaktivität gegenüber TGN1412 ging mit Tyrosin-Phosphorylierung sowie der Polarisierung von TCR Molekülen einher, war abhängig von Zellkontakten und konnte durch HLA-spezifische mAbs geblockt werden. Während der HDC durchlaufen sowohl CD4 T-Gedächtniszellen, als auch Monozyten eine voneinander abhängige funktionelle Reifung. TGN1412-induzierte Zellproliferation beschränkt sich jedoch auf CD4 T-Gedächtniszellen, die auch die Hauptquelle der proinflammatorische Zytokine sind. Antworten auf weitere T-Zell aktivierende Agenzien waren ebenfalls erhöht, wenn PBMC zunächst auf gewebeartige Bedingungen zurückgesetzt wurden.

Die vorliegende Arbeit beschreibt damit ein neuartiges in vitro Protokoll für humane PBMC, welches T-Zellen der Zirkulation in einen gewebeartigen funktionellen Status versetzt, in welchem sie auf TGN1412 antworten. Dieses Protokoll könnte auch einen verlässlicheren vorklinischen in vitro Test sowohl für aktivierende als auch für inhibierende immunmodulatorische Medikamente darstellen.

Im letzten Teil der Arbeit wird die erstaunliche Beobachtung vorgestellt, dass TGN1112, ein IgG1 Antikörper mit gleicher Spezifität wie der IgG4 Antikörper TGN1412, trotz seiner höheren Affinität für Fc-Rezeptoren eine viel geringere stimulatorische Aktivität zeigt. Sterische Hinderung konnte als eine mögliche Erklärung ausgeschlossen werden. Vielmehr scheint das Entfernen von TGN1112/CD28 Komplexen von der T-Zelloberfläche durch Trans-Endozytose eine mögliche Erklärung für die geringere Aktivität zu sein.

## 1. Introduction

### 1.1. Immune system

The immune system represents the body's defense against pathogens. It consists of two main branches, the innate and the adaptive immune system. Innate immunity is the first line of defense against microbes. It is comprised by (a) physical and chemical barriers such as epithelia and the chemicals produced by epithelial surfaces; (b) phagocytic cells (neutrophils, macrophages), dendritic cells (DC), and natural killer cells (NK cells); (c) proteins in the blood, for example complement system components; and (d) cytokines, proteins that orchestrate numerous functions during an immune response. The mechanisms of innate immunity recognize structures that are common on groups of related pathogenic organisms, for example, innate immune cells express pattern recognition receptors (PRR) that recognize pathogen-associated molecular patterns (PAMPs) expressed on microbes (Reviewed in Luster 2002).

Adaptive immunity, on the other hand, is activated upon antigen encounter and it is tailored to the specific threat. An important characteristic of adaptive immunity is that it generates memory, so if repeated exposures to the microbe occur the protective immune response will be faster, highly specific and more effective. The main effectors in an adaptive immune response are lymphocytes and their secreted antibodies (Ab), and they recognize antigens either on the cell surface of microbes or presented by DC in the form of peptides. There are two main types of adaptive responses. One is humoral immunity comprised by B cells and their secreted antibodies, which can block infections or coat extracellular microbes to be recognized by phagocytes or by complement in order to clear them. The other is cell-mediated immunity, which protects the body from intracellular pathogens such as viruses and some bacteria. It is mediated by T cells, which can activate macrophages to destroy phagocytosed microbes or can recognize and kill infected cells (Reviewed in Luster 2002).

A very important feature of adaptive immunity is tolerance, meaning that it has the ability to discriminate between self and non-self, so the body does not react to self-antigens. This is done via several mechanisms such as elimination of self-reactive lymphocytes during their development, or inactivation or suppression of these cells by regulatory T cells (Tregs) (Sakaguchi 2004). Tregs are major players in maintaining peripheral tolerance and in regulating the degree and duration of immune responses. They can suppress CD4 and CD8 T cell responses through cell-cell contact and IL-10 secretion, and they have shown to be very important in suppressing organ-specific and systemic autoimmunity in rodent models (Reviewed in Leipe et al. 2005). Disruption or dysregulation on any key mechanism involved

in tolerance development or maintenance can cause the body to "attack" itself, leading to the onset of autoimmune diseases (Reviewed in Davidson and Diamond 2001).

### **1.1.1. T cells**

T cells are part of the adaptive immune system and are the mediators of cellular immunity. Their precursors are generated in the bone marrow but they mature in the thymus. The two major subsets are CD4<sup>+</sup> T cells and CD8<sup>+</sup> cytotoxic T lymphocytes (CTL). CD4<sup>+</sup> regulatory T cells are another subset (Hori, Nomura, and Sakaguchi 2003), and all three of these subsets express an antigen receptor called  $\alpha\beta$  receptor (Reviewed in Kuhns and Davis 2012). Another T cell population are the  $\gamma\delta$  T cells with a functionally distinct type of antigen receptor (Reviewed in Pang et al. 2012).

#### **1.1.1.1. Structure of the T cell receptor and T cell receptor complex**

The  $\alpha\beta$  T cell receptor (TCR) is a heterodimer composed of two transmembrane polypeptide chains, the  $\alpha$  and the  $\beta$  chain, each consisting of one Ig-like N-terminal variable domain, one Ig-like constant domain, a hydrophobic transmembrane region, and a short cytoplasmic region (Clevers et al. 1988).

The human  $\alpha\beta$  TCR complex consists of one  $\alpha\beta$  TCR heterodimer noncovalently linked to one  $\gamma\varepsilon$  CD3 heterodimer, one  $\delta\varepsilon$  CD3 heterodimer, and one disulfide-linked  $\zeta\zeta$  homodimer. These TCR-associated proteins play a role in intracellular signal transduction and not in antigen recognition, by phosphorylation of their intracellular immunoreceptor tyrosine-based activating motifs (ITAM) (Reviewed in Smith-Garvin, Koretzky, and Jordan 2009).

#### **1.1.1.2. T cell activation and costimulation**

T cells have a high specificity for the antigen that elicits the response. After activation cells proliferate and generate a large number of functional effector cells from a small pool of naive lymphocytes, some of which become memory cells and remain for long periods of time in the body maintaining protective immunity against reinfection (Sprent and Surh 2002).

T cells are activated through the T cell receptor (TCR) complex after peptide loaded MHC molecules on antigen presenting cells (APC) are recognized, which is termed "signal 1". The second signal or "signal 2" is given by costimulatory molecules expressed on activated APC. Lack of costimulation leads T cells to an anergic state in which they are refractory to restimulation. When both signals are present clustering of coreceptors around the TCR complex is initiated, and ITAM tyrosine residues are phosphorylated by active Src family kinases, events that initiate signal transduction. A supra-molecular activation cluster

(SMAC) forms, a structure resembling a bulls-eye with two concentric rings. It consists of a central SMAC (cSMAC) and a peripheral SMAC (pSMAC). The cSMAC is formed by the TCR complex, CD4 or CD8 coreceptors, costimulation receptors (such as CD28), enzymes such as PKC- $\theta$  and adaptor proteins. The pSMAC is formed by integrins such as talin and lymphocyte-associated antigen 1 (LFA-1), which main role is to stabilize the T-cell-DC interaction. CD45, known also as common leukocyte antigen, stays outside the pSMAC in an area termed distal SMAC (dSMAC) (Monks et al. 1998).

#### **1.1.1.2.a. T cell receptor signaling**

The first steps following TCR-MHC+peptide recognition involve many phosphorylation events of ITAMs, as well as the activation of downstream tyrosine kinases. The CD4 and CD8 coreceptors participate in the signal transduction by bringing the Src family kinase Lck (lymphocyte-specific protein tyrosine kinase) close to the CD3 and  $\zeta$  ITAMs, which phosphorylates them together with the kinase Fyn. Subsequently, ZAP-70 is recruited and a cascade of phosphorylation events is initiated which ends up with activation of transcription factors (NFAT, NF $\kappa$ B and AP-1), gene transcription and protein expression (Reviewed in Smith-Garvin, Koretzky, and Jordan 2009).

#### **1.1.1.2.b. CD28 costimulation**

The most important and best characterized costimulatory receptor expressed on T cells is the homodimeric glycoprotein CD28 (Hara, Fu, and Hansen 1985), which in humans is expressed in approximately 95% of CD4<sup>+</sup> T cells and 50% of CD8<sup>+</sup> T cells (Lum et al. 1982). The ligands of CD28 are CD80 (B7-1) and CD86 (B7-2) expressed on activated APC (Sharpe and Freeman 2002). CD80 is a homodimer whereas CD86 is a monomer; nevertheless the CD28 homodimer binds to both molecules monovalently due to steric interference (Collins et al. 2002; Evans et al. 2005).

CD28 is part of the immunoglobulin family of costimulatory receptors (Hansen, Martin, and Nowinski 1980; Gmunder and Lesslauer 1984), together with cytotoxic T-lymphocyte antigen 4 (CTLA-4 or CD152) (Dariavach et al. 1988), programmed-death receptor 1 (PD-1), inducible T-cell costimulator (ICOS or CD278) (Hutloff et al. 1999; Tezuka et al. 2000) and B- and T-lymphocyte attenuator (BTLA) (Watanabe et al. 2003). CTLA-4, PD-1 and BTLA are inhibitory receptors, while CD28 and ICOS are predominantly enhancing T-cell activation (Sharpe 2009).

The more robust T cell-signal enhancer is CD28. It promotes T cell proliferation, cytokine production, cell survival, and cellular metabolism. It can be addressed in vitro with monoclonal antibodies (mAbs), in combination with anti-TCR mAbs, leading to full T-cell

activation. Recently, Sanchez-Lockhart et al. (2011) showed that TCR ligation might lead to a conformational change of the extracellular domains of CD28, enabling ligand binding and signaling, a mechanism similar to integrin inside-out signaling. CD28 ligation leads to an intracellular signaling cascade that is initiated by phosphorylation of a tyrosine residue and subsequent recruitment of the p85 subunit of phosphatidylinositol 3-kinase (PI3K), although its role is still controversial. Grb2 and GADS are adaptor proteins that can bind the same region as PI3K and are also involved in signaling. Another molecule that is also likely involved in CD28 signaling, but binds to a different region, is Lck. Binding of PI3K and the adaptor proteins initiates signaling pathways that lead to activation of the transcription factors AP-1, NF $\kappa$ B and NFAT, leading to T-cell survival signals, IL-2 production, and cell proliferation (Reviewed in Boomer and Green 2010).

While CD28 costimulation represents a stimulatory signal for T cells, there is a parallel mechanism which competes for CD80/86 binding and gives a negative signal for T-cell response termination, and that is the CTLA-4 homodimer, which is upregulated on effector T cells upon activation and constitutively expressed on regulatory T cells. CTLA-4 binding affinity is 20-fold higher to CD80 and up to 100-fold higher to CD86 than CD28. Moreover, CTLA-4 binds to ligand in a bivalent fashion increasing the avidity considerably, although for CD28 it is still not clear if it binds mono- or bivalently in the immunological synapse (Sanchez-Lockhart, Kim, and Miller 2011). CTLA-4 plays an important role in keeping immune responses in check (Collins et al. 2002).

## **1.2. Immune pathologies**

Immune responses are tightly controlled. Nevertheless the possibility that a person's immune system reacts against self-antigens causing damage exists. There are two different circumstances in which the body can harm itself, one is under excessive inflammatory conditions tissue can be damaged by the immune system, which is sometimes grouped under "immune-mediated inflammatory diseases" or "hypersensitivity diseases", but they are not associated with recognition of self-antigens. On the other hand, if tolerance is breached immune cells can react against self-antigens causing damage, which is termed "autoimmunity". It results from a dysregulation of tolerance mechanisms on T and B cells. The major factors contributing to the development of autoimmune diseases are genetic susceptibility and environmental triggers, such as infections and tissue injury.

Rheumatoid arthritis (RA), a very common autoimmune disease, is associated with high levels of TNF production, which seems to down-modulate the suppressive function of

human CD4<sup>+</sup>CD25<sup>hi</sup> Treg cells through TNF receptor II (TNFRII) by lowering *FOXP3* mRNA as well as protein expression (Valencia et al. 2006). An approach to treat RA, besides the already established TNF blockade, could include manipulation of the Treg compartment. Adoptive transfer of Treg cells has proven beneficial in animal models of RA, but the consequences of these kind of therapy in humans remains to be established (Fox 2012).

### **1.2.1. Classic therapies to control autoimmune diseases**

There are over 80 types of autoimmune diseases affecting the human population. The need for treatments that ameliorate the symptoms or even cure the disease are clearly necessary (Dugdale and Zieve 2011). There are numerous treatments that are prescribed to control or reduce the immune response. Some of these immunosuppressive drugs include corticosteroids (such as prednisone, methylprednisolone), and non-steroid drugs such as azathioprine, cyclophosphamide, mycophenolate, which inhibit T and B cell proliferation by different mechanisms; rapamycin, which prevents activation of T cells and B-cells by inhibiting their response to interleukin-2 (IL-2); tacrolimus or cyclosporine, both of which inhibit calcineurin and therefore activation of NFAT, T-cell signal transduction and IL-2 transcription, and methotrexate, an antimetabolite and antifolate drug which inhibits purine metabolism, consequently blocking the synthesis of DNA, RNA, and proteins. These immunosuppressive drugs are used to prevent transplant rejection, cancer treatment or to ameliorate the symptoms in autoimmune diseases (Wikipedia).

### **1.2.2. Biologics**

Biologics are genetically engineered proteins derived from human genes. They are designed to inhibit key components of the immune system that promote inflammation, therefore they are much more specific than the classical treatments.

Many biologics are used to treat a wide range of autoimmune diseases such as systemic lupus erythematosus, multiple sclerosis, type 1 diabetes, ulcerative colitis, as well as a cancer treatment, because they target elements involved in inflammation processes. The gold standard treatment for many autoimmune diseases associated with excessive TNF release are TNF blockers in combination with methotrexate, which in many patients changes the course of the disease from progressive damage to a manageable chronic inflammation (Bingham 2012). Although TNF inhibitors are quite effective in ameliorating the symptoms they are not specific to the disease and are associated with a variety of side effect such as lymphoma, infections, congestive heart failure, lupus-like syndrome, induction of auto-antibodies and injection site reactions, although the risk of these side effects is very low (Scheinfeld 2004).

### **1.3. Immunomodulatory monoclonal antibodies**

Antibodies directed against inflammatory mediators or cell surface molecules are an attractive approach to develop immune therapies for a wide range of diseases. In 1986, the first monoclonal antibody (mAb) for human therapy was approved by the FDA, Muronomab (Orthoclone OKT3), and since then more than 30 mAb have been approved and are currently used to treat autoimmune diseases, cancer and other maladies.

#### **1.3.1. Muronomab (Orthoclone OKT3)**

OKT3 was used as an immunosuppressant against transplant rejection. However, because of its numerous side effects, better-tolerated alternatives and declining usage, OKT3 was removed from the market in 2010 (Reichert 2012).

It is a mouse mAb that binds the epsilon chain of the CD3 molecule on the T-cell surface initially leading to T-cell activation and systemic cytokine release, namely a cytokine release syndrome (CRS) that can be controlled with the use of corticosteroids (Gaston et al. 1991), but subsequently results in CD3<sup>+</sup> cell depletion (Stankova, Hoskin, and Roder 1989). T cell activation is mediated by Fc receptor (FcR) cross-linking on the surface of cells such as monocytes (Rinnooy Kan et al. 1986; Landegren, Andersson, and Wigzell 1984). The therapeutic effect consists in T-cell depletion by opsonization and T-cell function blockade by removal of CD3 from the cell surface (Goldstein 1987).

### **1.4. Regulatory T cells as a target for therapy**

“Natural” regulatory T cells are key effectors in keeping immune responses in check. They protect against development of autoimmunity and other immunopathologies such as allergies (Sakaguchi et al. 2006). Because of these features, manipulation of the Treg-cell compartment represents an attractive target for therapy. Tregs are characterized by CD4 and CD25 (IL-2R $\alpha$ ) expression, as well as the transcription factor FoxP3 (Fontenot and Rudensky 2005). The high levels of CD25 expression are related to the dependence of Tregs on IL-2 for their survival and activation, as seen in knock-out animal models where the lack of IL-2 or IL-2R gives a phenotype of an autoimmune lymphoproliferative disease (Papiernik et al. 1998; Maloy and Powrie 2005; Furtado et al. 2002; Krämer, Schimpl, and Hunig 1995; Schimpl et al. 2002; Wolf, Schimpl, and Hunig 2001). Besides FoxP3 expression, another difference with CD4<sup>+</sup> effector cells is that Tregs constitutively express CTLA-4 (Takahashi et al. 2000). This might be involved in their suppressive function, although it is still not clear

whether CTLA-4 might play a role in *cis* regulation of Treg function or if the role is in negative regulation of the CD4<sup>+</sup> T-cell compartment (Reviewed in Sansom and Walker 2006). Recently, Qureshi et al. (2011) demonstrated a cell-extrinsic inhibitory effect of CTLA-4<sup>+</sup> cells over T-cell activation via CD28. They suggested a model in which activation of conventional T-cells or Treg cells promotes the removal and degradation of CD80 and CD86 from the surface of APC by CTLA-4, a process termed “trans-endocytosis”.

CD28 is expressed on both regulatory and conventional T cells. CD28 expression on Tregs seems to play an important and non-redundant role in the generation, homeostasis, and activation of the cells. This is supported mainly by the finding that CD28-deficient mice have a reduced Treg cell compartment (Salomon et al. 2000). As mentioned, IL-2 production by conventional T cells depends on CD28 costimulation. When this cytokine is produced, Treg cells are activated and expanded, which in turn switch off IL-2 production by effector cells. Manipulation of CD28 costimulation is a subject of interest in the field of immunological therapies, since this molecule is involved in homeostasis of both CD4<sup>+</sup> effector and regulatory T cells.

A therapy engineered with the aim of blocking T-cell activation was the generation of CTLA-4-Ig, which is a recombinant fusion protein consisting of the extracellular domain of CTLA-4 fused to the Fc portion of IgG. It competes with binding to CD80 and CD86, blocking CD28 costimulation (Reviewed in Najafian and Sayegh 2000). CTLA-4-Ig has been used as a successful therapy on rheumatoid arthritis (Nogid and Pham 2006).

Functional impairment or reduced numbers of Treg cells have been associated with generation of autoimmunity in several animal models (Reviewed in Sakaguchi 2000). In humans, defects in the Treg compartment have also been associated with autoimmune diseases such as multiple sclerosis (Viglietta et al. 2004), rheumatoid arthritis (Ehrenstein et al. 2004), or type-1 diabetes (Lindley et al. 2005). Therefore, manipulation of the Treg compartment is of great interest in the development of immune therapies.

#### **1.4.1. Conventional and superagonistic anti-CD28 mAbs**

The CD28 molecule was first identified in humans by the use of mAbs. These showed to act as T cell costimulators during polyclonal T cell activation *in vitro* (Hara, Fu, and Hansen 1985). The first mAbs directed against CD28 in mice (Gross, Stjohn, and Allison 1990) and rat (Tacke et al. 1995) were developed much later. These also showed to act as costimulators *in vitro*, in combination with TCR activation, but were not stimulatory by themselves. This kind of CD28-specific mAb is referred to as “conventional”.

When mAbs recognizing rat CD28 were generated, two functionally distinct categories were detected, conventional antibodies which acted as “signal 2” during T cell activation, and another kind that surprisingly activated T cells without the need of TCR ligation, termed “superagonistic” (Tacke et al. 1997). This unexpected functional difference was not related to the antibody isotype or differential binding avidity. Instead it showed to be related to the binding epitope on the CD28 molecule (Luhder et al. 2003). Conventional mAbs bind close to the ligand binding site of CD80/86, while superagonistic mAbs bind laterally to the CD28 molecule, specifically to the C'D loop (Figure 1A and B). Human, mouse and rat conventional and superagonistic monoclonal antibodies bind to CD28 as shown in Figure 1 (Luhder et al. 2003; Dennehy et al. 2006; Evans et al. 2005).

The mode of binding of human superagonistic or mitogenic  $\alpha$ CD28 mAbs was determined by cocrystallization of Fab fragments of the antibody with recombinant soluble CD28, and a lateral binding mode was observed (Evans et al. 2005). This suggests that CD28SA might crosslink CD28 molecules on the cell surface forming a lattice (Figure 1C). CTLA-4 mode of binding to its natural ligands is also bivalent, while CD28 binds monovalently (Collins et al. 2002). It has been hypothesized that the bivalent mode of binding of CD28SA, resembling the one of CTLA-4, may be related to their activation properties on T cells; or, on the other hand, it is possible that the monovalent binding of CD28 is a mechanism by which the activation signal stays under the control of the TCR (Dennehy et al. 2006).

#### **1.4.1.1. Signaling pathways of CD28 superagonistic mAbs**

CD28 superagonists stimulate T cells without TCR engagement by inducing intracellular signaling cascades (Bischof et al. 2000; Hünig and Dennehy 2005). Importantly, during CD28SA T cell activation, the proximal components of the TCR signaling machinery TCR  $\zeta$  chain and ZAP-70 do not show phosphorylation above background levels (Dennehy et al. 2007; Dennehy et al. 2003; Luhder et al. 2003). However, it has been observed that CD28SA T cell stimulation depends on constitutive proximal TCR signals, or what is called “tonic signals”. These signals are amplified at the level of the SLP-76 signalosome, where the adaptor molecule Vav1 plays an essential role (Dennehy et al. 2007).

CD28 superagonist stimulation polarizes resting T cells predominantly into a Th2 phenotype (Rodriguez-Palmero et al. 1999). It also induces a significant upregulation of Bcl-xL, which is involved in the FAS-L pathway, and there is no induction of CD95L expression, which translates into T cells being more resistant to apoptosis (Kerstan and Hunig 2004).

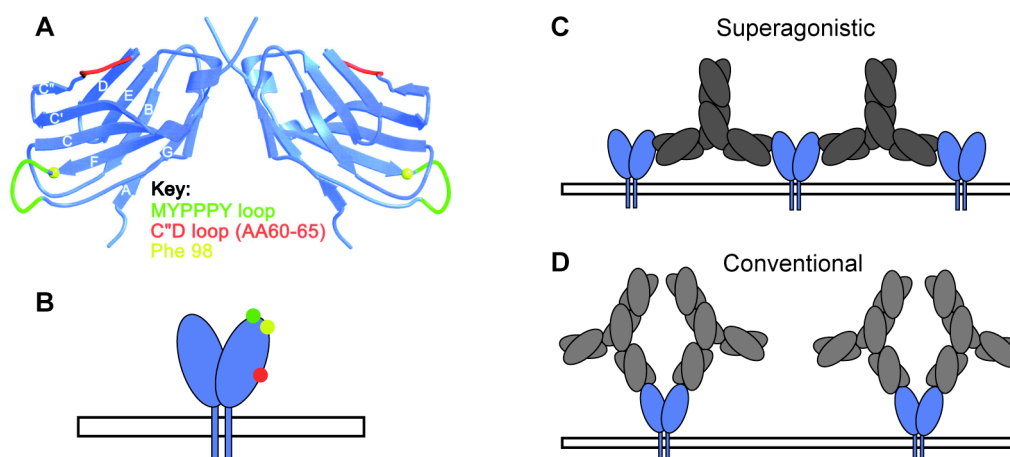


**Figure 1. Binding of the superagonistic and conventional  $\alpha$ CD28 monoclonal antibodies to CD28.** **A.** Three dimensional model of the extracellular portion of human CD28 (blue) showing the binding epitopes of conventional rat and mouse CD28-specific mAb (yellow), of rat and human superagonistic  $\alpha$ CD28 mAb (red), and of B7 molecules (CD80/86) (green, MYPPPY loop) (Luhder et al. 2003)<sup>§</sup>. **B.** Simplified view of the binding epitopes on CD28 molecules; colors represent same as in A. **C, D.** Mode of binding of CD28SA (dark grey) and conventional (light grey)  $\alpha$ CD28 mAbs to the extracellular portion of the CD28 homodimer (blue) (B-D from Beyersdorf, Hanke, et al. 2005)<sup>||</sup>.

#### 1.4.2. In vitro regulatory T cell expansion by $\alpha$ CD28 conventional and superagonistic mAbs

CD28 costimulation is necessary for the in vivo generation of Treg cells, as seen in a model of CD28 and/or B7 molecules deficient mice (Salomon et al. 2000). The cytokine IL-2 is also crucially involved in the generation and homeostasis of Treg cells (Malek and Bayer 2004; Setoguchi et al. 2005). Therefore, efficient in vitro expansion of Treg cells requires CD28 costimulation, TCR stimulation, and IL-2. For in vitro studies, the use of activated APC to deliver signal 1 and 2 is highly efficient, but for ex vivo Treg expansion to be re-infused into animals or patients purity is essential. Currently, the most widely employed tool for Treg expansion is the use of beads coated with anti-CD3 and anti-CD28 antibodies (Hoffmann et al. 2004; Tang et al. 2004).

Given the fact that CD28 superagonists activate T cells without the need of TCR ligation, expansion of Treg cells with the use of these antibodies is an interesting approach. In fact, Treg cells showed to respond very well to CD28SA stimulation, but they also need IL-2 for long term expansion (Beyersdorf, Hanke, et al. 2005); it even proved superior than

<sup>§</sup> ©LUHDER et al. 2003. Originally published in JEM. doi:10.1084/jem.20021024

<sup>||</sup> Reprinted from Annals of the Rheumatic Diseases, 64/suppl 4, Niklas Beyersdorf, Thomas Hanke, Thomas Kerkau, Thomas Hünig, Superagonistic anti-CD28 antibodies: potent activators of regulatory T cells for the therapy of autoimmune diseases, iv91-5, 2005, with permission from BMJ Publishing Group Ltd.

standard costimulation in Treg expansion protocols (Beyersdorf et al. 2006). A schematic view of in vivo T-cell activation by CD28SA is depicted in Figure 2 (Hünig 2007).

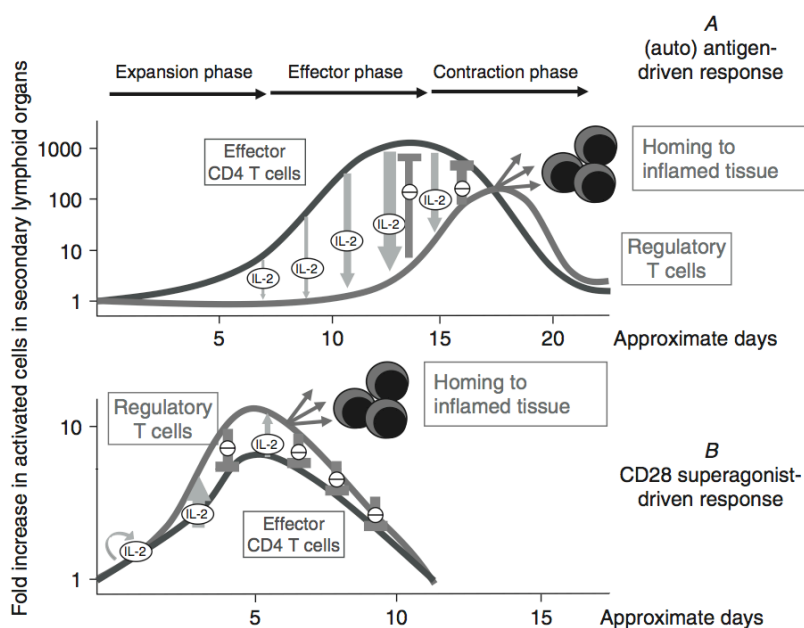


**Figure 2. Clonal expansion of Treg cells during a normal immune response and by a CD28 superagonist. A.** Antigen-driven immune response, where IL-2 produced by effector T cells promotes the later expansion of Treg cells. **B.** Model of a CD28SA driven response where both effector and Treg cells are stimulated simultaneously and Treg cell expansion is favored (Hünig 2007)\*.

## 1.5. CD28SA preclinical rodent models

### 1.5.1. Studies in mice and rats

Injection of CD28SA in rats (JJ316) (Tacke et al. 1997) or mice (D665) (Dennehy et al. 2006) had a very similar effect. Cytokine production at the peak of the response was mainly associated with IL-10 production and, to a lesser degree, IL-4, both anti-inflammatory cytokines (Rodriguez-Palmero et al. 1999; Hünig 2007). In rats, IL-10 was traced back to be produced by Treg cells ( $CD4^+CD25^+CTLA-4^+FoxP3^+$ ) (Beyersdorf, Hanke, et al. 2005; Lin and Hünig 2003). Importantly, the proportion of these cells among the CD4 compartment increased from an initial percentage of about 5% to 20% in rats, and had a 10 to 20-fold increase in mice on day 3 after CD28SA administration, which decreased gradually to normal levels by day 10. At the peak of the stimulation, these cells showed to have an activated phenotype ( $CD25^{high}CTLA-4^{high}$ ) and, of importance, a dose dependent suppressive activity

\* Reprinted from *Advances in Immunology*, 95, Thomas Hünig, Manipulation of regulatory T-cell number and function with CD28-specific monoclonal antibodies, 111-148, 2007, with permission from Elsevier.

was measured, which was up to 10-fold higher than Tregs isolated from unstimulated animals. Expanded cells had the phenotype of “natural” Treg cells (Lin and Hunig 2003; Beyersdorf, Hanke, et al. 2005).

When these observations were made several hypothesis arose to try to explain why Treg cells were preferentially activated over effector T cells by the superagonistic monoclonal antibodies. One was that since Treg cells generated in the thymus recognize self peptides, they receive strong signals in the periphery by self-peptide-MHC class II complexes, which leads to hyper-phosphorylation of downstream signaling molecules that CD28SA expands, and therefore overrule conventional T cell responses (Beyersdorf, Hanke, et al. 2005). Another explanation is related to the anti-apoptotic nature of the CD28SA signals, which avoids induction of strong pro-apoptotic signals and actively induces anti-apoptotic molecules such as BCL-X<sub>L</sub>, given the fact that Treg cells are highly prone to undergo apoptosis (Kerstan and Hunig 2004).

### **1.5.2. CD28SA in autoimmune and inflammatory disease models**

Animal studies showed that the Treg cells that are expanded by CD28SA stimulation are derived from “natural” Tregs originated in the thymus, which are CD25<sup>+</sup>, and not from converted conventional CD4<sup>+</sup> T cells (Lin and Hunig 2003). Naturally occurring Tregs pass through a positive selection process in the thymus for autoreactivity, and that makes them protective against possible immune reactions against self (Sakaguchi et al. 2006). Based on these, CD28SA expansion of Tregs was considered to possibly be a very good approach to treat autoimmune or inflammatory diseases, since specificity to antigens related to the disease is not necessary (Hünig 2007).

To date, treatment with CD28SA has proven effective in a number of animal models of autoimmunity or inflammatory diseases; several examples are shown in Table 1. In general, they are based on the anti-inflammatory effects of expanded Tregs, either therapeutic or preventive, before or after onset of the disease, accomplished by rat (JJ316) (Tacke et al. 1995; Tacke et al. 1997) or mouse CD28SA (D665) (Dennehy et al. 2006).

Cytotoxic cancer therapies leave the patient with severe lymphopenia which is slowly recovered (months to years) (Mackall et al. 1996), contributing to the high incidence of life-threatening opportunistic infections. CD28SA proved effective in the recovery of lymphopenic rats (lethally irradiated, bone marrow-reconstituted) by a dramatic acceleration of T cell recovery, mainly CD4 cells, after a single antibody injection (Elflein et al. 2003).

**Table 1. Examples of rodent models of autoimmune diseases or inflammatory conditions where CD28SA treatment has proven its efficacy either as a preventive measure and/or as a therapy.**

Strain/species	Model	Human equivalent	References
Lewis rat	Experimental autoimmune neuritis	Guillain–Barré syndrome	Schmidt et al. (2003)
Lewis, DA rat	Experimental autoimmune encephalomyelitis	Multiple sclerosis	Beyersdorf, Gaupp, et al. (2005)
Wistar rat	Adjuvant arthritis	Rheumatoid arthritis	Rodriguez-Palmero et al. (2006)
Lewis, DA rat	Allogeneic liver transplantation	Liver transplantation	Urakami et al. (2006)
BB rat	Spontaneous autoimmune diabetes	Diabetes mellitus type 1	Beaudette-Zlatanova et al. (2006)
Lewis, DA rat	Allogeneic heterotropic heart graft	Cardiac transplantation	Kitazawa et al. (2008)
Lewis, DA rat	Graft-versus-host disease (GvHD)	GvHD	Kitazawa et al. (2009)
Wistar rat	Experimental glomerulonephritis	Mesangial proliferative glomerulonephritis	Miyasato et al. (2011)
Brown-Norway and Lewis rat	Obliterative bronchiolitis in allo-orthotopic tracheal transplantation	Obliterative airway disease in lung transplantation	Shi et al. (2012)
C57BL/6, BALB/c mouse	<i>T. brucei</i> and <i>T. congolense</i> infection	African trypanosomiasis	Guilliams et al. (2008)
C57BL/6 mouse	Experimental autoimmune encephalomyelitis	Multiple sclerosis	Gogishvili et al. (2009)
C57BL/6 mouse	Non-T cell–dependent inflammatory arthritis	Inflammation-induced bone loss in rheumatoid arthritis	Zaiss et al. (2010)
C57BL/6 mouse	DSS-induced colitis	Inflammatory bowel disease	Chen et al. (2011)

Abbreviations: *T.*: *Trypanosoma* DA: dark Agouti DSS: dextran sulfate sodium (Hünig 2007)<sup>⊕</sup>

These promising results highlight the potential of Treg cell expansion as an immunological therapy, especially because of the fact that knowledge of the autoantigen recognized is not required, which is a great advantage for human autoimmune disease

<sup>⊕</sup> Reprinted from *Advances in Immunology*, 95, Thomas Hünig, Manipulation of regulatory T-cell number and function with CD28-specific monoclonal antibodies, 111-148, 2007, with permission from Elsevier.

therapy, and it can be both beneficial on thymic T-cell production as well as Treg accumulation.

### **1.6. TGN1412 – a human anti-CD28 superagonistic monoclonal antibody**

Based on the promising results obtained with numerous animal models on the therapeutic potential of CD28SA, a human equivalent was of great interest as a possible therapy for several autoimmune diseases. The German Biotech TeGenero generated a set of mouse anti-human CD28 mAbs and isolated both conventional and superagonistic antibodies, which followed the epitope-function relationship explained in section 1.4.1 (Luhder et al. 2003). One of the superagonistic antibodies isolated was developed into fully humanized by genetic engineering. Based on the knowledge that IgG4 antibodies have a lower affinity for Fc receptors (Presta and Namenuk 2005), and hence might be less likely to recruit cytotoxic mechanisms, the superagonistic IgG4 mAb was developed and it was named TGN1412. The aim of this antibody was to be used as a treatment of human immune diseases, such as rheumatoid arthritis, multiple sclerosis, and B-cell chronic lymphocytic leukemia (Duff 2006).

#### **1.6.1. TGN1412 preclinical studies – Animal models**

Preclinical studies in rodent models with the rodent-specific CD28SA showed that regulatory T cells were preferentially activated, and hence conferred protection against autoimmune and inflammatory diseases. Preclinical safety and toxicity tests were performed on cynomolgus monkeys based on the following knowledge: affinity of TGN1412 for CD28 on cynomolgus monkeys T cells showed to be very similar to human CD28, a finding which correlates with the fact that the extracellular domain of cynomolgus monkeys CD28 showed 100% identity at the amino acid level compared to the human equivalent. Fc receptor interaction of an antibody also influences its biological activity. It was determined that human and cynomolgus monkeys FcR are highly conserved, specially the critical motifs involved in signal transduction (Hanke 2006). Importantly, cynomolgus monkeys showed no sign of cytokine release or toxicity, even at very high doses of 50 mg/kg weight, as reported by TeGenero and reproduced by the National Institute for Biological Standard and Control (NISBC) study, commissioned by the Expert Commission on Phase I Trials (Duff 2006).

#### **1.6.2. TGN1412 first-in-man clinical trial**

Based on the promising results obtained in animal models, and the lack of toxicity in cynomolgus monkeys, TGN1412 was approved to proceed to a clinical trial. On March 13, 2006, Parexel International, Northwick Park, London, started the TGN1412 first-in-man

clinical trial. Six healthy male volunteers received TGN1412 and two received a placebo. Within hours of receiving the TGN1412 infusion the volunteers presented a series of adverse effects that progressed to multi-organ failure. They presented a systemic inflammation caused by a cytokine release syndrome (CRS) also termed “cytokine storm”, that started with high levels of the proinflammatory cytokine TNF- $\alpha$ , followed by IFN- $\gamma$  and several other cytokines. Volunteers were transferred to an intensive care unit, where the symptoms were successfully treated with high dose corticosteroids (Suntharalingam et al. 2006).

### **1.6.3. Current knowledge on CD28 superagonists – After the CRS**

After the unexpected and shocking outcome of the TGN1412 first-in-man trial the scientific community was in desperate need of answers. Why wasn't this foreseen in animal and/or in vitro models? Why did the mechanisms observed in rodent models, namely Treg cell proliferation and activation, failed to protect the human volunteers? By now it is clear that the cell type that mainly released the proinflammatory cytokines were the effector memory T cells (Eastwood et al. 2010). These cells are mostly located in tissues and respond very rapidly to secondary stimulation. Laboratory animals are kept under clean conditions, so they have very few numbers of memory cells due to low exposure to infections, so the balance of the T cell compartment is different than in humans, which accumulate a great number of memory cells throughout their life (Hünig 2012). Gogishvili et al. (2009) showed in a mouse model that Treg cell depletion previous to CD28SA (D665) treatment leads to considerable cytokine release and, importantly, it could be controlled by the use of corticosteroids, which in turn did not affect Treg cell expansion and function.

Regarding cynomolgus monkeys, despite many attempts to explain the non-toxic effect of TGN1412, the reason was surprisingly simple. It was recently found that the CD4<sup>+</sup> effector memory cells do not express CD28, which is the cell type that responds to TGN1412 stimulation (Eastwood et al. 2010).

Finally, human PBMC in vitro assays failed to predict the cytokine storm observed. To date several approaches have been made, which will be discussed later, both to find an in vitro method that allows to predict the CRS induced by TGN1412, and to explain the differences between the in vitro and the in vivo situation. In this study, an in vitro assay was developed that allowed both to find a plausible explanation on why circulating PBMC did not respond to soluble TGN1412 stimulation, and to improve the current PBMC in vitro assays for immunological drug testing.

## **2. Introductory statement on contributions and previous publication**

This thesis was conducted in the research laboratory of Prof. Thomas Hünig (Institute for Virology and Immunobiology, University of Würzburg). Experimental procedures of this PhD project were performed by myself, with technical assistance from Susanne Berr - unless stated otherwise. Shin-Young Na (Postdoc, Prof. Hünig's group) performed confocal analysis of human lymph node sections, and Elita Avota (Postdoc, Prof. Schneider-Schaulies' group) of human PBMC. Manuela Battaglia (San Raffaele Diabetes Research Institute, Milan, Italy) obtained, stimulated, and measured proliferation of human lymph node cells. Ineke ten Berge (Academic Medical Center, University of Amsterdam, Amsterdam, Netherlands) provided paired human lymph node and PBMC samples. The bulk of this research was originally published in *Blood*. Authors: Paula S. Römer, Susanne Berr, Elita Avota, Shin-Young Na, Manuela Battaglia, Ineke ten Berge, Hermann Einsele, Thomas Hünig. Title: Preculture of PBMCs at high cell density increases sensitivity of T-cell responses, revealing cytokine release by CD28 superagonist TGN1412. *Blood*. 2010;118:6772-6782. © the American Society of Hematology.

### **3. Methods**

#### **3.1. Cell isolation and preparation**

##### **3.1.1. Human PBMC isolation**

Human PBMC were obtained either from healthy donors as a byproduct of platelet concentrates from leukoreduction system chambers (LRS-C) (7-9 mL), and filled up with Versene to 60 mL; or directly from heparinized venous blood. PBMC were separated by density gradient centrifugation using Lymphocyte Separation Medium and Leucosep tubes, and washed twice with ice-cold balanced salt solution (BSS) / 0.2% bovine serum albumin (BSA).

##### **3.1.2. Human lymph node cells**

Lymph nodes were obtained from two sources, one from the pancreas of non-diabetic brain-dead multi-organ donors, from the San Raffaele Hospital, Milan, Italy.

Alternatively, lymph nodes were collected from the para-iliac region of renal transplant recipients, received from the Academic Medical Center, Amsterdam, Netherlands. Paired peripheral blood samples were collected before the transplantation procedure. Cells were frozen in IMDM supplemented with 10% DMSO, 20% FCS, penicillin, streptomycin and 0.00036%  $\beta$ -mercaptoethanol.

##### **3.1.3. Cell culture**

Cells were cultured under sterile conditions in a humidified incubator at 37 °C, 5% CO<sub>2</sub> in AB medium.

##### **3.1.4. Freezing and thawing**

Cells were cryopreserved at -140°C.  $5 \times 10^7$  cells in 1 mL of freezing medium in cryotubes, kept at -80°C in a pre-cooled (4°C) "Mr. Frosty" Cryogenic Freezing Container filled with isopropanol for 24h, then transferred to a -140°C freezer.

Vials were thawed in a 37°C water bath until there was a pea-sized pellet of ice remaining. Cell suspensions were then transferred to a correspondingly labeled 50 mL Falcon tube containing 8 mL of pre-warmed AB medium with DNase (5 U/mL), and incubated for 10 min at room temperature (RT); centrifuged and washed once more with AB medium, resuspended in AB medium and left 20 min at RT, then kept on ice until use.

### 3.1.5. Depletion and isolation of cell subsets

CD4<sup>+</sup> T cell isolation from human PBMC was performed using the CD4<sup>+</sup> T Cell Isolation Kit II from Miltenyi Biotec, following the manufacturer's instructions, and for monocytes, the Monocyte Isolation Kit II from Miltenyi Biotec was used following the manufacturer's instructions; with the only modifications of using BSS/BSA instead of their recommended buffer, in both cases. MACS LS columns were used for positive or negative selection, and MACS LD columns for cell depletion.

For cell subset depletion, anti-PE microbeads, anti-FITC microbeads, and goat anti-mouse IgG microbeads were used accordingly, following the manufacturer's instructions. PBMC were stained with CD19-PE, CD83-PE, CD14-FITC, or Tü39 (anti-HLA-DR,DP,DQ). Cells expressing CD19, CD83 and CD14 were depleted simultaneously. In this case, PBMC were stained with CD14-FITC, CD19-PE and CD83-PE. CD19 and CD83 positive cells were depleted using anti-PE microbeads, and CD14<sup>+</sup> cells were subsequently depleted using anti-FITC microbeads.

### 3.2. Stimulation assays – RESTORE protocol

The optimized "RESTORE" protocol was done by preculturing PBMC at a high cell density of  $1.5 \times 10^7$  cells in 1.5 mL ( $1 \times 10^7$  cells/mL) in 24 well suspension culture plates for 2 days, in a humidified incubator at 37°C, 5% CO<sub>2</sub>. After this preculture period, cells were harvested using ice-cold AB medium, washed, and prepared for stimulation.

Cells stimulated at  $1 \times 10^6$  cells/mL in 96-well flat bottom plates (200 µL/well,  $2 \times 10^5$  cells). GMP-grade TGN1412 and clinical grade OKT3 were used.

During the optimization process, cells were precultured at low cell density ( $1 \times 10^6$  cells/mL), and several preculture times were performed.

### 3.3. Western blotting

#### 3.3.1. Cell lysis

Cells were lysed in lysis buffer and incubated on ice for 1h, vortexing for 5 sec. medium speed every 5 min. The lysate was centrifuged at 20,000 x g at 4°C for 10 min.

### **3.3.2. Pre-clearing of cell lysate**

The cell lysate was pre-cleared by mixing it with 30  $\mu$ L of 50% protein-G sepharose, and incubated 30 min in rotation at 4°C. Repeated 2x if the lysate was prepared from cells expressing immunoglobulins.

### **3.3.3. SDS-polyacrylamide gel electrophoresis**

Protein extracts were separated on 12.5-15% SDS polyacrylamide gels under reducing conditions (boiled 10 min, 96°C with 1x SDS reducing sample buffer). The separating gel mix was prepared, poured into the gel apparatus, and overlaid with water. After the gel polymerized, the water was decanted and the stacking gel was poured. Protein samples were loaded, and ran in 1x SDS PAGE running buffer.

### **3.3.4. Western Blot**

Proteins from the SDS-PAGE gel were blotted to a nitrocellulose membrane at 50 mA, 500 V for 2h at 4°C. The membrane was washed with H<sub>2</sub>O for 5 min., then with methanol 5 min., and incubated with 5% milk powder in PBS-0.1% Tween for 1h at RT on a rocker platform.

The nitrocellulose membrane was incubated with the primary Ab diluted in 1% milk powder in PBS-0.1% Tween, O/N at 4°C. The membrane was washed 6x with PBS-0.1% Tween for 5 min each time, on the rocker platform at RT, then incubated with a horseradish-peroxidase-conjugated secondary Ab for 1-2h, on the rocker platform at RT. After incubation, the membrane was washed again 6x with PBS-0.1% Tween for 5 min each time, on the rocker platform at RT, then treated with enhanced chemiluminescent substrate and developed in the dark box (LAS-3000).

## **3.4. Cell proliferation assays**

### **3.4.1. 3H-thymidine incorporation**

After cell stimulation, proliferation was measured as radioactivity incorporated from day 2 to 3 from 3H-thymidine (1  $\mu$ Ci per well) into DNA, using a Liquid Scintillation Counter. Results are expressed as counts per minute (cpm).

### **3.4.2. Ki67 staining**

Cells were stimulated for 3 days, and cold harvested. PBMC were surface stained, washed once with FACS buffer, then incubated with fixation/permeabilization buffer (eBioscience) for 30 min. in the dark in order to fix and permeabilize the cells allowing intracellular (nuclear)

staining, washed 1x with FACS buffer, 1x with Perm/Wash, and incubated with anti-Ki67 antibody diluted in Perm/Wash for 30 min. at 4°C, in the dark. Washed with FACS buffer and resuspended in either FACS buffer for immediate analysis or fixed with 2% PFA until analysis (maximum 1 day). Kept at 4°C.

### **3.5. Cell dissociation experiment**

Lymph node cells were prepared at  $1 \times 10^6$  cells/mL in AB medium, and either stimulated immediately or placed in a humidified incubator at 37°C for two or four hours, in a 50 mL Falcon tube without the lid to allow gas exchange. The cells were gently mixed every 20 min. to keep them in suspension.

### **3.6. Transwell assay**

Freshly isolated PBMC were placed in the lower compartment of the transwell system in low cell density ( $1 \times 10^6$  cells/mL), while high-cell density PBMC ( $1 \times 10^7$  cells/mL) from the same donor were placed in the upper compartment of the transwell insert, therefore allowing exchange of soluble factors, but not of cells. Controls were included with only low or high-density cells. The system was incubated for two days at 37°C, 5% CO<sub>2</sub>.

Cells were recovered from the wells with or without the transwell insert and stimulated at  $1 \times 10^6$  cells/mL in 96-well flat bottom plates (200 µL/well) for 24 h at 37°C. Cell culture supernatant was taken and cytokine levels measured by Cytometric Bead Array (CBA).

### **3.7. Flow cytometry (phenotyping)**

Cells were washed with FACS buffer, resuspended in the antibody preparation, and incubated for 20 min. at 4°C. Washed with FACS buffer and resuspended in either FACS buffer for immediate analysis or fixed with 2% PFA until analysis (maximum 1 day). Kept at 4°C.

### **3.8. Cytokine release quantification**

Cytokine release was evaluated by three methods: Cytometric Bead Array (CBA), enzyme-linked immunospot assay (ELISPOT) or by intracellular cytokine staining. The first two were performed following the manufacturers instructions.

### 3.8.1. Intracellular cytokine staining

Brefeldin A was added on the last four hours of a 6 or 16h stimulation in order to block the cytokine secretion. Cells were surface stained, washed once with FACS buffer, then incubated with fixation/permeabilization buffer (BD) for 30 min. in the dark in order to fix and permeabilize the cells for intracellular (cytoplasmic) staining, washed 1x with FACS buffer, 1x with Perm/Wash, and incubated with an antibody directed against the cytokine of interest, diluted in Perm/Wash for 30 min. at 4°C, in the dark. Washed with FACS buffer and resuspended in either FACS buffer for immediate analysis or fixed with 2% PFA until analysis (maximum 1 day, 4°C).

### 3.8.2. Responding cell subset determination

To determine which subset of the memory CD4<sup>+</sup> T cell compartment responds to TGN1412, purified CD4<sup>+</sup>, CD4<sup>+</sup>CCR7<sup>+</sup>, or CD4<sup>+</sup>CCR7<sup>-</sup> T cells (MACS separation) were obtained. CD4<sup>+</sup> T cells were isolated using the CD4<sup>+</sup> T Cell Isolation Kit II, following manufacturers instructions. Cells were then surface stained with  $\alpha$ -human CCR7-FITC antibody, positive and negative cells were separated using  $\alpha$ -FITC microbeads and an LS column. Positive cells were passed again through an LS column, and negative cells through an LD column, to improve the purity of the obtained fractions.

CD4<sup>+</sup>, CD4<sup>+</sup>CCR7<sup>+</sup>, and CD4<sup>+</sup>CCR7<sup>-</sup> T cells were CFSE labeled, mixed with intact PBMC in high cell density ( $1 \times 10^7$  cell/mL) by including 20% of CFSE labeled cells, and incubated for two days at 37°C, 5% CO<sub>2</sub>. Cells were harvested, placed in low cell density ( $1 \times 10^6$  cell/mL), stimulated for 6 hours with 1  $\mu$ g/mL TGN1412 or OKT3. Brefeldin A was added at the beginning of the stimulation. PBMC were cold harvested, washed, and stained for intracellular TNF. Gates were done in CFSE<sup>+</sup> cells.

### 3.9. CFSE labeling

Wash cells 2x with 10 mL PBS, resuspend in CFSE 1:25,000 at  $1 \times 10^7$  cells/mL. Incubate for 5 min., RT, in the dark. Centrifuge for 5 min., 300 x g, 4°C, and wash 2x with cold RPMI-1640 medium with 10% fetal calf serum (FCS) (RPMI-10). Resuspend in AB medium.

### 3.10. Confocal microscopy

Paraffin embedded human lymph node sections (3  $\mu$ m) were deparaffinized, boiled in citrate buffer, and blocked with PBS / 10% BSA.

Human PBMC kept in ice-cold PBS / 0.02% sodium azide were allowed to adhere to poly-lysine-coated glass slides, fixed with paraformaldehyde and permeabilized with 0.1% Triton X-100 for 5 min.

### **3.11. Statistical analysis**

To evaluate statistically significant differences, the Wilcoxon signed rank sum test, paired t test, unpaired t test, and two-way ANOVA were used. In all cases a *P* value less than 0.05 was considered as significant.

## 4. Results

### 4.1. PBMC response to soluble TGN1412

In order to study why the cytokine storm elicited by TGN1412 was not predicted by in vitro assays, the response to soluble TGN1412 was evaluated. Initially, freshly isolated circulating human PBMC were used in the stimulations. As a positive control, the anti-CD3 mAb Muromonab (OKT3) was used, which is known to generate a strong cytokine release in vivo (Abramowicz et al. 1989B; Chatenoud et al. 1990). Both reagents were added at 1  $\mu$ g/mL, which is in the range of the estimated concentration reached in the blood of the volunteers during the TGN1412 Phase I Clinical Trial (Waibler et al. 2008).

Cell culture supernatant was collected after 24 h stimulation, and cytokine levels were determined (TNF, IL-2 and IFN- $\gamma$ ) by Cytometric Bead Assay (CBA). These cytokines were highly elevated in the blood of the healthy London trial volunteers after TGN1412 infusion (Suntharalingam et al. 2006). Figure 3A shows that freshly isolated PBMC respond by cytokine release to soluble OKT3, but not to TGN1412, as it has been previously reported (Duff 2006; Stebbings et al. 2007).

After failing to reproduce in vitro the cytokine storm generated by TGN1412 in vivo, there was an unexpected breakthrough. In one opportunity isolated PBMC were kept for two days in the incubator at a high cell density, while waiting for a missing reagent. When the stimulation assay was repeated with these cells, TGN1412 induced a high cytokine release of comparable magnitude as the one elicited by OKT3 (Figure 3B) (Römer et al. 2011). This methodology was termed “RESTORE” protocol, for RESetting T-cells to Original REactivity.

The results are highly reproducible (over 150 healthy donors). Figure 3C shows results obtained from the first 22 individuals tested. There is a consistent induction of TGN1412 reactivity by preculture, whereas fresh PBMC do not respond to stimulation. This phenomenon of an “in vitro cytokine storm” resembles the in vivo situation, and is comparable to the OKT3 response (Goldman et al. 1989).

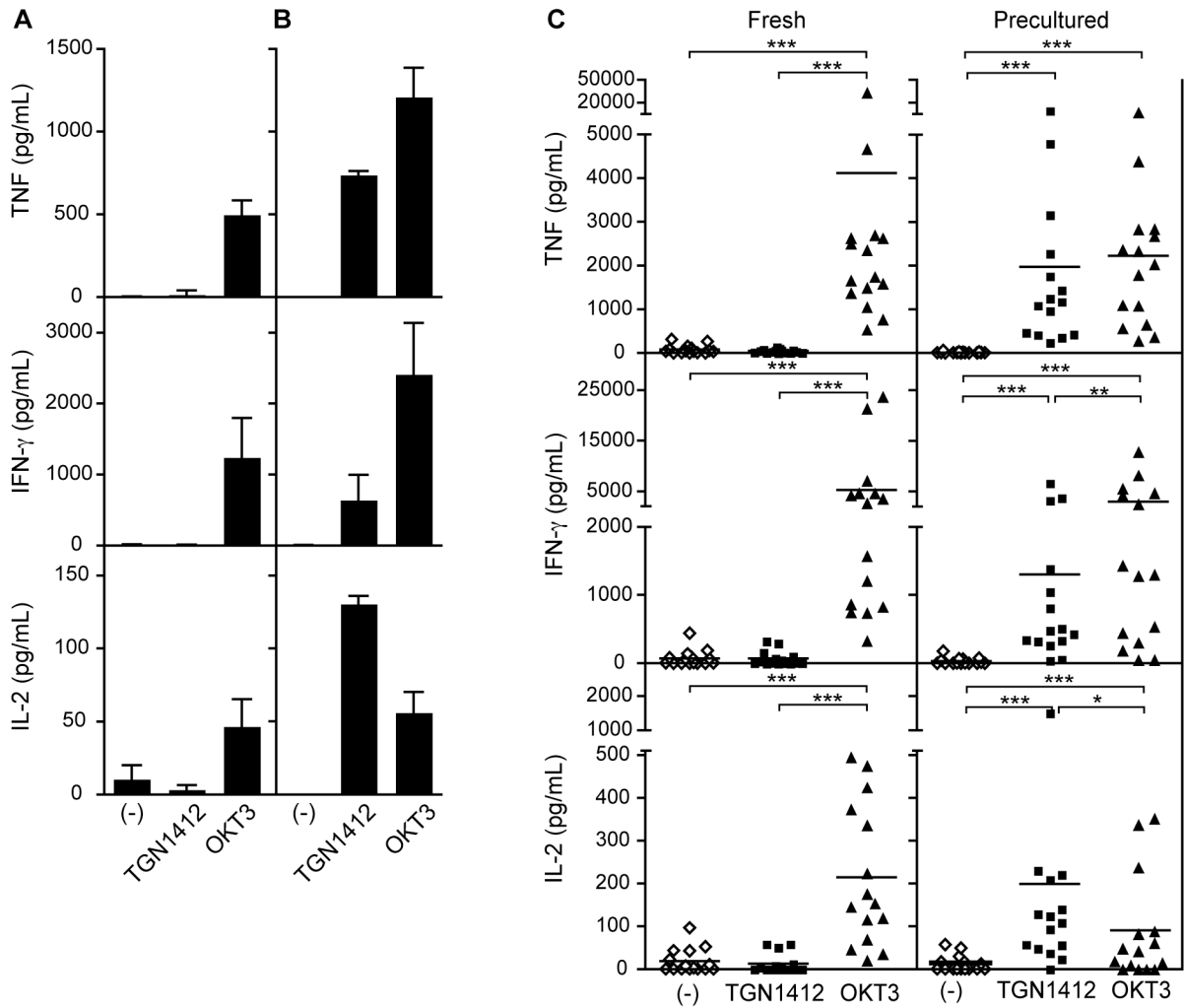


**Figure 3. Human PBMC cytokine release response to soluble TGN1412.** **A.** Fresh and **B.** precultured PBMC are compared by their cytokine release profile in response to TGN1412 or OKT3. Data are mean  $\pm$  SD of triplicate samples. **C.** Compilation of the results obtained from 22 healthy individuals. Cytokines determined by CBA in cell culture supernatant after 24h stimulation with 1  $\mu$ g/mL TGN1412 or OKT3. Wilcoxon signed rank test: \* $P < .05$ , \*\* $P < .005$ , \*\*\* $P < .0001$ . (-) represents unstimulated cells.

TGN1412 acts as a mitogen on precultured PBMC, with comparable strength to OKT3 (Figure 4A). In contrast, fresh PBMC did not proliferate when stimulated with TGN1412, but did with OKT3 stimulation, in accordance with the results obtained with cytokine release as a read-out (Figure 3). The response of precultured PBMC elicited by TGN1412 can be titrated and is of comparable magnitude to the response to OKT3, as shown by TNF release in Figure 4B. There is a detectable TGN1412 response already at 0.06  $\mu$ g/mL, which is equivalent to  $\approx$  1% receptor occupancy (Waibler et al. 2008). At 1  $\mu$ g/mL the maximum biological response is achieved, which is now known to represent 45 to 80% of occupied CD28 molecules (Waibler et al. 2008).

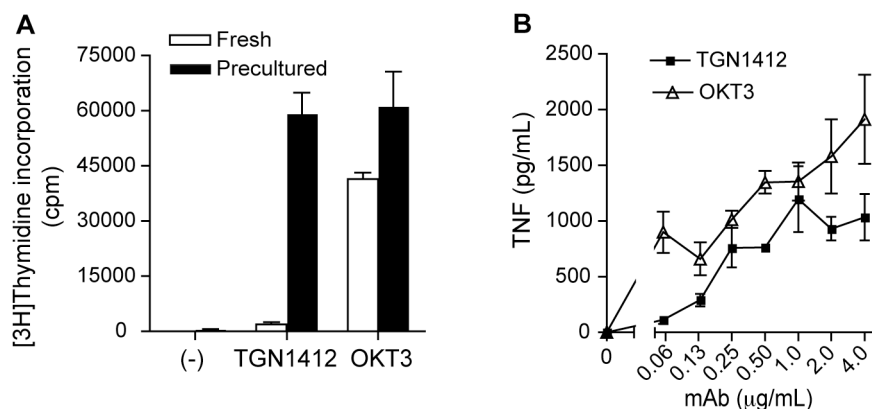


**Figure 4. Properties of the RESTORE response to TGN1412. A.** Proliferative response of fresh and high-density precultured PBMC to stimulation with 1  $\mu\text{g}/\text{mL}$  TGN1412 or OKT3. **B.** TNF in cell culture supernatants after 24h stimulation to titrated amounts of TGN1412 and OKT3. Data are mean  $\pm$  SD of triplicate samples.

#### 4.2. Optimization of the RESTORE protocol

In order to determine the optimal preculture time for the RESTORE protocol, cells were stimulated either fresh or kept in the incubator at  $1 \times 10^7$  cells/mL for 24 or 48 h (Figure 4B). The best proliferative response was obtained after 48 h of high-density PBMC preculture. Preculture of PBMC is performed at a 10-fold higher cell density than the concentration used in standard PBMC assays. Preculture at high ( $1 \times 10^7$  cells/mL) but not at low ( $1 \times 10^6$  cell/mL) cell density rendered PBMC reactive to TGN1412 stimulation, suggesting the requirement for cell contact (Figure 5B). Further increase in cell density or pre-incubation time did not improve the response (not shown).

To find the optimal conditions for the preculture, tissue and suspension culture plates were compared. PBMC were placed in high cell density for 2 days in each plate type, and stimulated as described previously. As shown in Figure 5C, a slightly better response is obtained when suspension culture plates are used during the preculture, although tissue culture plates also allow the acquisition of TGN1412 reactivity.

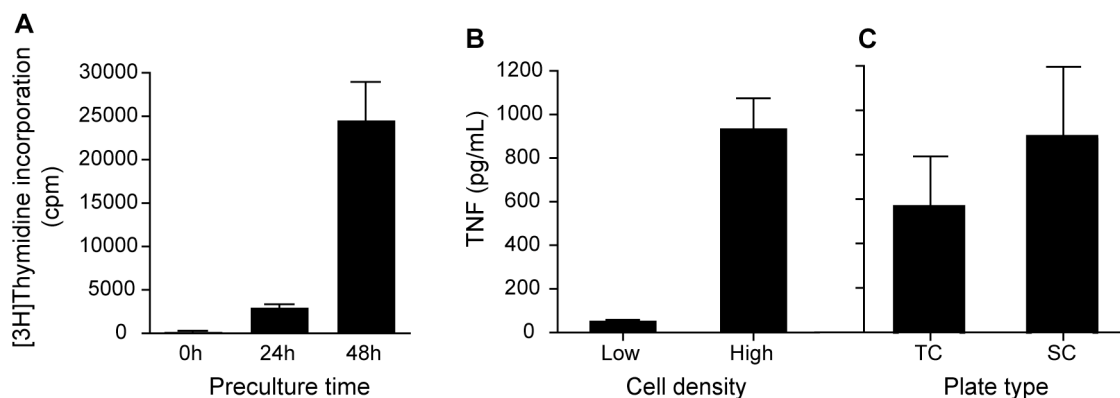


**Figure 5. Optimization of the RESTORE protocol.** **A.** Proliferative response of precultured PBMC to 1  $\mu\text{g/mL}$  TGN1412 **B.** TNF release in cell culture supernatants after 24h stimulation with 1  $\mu\text{g/mL}$  TGN1412 from low or high-density precultured PBMC. Data are mean  $\pm$  SD of triplicate samples. **C.** Comparative TNF release response to 1  $\mu\text{g/mL}$  TGN1412 between PBMC precultured at a high cell density in either tissue culture (TC) or suspension culture (SC) plates. Data from single values of two independent experiments  $\pm$  SD is shown.

Based on these findings, optimal RESTORE preculture conditions were used in all subsequent experiments,

**Preculture:**

Time: 2 days

Cell density:  $1 \times 10^7$  cells/mL or  $2 \times 10^6$  cells/cm<sup>2</sup>

Plate type: Suspension culture plates

Medium: AB medium

**Stimulation:**

TGN1412: 1  $\mu\text{g/mL}$

OKT3: 1  $\mu\text{g/mL}$

Cell density:  $1 \times 10^6$  cells/mL or  $2 \times 10^5$  cells/cm<sup>2</sup>

#### 4.3. Loss of suppression vs. gain of function after high-density preculture

There could be several explanations for the acquisition of TGN1412 reactivity. One of the hypotheses on why PBMC are suddenly responding after a two-day preculture period at a high cell density is that a specific cell subset is changing, i.e. regulatory T cells dying or enrichment of a subset. To verify if this is the case, fresh and precultured PBMC were stained for a variety of cell markers. Figure 6 shows that there is no remarkable change in cell subset composition after the preculture period. Dendritic cells (CD83<sup>+</sup>) remained under 1% before and after preculture (not shown).

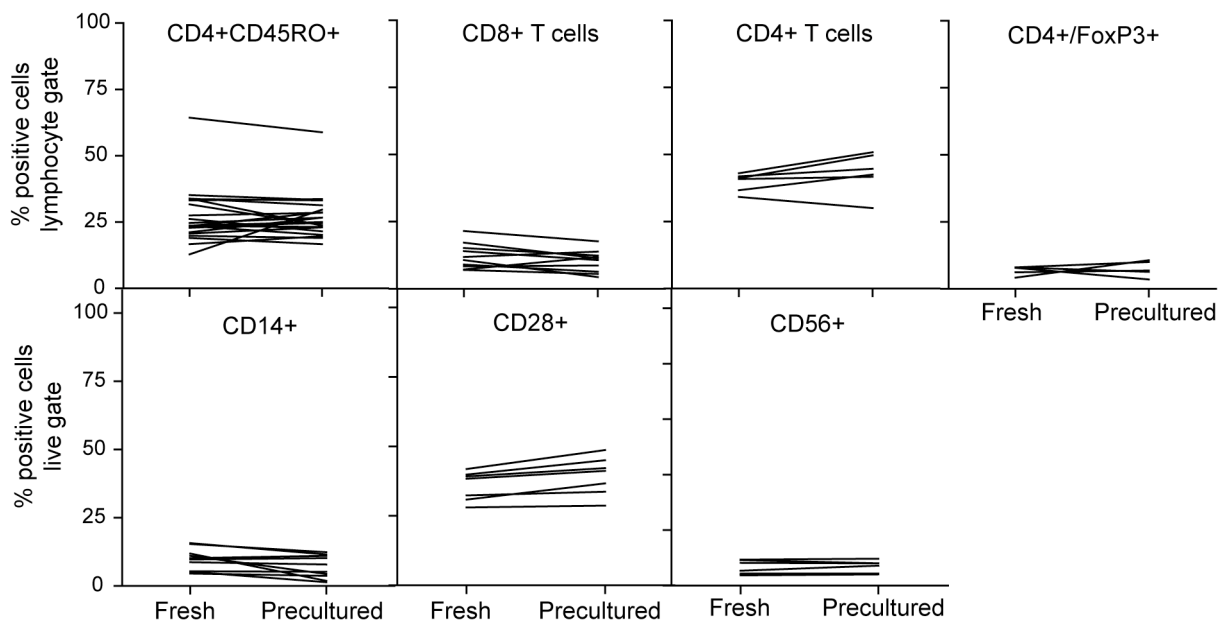


**Figure 6. Cell subset composition of fresh and precultured PBMC. A.** Fresh and precultured PBMC were stained surface or intracellularly (FoxP3) with the given antibodies. Each line represents a different blood donor. Gating strategy is shown in the Y-axis.

To further verify that the preculture effect was not due to a loss of suppression, but to a gain of function, fresh and precultured cells from the same donor were mixed at different ratios. TNF release measured after TGN1412 stimulation was directly proportional to the fraction of precultured cells (Figure 7), showing that fresh cells did not suppress the response, which suggests that the effect of 2-day high density preculture is not due to a loss of suppression, i.e. Tregs losing their suppressive capacity or missing anti-inflammatory cytokines. It rather seems to be due to a gain of function of the precultured PBMC, which renders them TGN1412 reactive.

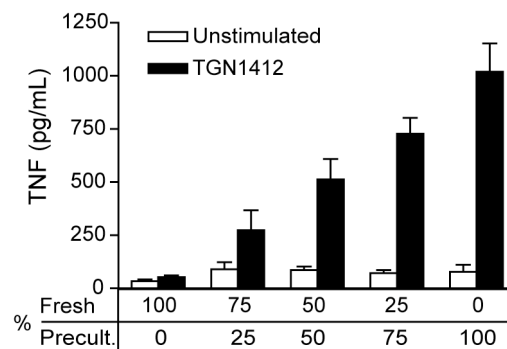


**Figure 7. TNF release of fresh and precultured PBMC mixed at different ratios during stimulation.** TNF concentrations measured in cell culture supernatants by CBA after 24h stimulation with 1  $\mu$ g/mL TGN1412. Data are mean  $\pm$  SD of triplicate samples.

#### 4.4. Properties of the RESTORE response of PBMC to soluble TGN1412

TGN1412 binds to CD28 which is expressed on T cells, but which subset of T cells respond to TGN1412 stimulation after preculture? In Figure 8 we can clearly see that production of TNF and IFN $\gamma$  in response to TGN1412 is restricted to CD4<sup>+</sup> memory cells (CD45RO<sup>+</sup>), a finding also shown by Eastwood et al. (2010). There was a significant positive correlation between cytokine production and the percentage of CD4<sup>+</sup>CD45RO<sup>+</sup> cells (N = 15, Spearman  $r = 0.70$ ,  $P = .0039$ ).

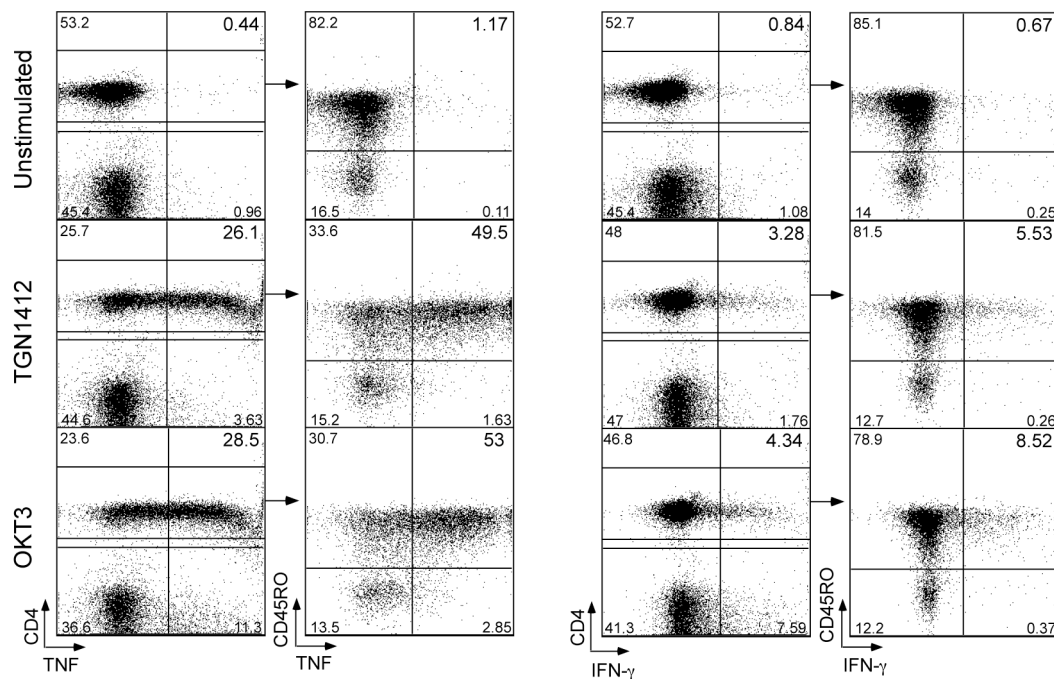


**Figure 8. Intracellular cytokine staining of precultured PBMC.** Cells were stimulated for 16h with 1  $\mu$ g/mL TGN1412 or OKT3. For optimal resolution, a donor with a particularly high TNF release was chosen.

Recently published work using plastic-immobilized TGN1412 suggests that the CD4 effector memory T cells (CD45RO<sup>+</sup>CCR7<sup>-</sup>) are the main cytokine producers to TGN1412 stimulation (Eastwood et al. 2010). In Figure 9 this finding could be corroborated (see method in section 3.8.2). Of the CD4<sup>+</sup> T cells added to the preculture, 2.3% released TNF in response to TGN1412. When CD4 effector memory T cells (CCR7<sup>-</sup>) were enriched the TNF responder cells to soluble TGN1412 stimulation increased considerably (9% responder cells), while in contrast central memory T cells (CCR7<sup>+</sup>) were only 0.5% (Figure 9). This finding reveals that the main source of proinflammatory cytokines to TGN1412 stimulation are the CD4 effector memory T cells.

To determine whether the proliferating cells are the same cell type that releases the cytokines, an intracellular Ki67 staining was performed. As shown in Figure 10, proliferating

cells to soluble TGN1412 stimulation are indeed of the memory cell compartment ( $CD4^+CD45RO^+$ ), the same cell type producing cytokines (Figure 8).

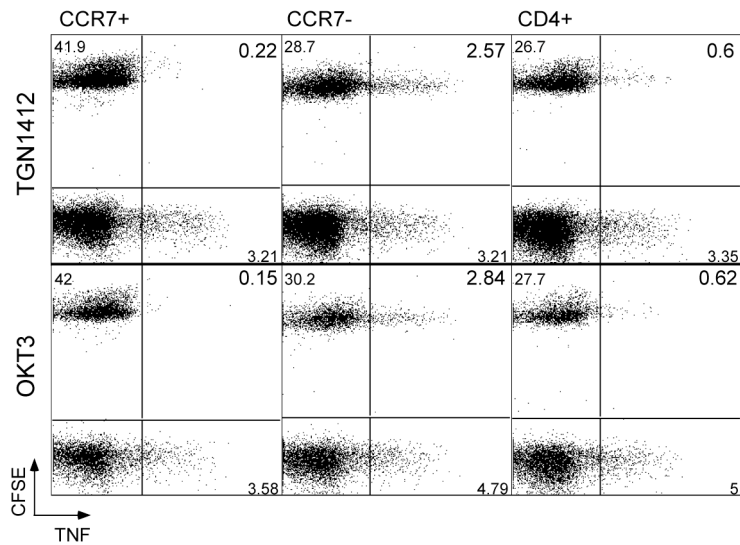


**Figure 9. TNF release by effector memory T cells from precultured PBMC in response to TGN1412.** Purified  $CD4^+$  T cells, and either  $CCR7^+$  or  $CCR7^-$  were separated and CFSE labeled. Mixed 1:5 with intact PBMC in high cell density and incubated for 2 days,  $37^\circ C$ ,  $5\% CO_2$ . Stimulation was done for 6h with  $1 \mu g/mL$  TGN1412 or OKT3. Gated on  $CD4^+$  T cells.

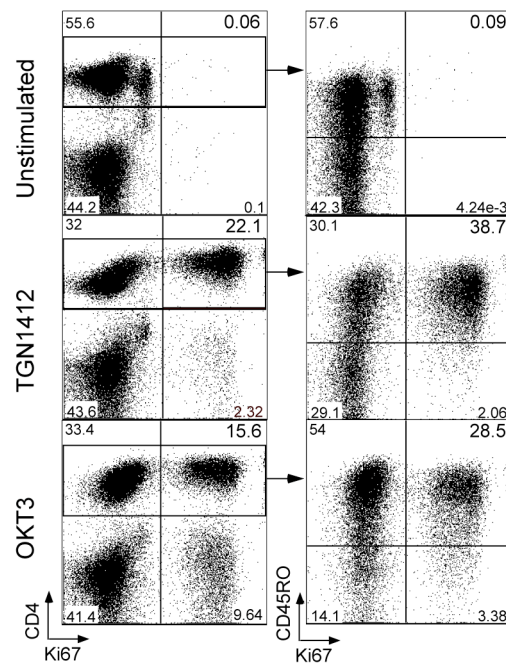


**Figure 10. Proliferation of high density precultured PBMC in response to TGN1412 and OKT3 determined by Ki67 staining.** Intact PBMC were stimulated with  $1 \mu g/mL$  TGN1412 or OKT3 for 3 days. Gated on lymphocytes.

#### 4.5. Cellular interactions during high-density preculture

Acquisition of TGN1412 reactivity by preculture requires high cell density (Figure 5B). In order to confirm if cell contact is indeed necessary, a transwell assay was employed (section 3.6). In this system soluble factors can be exchanged between low density and high-density cells through a semipermeable membrane, which cells cannot cross.

The low density PBMC precultured in the presence of high density PBMC separated by a semipermeable membrane did not respond to TGN1412 (Figure 11), meaning that a soluble factor is not sufficient for the acquisition of reactivity. This confirms the need of cell-cell contact for the acquisition of TGN1412 reactivity.

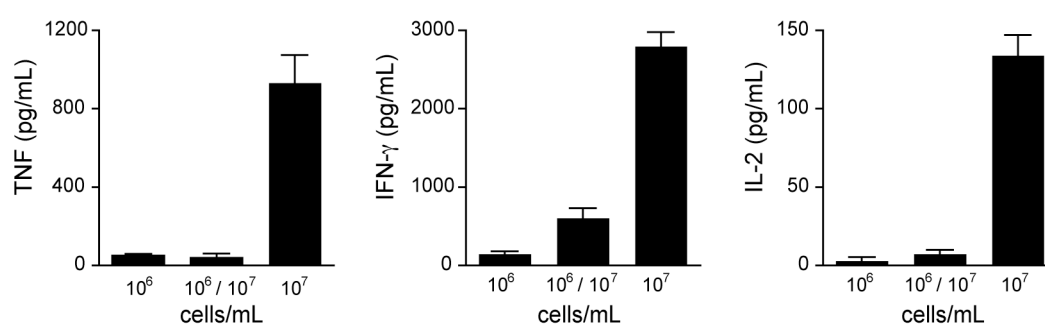


**Figure 11. Cell contact is required for acquisition of TGN1412 reactivity.** Cytokine release upon TGN1412 stimulation (24 h, 1  $\mu$ g/mL) after preculture at high ( $10^7$  cells/mL) and low ( $10^6$  cells/mL) cell density, or at low cell density with a transwell insert containing high-density PBMC ( $10^6$  /  $10^7$ ). Measured by CBA. Data are mean  $\pm$  SD of triplicate samples.

To study the effect of high-density culture on the T cells it is important to characterize the interactions and effects that happen within the system. It has been shown that CD28SA require weak or “tonic” TCR signals in order to elicit a response (Dennehy et al. 2007; Levin et al. 2008); and priming of the TCR complex of mouse lymph node CD4 T cells can occur by cellular adhesion (Randriamampita et al. 2003), or by MHC scanning of APC within the organ (Stefanova, Dorfman, and Germain 2002; Hochweller et al. 2010). These signals promote the preassembly and phosphorylation of proximal intracellular signaling proteins of the TCR complex, keeping the cells in an optimal state of sensitivity, allowing them to respond faster and more efficiently to a foreign peptide (Stefanova, Dorfman, and Germain 2002). Importantly, mouse CD4 T cells lose this quality when entering the blood stream, because they lack cell contacts (Stefanova, Dorfman, and Germain 2002).

Based on these previous findings, a possible explanation for the unresponsiveness of circulating human PBMC to TGN1412 is that they have lost their “primed” status, which can

be recovered by allowing cell-cell interactions, i.e. MHC scanning. Placing circulating PBMC in high cell density allows the recovery of this sensitive state.

One of the features of the assembly of the TCR complex and the immunological synapse involves phosphorylation of tyrosine residues in proteins involved in the signal transduction cascade downstream of the TCR. Therefore studying the tyrosine phosphorylation status of the cells in the RESTORE system could shed a light on the mechanism behind the acquisition of TGN1412 reactivity by preculture.

The distribution of the TCR component CD3 molecule and of tyrosine-phosphorylated proteins in human lymph node sections was studied, as well as in fresh and high density precultured PBMC. Figure 12 (experiment by Dr. Shin-Young Na) shows a clear co-localization of CD3 with phosphotyrosine (pTyr) staining (overlay) in the human lymph node section. CD3 is not evenly distributed in the cell surface, but in a polarized fashion, while CD45 (common leukocyte antigen) shows an even distribution (control staining) and, more importantly, does not co-localize with pTyr.

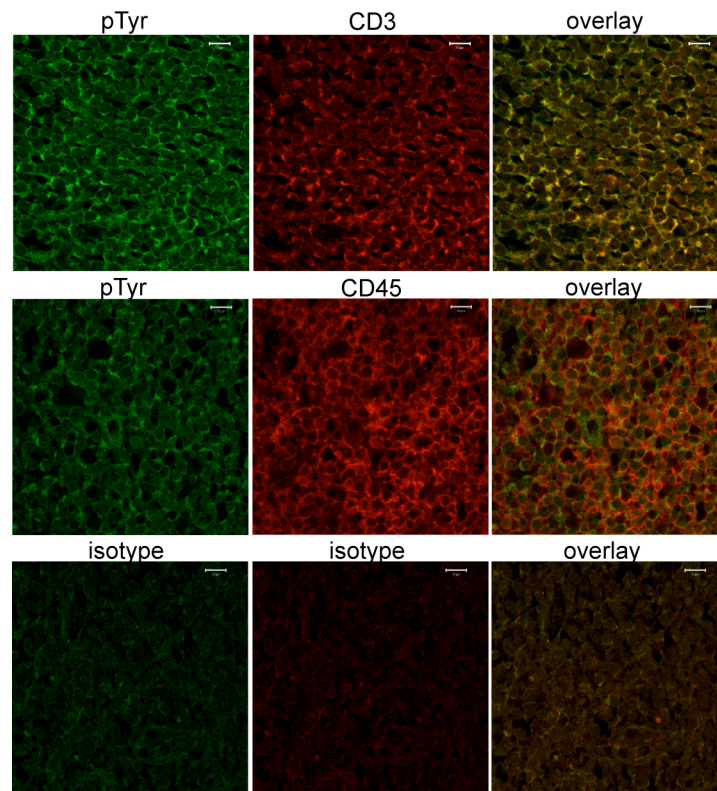


**Figure 12. Colocalization of CD3 with tyrosine-phosphorylated proteins in human lymph node sections.** Human lymph node sections were co-stained with anti-CD3 mAb (red) and anti-phosphotyrosine (pTyr, green). Anti-CD45 mAb was included as a negative control. Appropriate isotype controls were included. Experiment performed by Dr. Shin-Young Na.

In contrast, freshly isolated PBMC show a homogeneous distribution of CD3 on the cell surface, and barely any tyrosine phosphorylation on the T cells, as compared to non-T cells (Figure 13, experiment by Dr. Elita Avota). Precultured PBMC, on the other hand, show a remarkably high and polarized tyrosine phosphorylation, which co-localizes with CD3, forming cap-like structures. These structures suggest the formation of a partially activated TCR complex in the lymph node, and tyrosine phosphorylation after the 2-day preculture at a high cell density, as seen in the human LN sections (Figure 12), suggesting that the T cells have returned to tissue-like conditions.

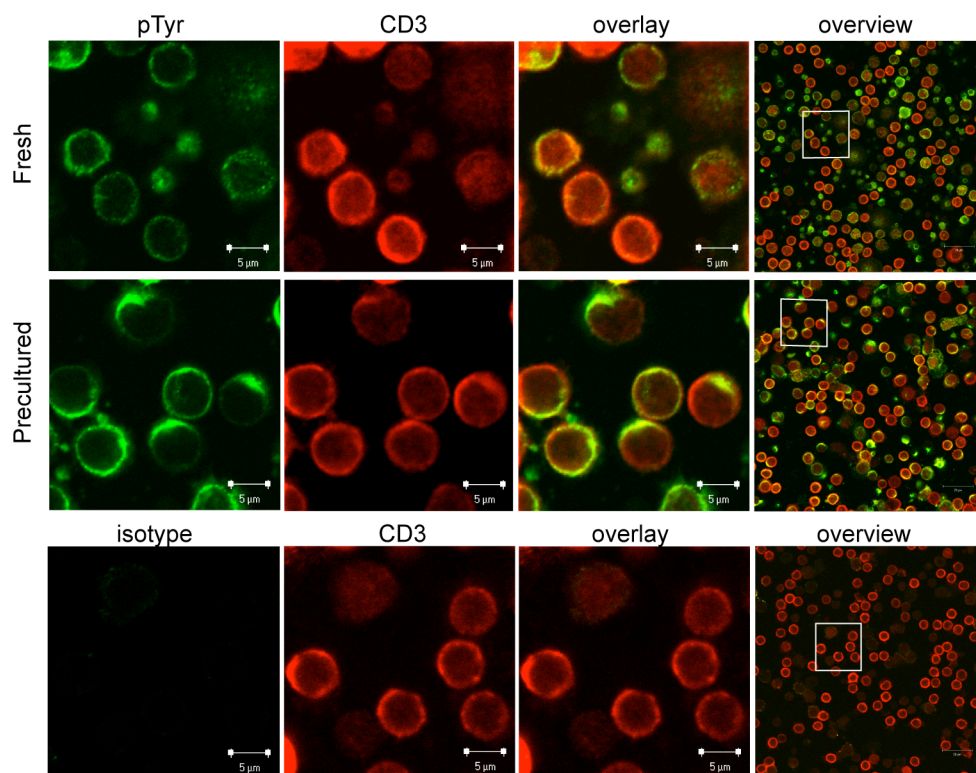


**Figure 13. Colocalization of CD3 with tyrosine-phosphorylated proteins in fresh and high density precultured human PBMC.** Human lymph node sections were co-stained with anti-CD3 mAb (red) and anti-pTyr (green). An isotype control for pTyr was included. For statistical analysis of colocalization, see Figure 14. Experiment performed by Dr. Elita Avota.

Statistics and colocalization coefficients were calculated for the confocal microscopy images of fresh and precultured PBMC (Figure 14, analysis by Dr. Elita Avota). On freshly isolated cells, pTyr positive cells were not of T cell origin (CD3<sup>+</sup>) (Figure 14A). In contrast, 84% of the T cells analyzed in precultured PBMC (150 cells) showed significant colocalization of CD3 and pTyr on the cell surface (Figure 14B). 46% of the cells showed a high colocalization coefficient (above 0.65).

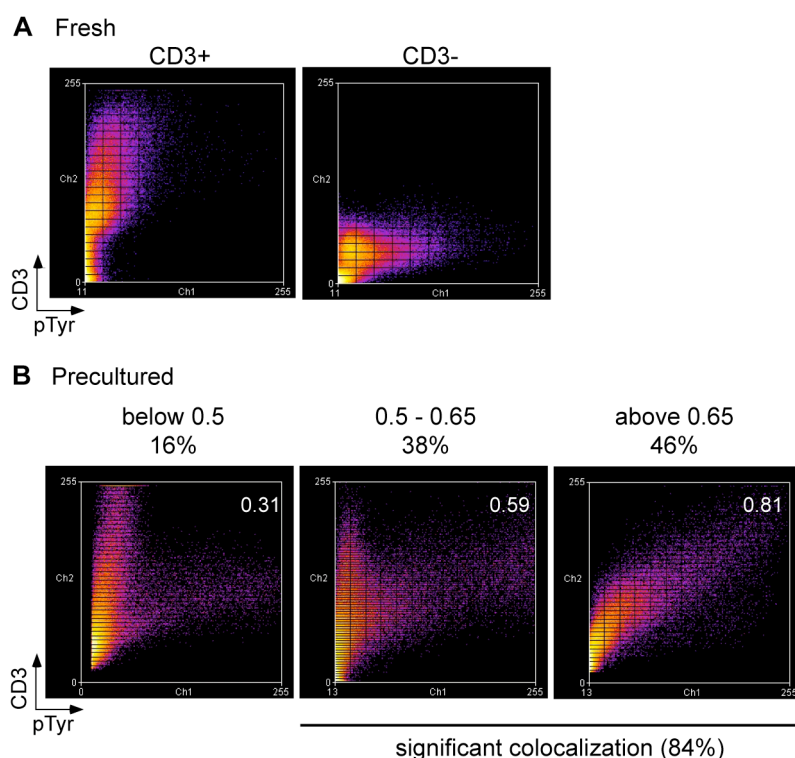


**Figure 14. Statistical analysis and colocalization coefficient of CD3 and pTyr in fresh and precultured PBMC.** Representative pseudocolored scatter plots from individual cells are shown. **A.** Representative CD3+ cell (left panel) of 150 analyzed. **B.** Representative examples and frequencies of T cells showing low, intermediate, or high CD3-pTyr colocalization values. Analysis performed by Dr. Elita Avota.

Western blots were performed to biochemically characterize fresh and precultured PBMC. As a primary antibody 4G10 was used, which is an anti-phosphotyrosine antibody. In high-density precultured cell lysates several phosphorylation events were detected. By this method it is not clear which ones belong to T cells. A band that presented consistent and strong phosphorylation in HDC cells and not in fresh PBMC presented a molecular weight of around 18 kD. The native form of CD3 has a molecular weight of 16-18 kD, but when it becomes phosphorylated it increases the molecular weight up to 21 kD. A control was performed using an  $\alpha$ CD3- $\zeta$  antibody (CD247), raised against amino acids 36-54 mapping within an N-terminal domain of CD3- $\zeta$  of human origin. This control showed the same level of CD3- $\zeta$  expression for both fresh and precultured cells, with a 17 kD band (not shown). In 7 independent experiments a band with a molecular weight higher than 17 kD appeared in precultured cells lysates, which was never present in fresh PBMC lysates (Figure 15). The observed band might correspond to the phosphorylated CD3- $\zeta$  chain, which when phosphorylated gives a typical molecular pattern with multiple bands ranging from 16-21 kD, representing the varying degrees of phosphorylation of the six cytoplasmic tyrosine residues

of the  $\zeta$  chain (Irving and Weiss 1991; van Oers 1999). The capacity of CD3- $\zeta$  to undergo multi-site tyrosine phosphorylation has been thought to constitute a molecular processor capable of translating the different types of TCR interactions into discrete phosphoforms and possibly distinct outcomes in the T cell response (Kersh, Shaw, and Allen 1998; Ardouin et al. 1999). Following this model, differential TCR signaling should depend on the integrity of the CD3- $\zeta$  ITAMs, therefore tonic signals through TCR-MHC interactions might give out a distinct pattern of tyrosine phosphorylation that makes T cells more sensitive to TCR activation. This observation was not further investigated, but it would be extremely interesting to study further the differences between fresh and precultured PBMC using biochemical tools.

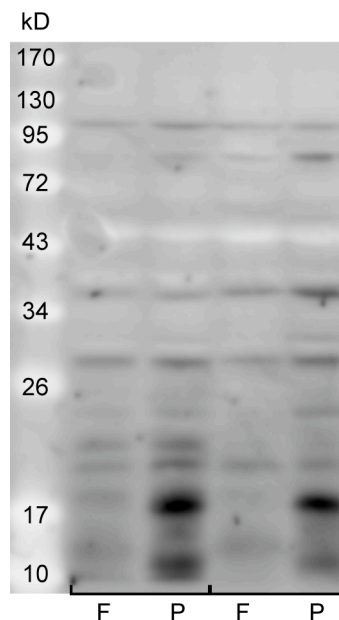


**Figure 15. Western blot of fresh and precultured PBMC lysates.** Fresh (F) and precultured (P) PBMC lysates from two different donors. Developed with 4G10 antibody (anti-pTyr). 15% polyacrylamide gel. Reducing conditions. One of 5 independent experiments is shown.

To determine whether the acquisition of TGN1412 reactivity depends on HLA scanning by the TCR, blocking mAb recognizing all HLA class I or class II molecules were added during the preculture. After 2 days the antibodies were washed out and the cells were stimulated with TGN1412 for 24 h. Figure 16A shows that intact antibodies efficiently prevented the acquisition of TGN1412 reactivity, as seen by decreased cytokine release. To avoid possible effects of the Fc portion of the blocking antibodies (negative signaling, FcR-mediated cytotoxicity) Fab fragments were generated. A strong reduction in the acquisition of TGN1412 reactivity was again observed (Figure 16B).

Since HLA recognition is important for sensitization of T cells to TGN1412, blockade of intracellular signaling proteins involved with the TCR complex during the high-density preculture should also have a negative effect. For this purpose, PP1 was used, which is an inhibitor of Src family kinases with selectivity for Lck. As expected, when PP1 was included during the subsequent stimulation assay there was a complete blockade of the response (Figure 17), since it is known that the CD28SA response depends on Lck (Bischof et al. 2000). Importantly, inclusion of PP1 during the 2-day high density preculture also strongly reduced the subsequent TGN1412 reactivity, while a brief pulse before harvest had no effect (wash out control; Figure 17).

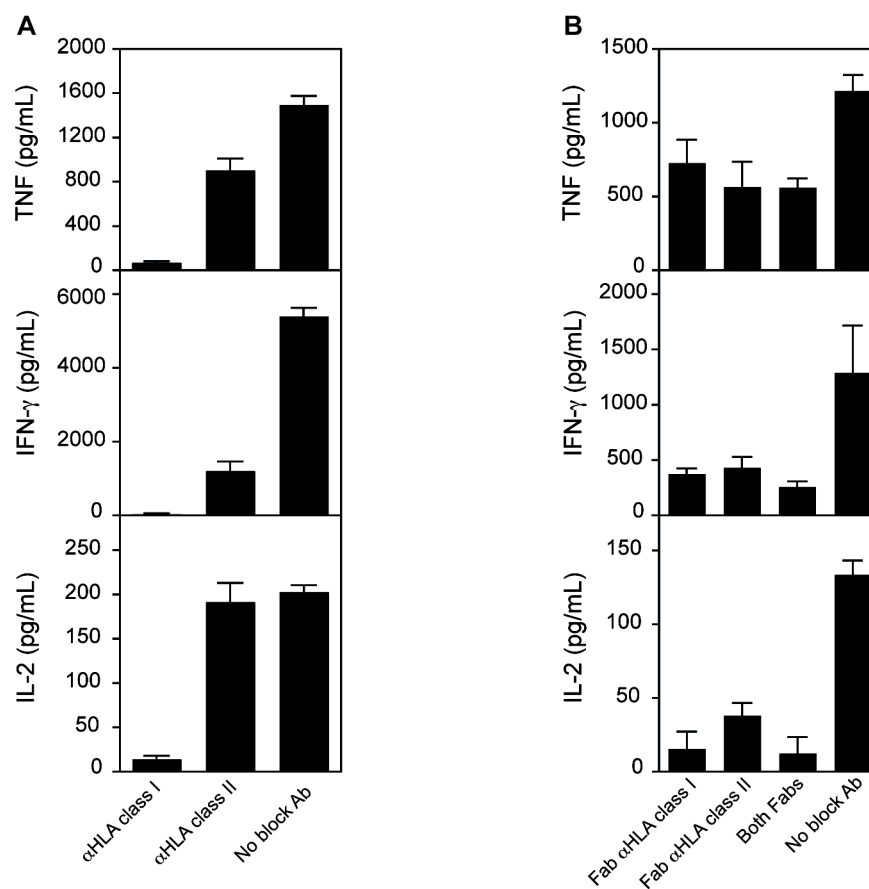


**Figure 16. Role of HLA recognition in TGN1412-reactivity acquisition during high-density preculture.**  $\alpha$ HLA class I clone W6/32 and  $\alpha$ HLA class II clone Tü39 antibodies were used either **A.** intact or **B.** as Fab fragments. Stimulation with 1  $\mu$ g/mL TGN1412 for 24h. Cytokines measured in cell culture supernatant by CBA. Two different donors are shown. Data are mean  $\pm$  SD of triplicate samples.

In the mouse lymphoid organs and other tissues, MHC scanning by T cells induces a basal activation level that allows subsequent responsiveness upon encounter with foreign antigens. This basal activation is provided by T-cell scanning of MHC molecules on the

surface of dendritic cells (Hochweller et al. 2010). In order to determine the cells involved in this process in the RESTORE protocol, distinct cell populations were depleted from human PBMC prior to preculture (Figure 18).

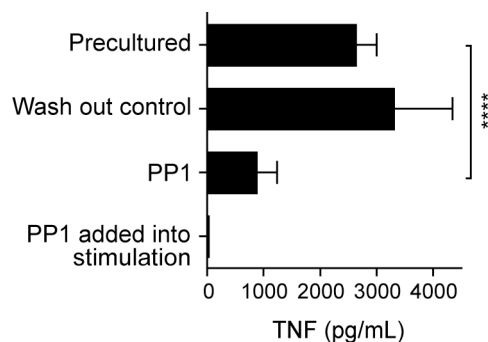


**Figure 17. LcK inhibitor PP1 affects acquisition of TGN1412 reactivity during preculture.** PP1 20  $\mu$ M added during preculture or into stimulation. Precultured PBMC stimulated with 1  $\mu$ g/mL TGN1412. TNF measured in cell culture supernatant by CBA. Two-way ANOVA:  $P < .0001$ . Data are mean  $\pm$  SD of triplicate samples.

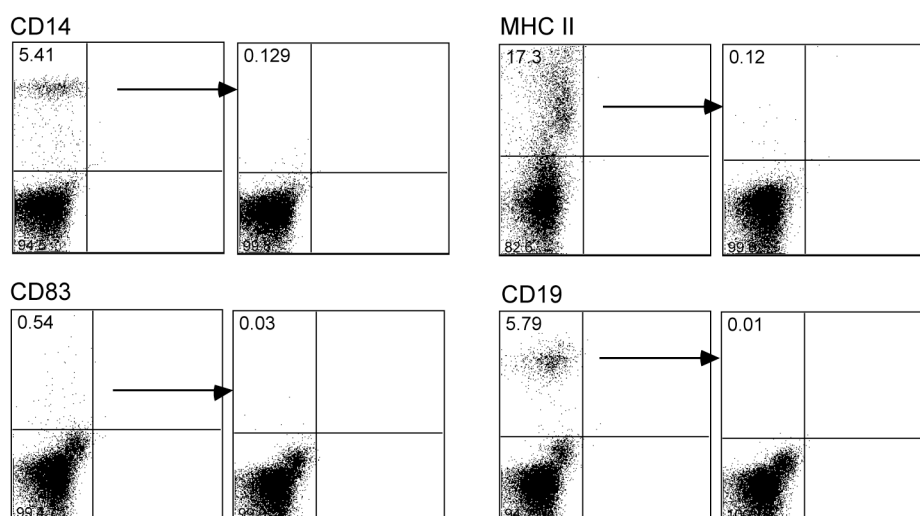


**Figure 18. Depletion of cell subsets from fresh human PBMC.** Dot plots showing cells before and after depletion. Depletion efficiency of CD14/CD19/CD83 simultaneously was 99%.

Reinstatement of T-cell reactivity by preculture depends on the presence of monocytes, the predominant APC in PBMC (Figure 19). The addition of 50% low-density precultured PBMC (not functionally mature, Figure 5) to the depleted group shows that the effect observed is due to lack of monocytes during the preculture supporting the idea of the need of T-cell–monocyte interactions for the restoration of T cell reactivity.

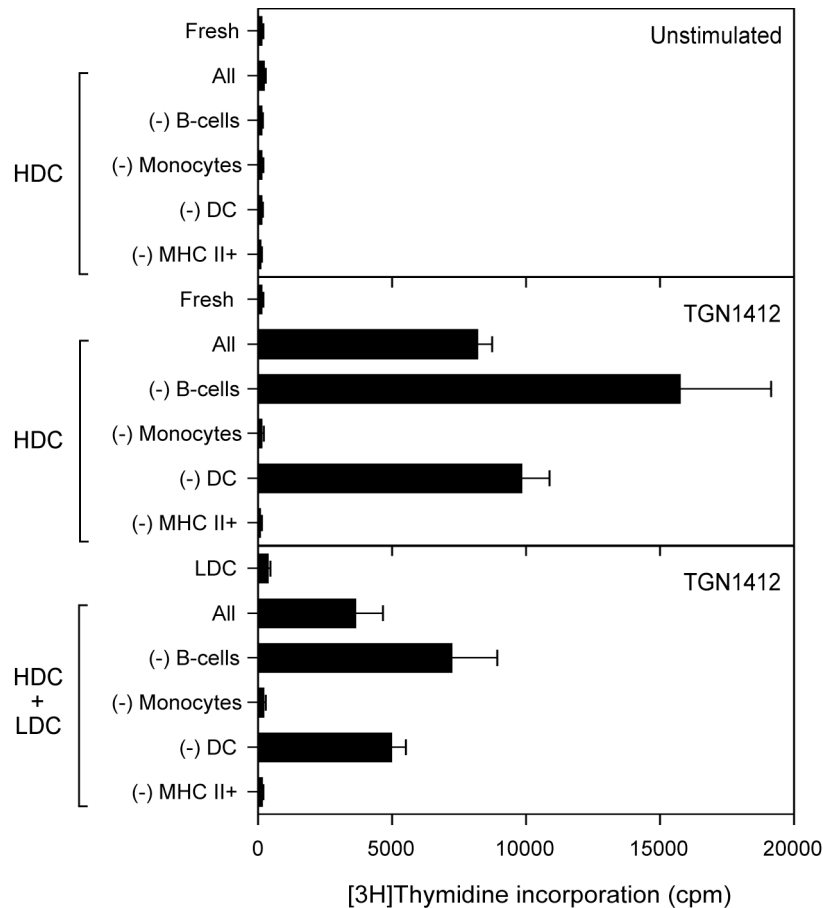


**Figure 19. Acquisition of TGN1412 reactivity requires the presence of monocytes during high-density preculture.** Before preculture at high cell density, PBMC were depleted from the cell subsets indicated with (-). The group "All" refers to undepleted PBMC. In the lower panel unseparated PBMC precultured at low cell density (LDC) were added as a source of the depleted subset at a 1:1 ratio during stimulation. HDC indicates high-density cell cultures; LDC, low-density cell cultures; DC, dendritic cells; and MHC II+ major histocompatibility complex class II-positive cells. Data are mean  $\pm$  SD of triplicate samples.

Mouse hyporesponsive T cells are able to quickly (30 min) regain their antigen sensitivity when co-cultured with DC (Hochweller et al. 2010). In contrast, in the RESTORE protocol, T cells take 2 days to regain tissue-like sensitivity (Figure 5). Since APC are involved in this process, the time requirement suggests that monocytes are not functionally mature, and therefore not able to provide T cells with the interactions needed to acquire a sensitive status.

To test if monocytes which had matured in high-density precultured PBMC would allow fresh T cells to respond, a 1:1 co-culture of fresh and HDC PBMC from the same donor was performed. Fresh cells were CFSE labeled in order to trace them back in the co-culture. The surface expression of CD69 after 16 h stimulation was used as readout, which provides information about early activation of T cells. Stimulation with either TGN1412 or OKT3 prompted the surface expression of CD69 on HDC cells when stimulated separately, but as

expected TGN1412 failed to do so on fresh PBMC (Figure 20). On the other hand, CD4<sup>+</sup> T cells from fresh PBMC in the presence of HDC PBMC (co-culture) expressed CD69, although to a lower extent than the HDC portion.

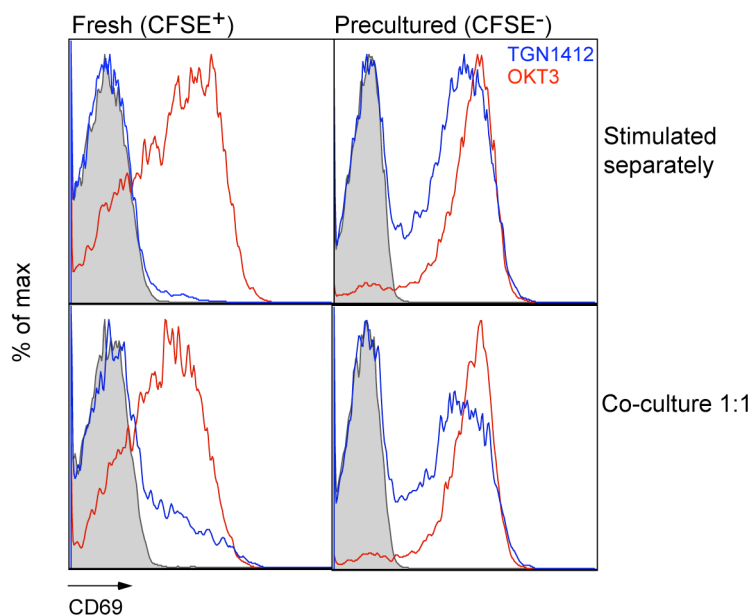


**Figure 20. CD69 expression by fresh PBMC in response to stimulation with soluble TGN1412 in the presence of HDC PBMC.** Fresh (CFSE labeled) and high-density precultured PBMC were stimulated for 16h at low density, either separately or in co-culture (1:1), with 1  $\mu$ g/mL TGN1412 (blue) or OKT3 (red). T cell activation was determined by CD69 surface staining, gated on CD4<sup>+</sup> T cells.

The kinetics of this response were studied in more detail. For this purpose, fresh and HDC PBMC were mixed 1:1 in high cell density and left for 0, 2 or 4 hours before dilution and addition of soluble TGN1412 (Figure 21). CD69 surface expression was assessed after 2 h of stimulation. The percentage of CD4<sup>+</sup> memory T cells from freshly isolated PBMC expressing CD69 in response to subsequent TGN1412 stimulation increased already after two hours of joint preculture. During the 4 h of high-density co-culture the percentage of responding fresh cells doubled from 5% to 10%, while responding precultured cells remained around 20%.

In conclusion, the presence of HDC cells allowed a percentage of fresh cells to get activated in response to TGN1412 stimulation. This suggests that the cellular environment in the 2-day high density precultured cells made the fresh CD4<sup>+</sup> memory T cells responsive, but to a lower extent than the CD4 memory cells from HDC (Figure 21).

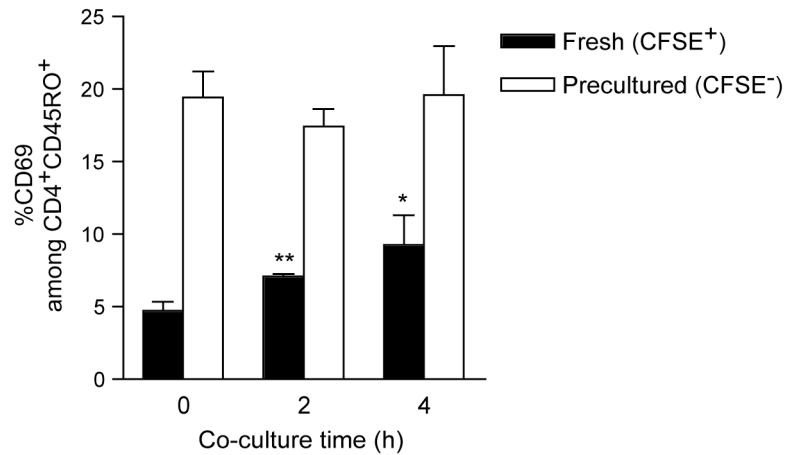


**Figure 21. Kinetics of CD69 expression by fresh PBMC in response to TGN1412 stimulation in a HDC co-culture.** Fresh CFSE-labeled PBMC were added to 2-day high-density precultured PBMC from the same donor and returned to high-density culture conditions for 0, 2, or 4 h before stimulation under standard conditions with 1  $\mu\text{g}/\text{mL}$  TGN1412 for 2 h. Activation status was assessed by CD69 surface. Results are shown as percentage of CD69<sup>+</sup> cells among the CD4<sup>+</sup>CD45RO<sup>+</sup> population. Unpaired t test: \* $P < .05$ , \*\* $P < .005$ . Data are mean  $\pm$  SD of triplicate samples.

Since monocytes are key players in the acquisition of TGN1412 reactivity in the RESTORE protocol, perhaps their functional status improves during the 2-day high-density culture of PBMC. Moreover, it is conceivable that such a maturation process again depends on interactions with the T-cells during HDC. To study this, monocytes were isolated from fresh PBMC and placed under high-density conditions, or were isolated from 2-day high-density PBMC cultures. These two sets of monocytes were titrated and mixed with fresh CD4<sup>+</sup> T cells from the same donor (Figure 22) in low cell density, and stimulated for 16 h. CD69 expression on fresh CD4<sup>+</sup> T cells was induced very efficiently in the presence of monocytes isolated from high-density PBMC cultures, and to a lesser extent by high-density cultured monocytes. The OKT3 response did not vary with the source of monocytes present. These results suggest that monocytes functionally mature under high-density conditions in the presence of lymphocytes. This maturation renders them more efficient “accessory cells” and allows them to provide the necessary pre-activation signals to T cells in order for them to enter the sensitive state, and therefore respond to TGN1412.

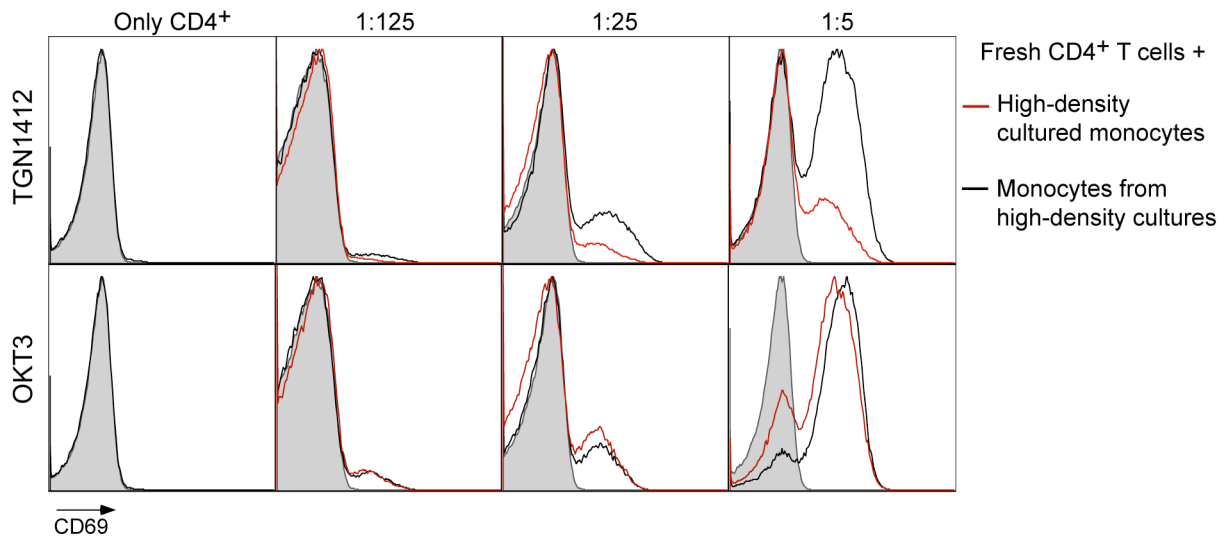


**Figure 22. Fresh CD4<sup>+</sup> T cells acquire TGN1412 reactivity in the presence of monocytes derived from high-density PBMC cultures.** Purified CD4<sup>+</sup> T cells ( $5 \times 10^5/0.5$  mL) were cocultured in 48-well plates at the ratios given with monocytes derived from high-density PBMC cultures, or with monocytes isolated from fresh PBMC and cultured for 2 days under high-density conditions. Stimulation with TGN1412 or OKT3 ( $1 \mu\text{g/mL}$ ) for 16 h. Activation status of CD4<sup>+</sup> cells was assessed by CD69 surface expression. Gray histograms represent unstimulated cells. Gated on CD4<sup>+</sup> T cells. Data are mean  $\pm$  SD of triplicate samples.

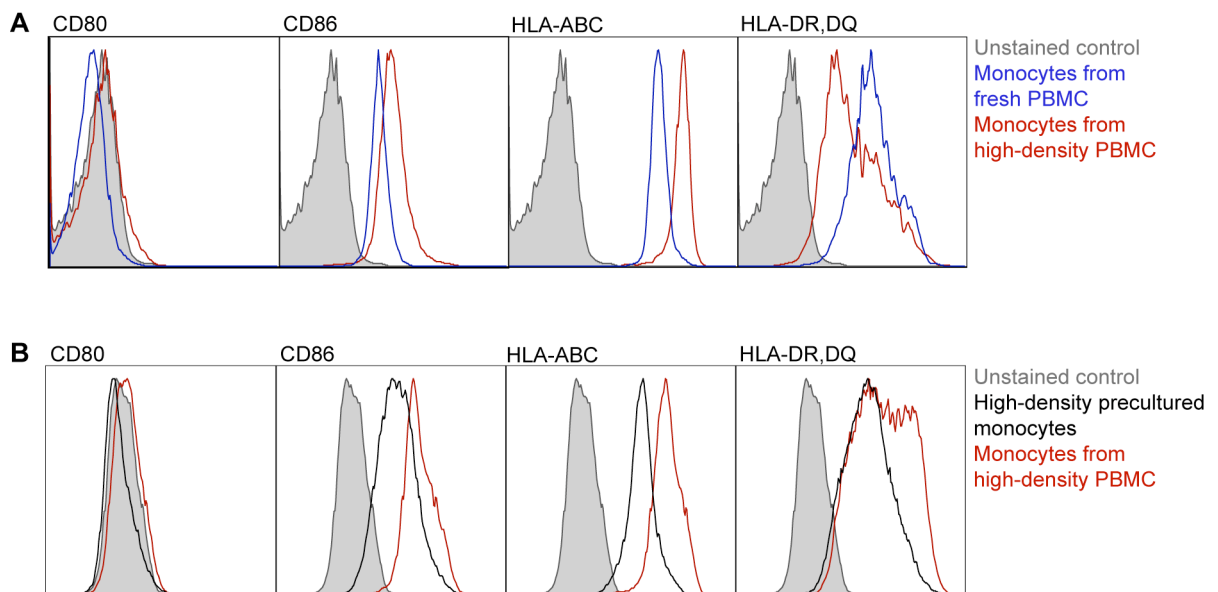


**Figure 23. Monocyte phenotype in fresh and precultured PBMC.** **A.** Monocyte phenotype from fresh and precultured PBMC, and **B.** phenotype of 2-day high-density precultured monocytes compared to monocytes within intact 2-day high density precultured PBMC. Gated on CD14<sup>+</sup> T cells. Two different donors are shown in A and B.

When cells mature they express or down regulate surface molecules that allow them to perform their functions. To identify a possible correlation between certain key surface markers and the monocyte function, surface stainings were performed for CD80, CD86, HLA-ABC (MHC class I), HLA-DR,DQ (MHC class II) (Figure 23). Characterized monocytes were

from freshly isolated PBMC, high-density PBMC, or isolated monocytes kept 2 days under high-density conditions. Monocytes within high-density precultured PBMC had up-regulated MHC class I and CD86, compared to monocytes in freshly isolated cells (Figure 23A). MHC class II expression was lower on monocytes from HDC than on fresh monocytes (Figure 23A). No major differences were observed for CD80. The up-regulation of surface markers depended on the presence of lymphocytes, since isolated monocytes cultured in high cell density for 2 days showed a similar phenotype to fresh monocytes (Figure 23B). These findings support the hypothesis of cell-cell interactions between different cell types during high-density PBMC culture.

#### **4.6. Human lymph node T cell response to TGN1412**

The toxic cytokine response elicited by TGN1412 during the clinical trial is most likely to have been by tissue resident CD4<sup>+</sup> effector memory T cells (Figure 9). These cells no longer routinely enter the lymph nodes but remain mainly in non-lymphoid tissues (Bevan 2011; Sallusto, Geginat, and Lanzavecchia 2004).

In rodent models it has been shown that tissue-resident memory T cells, as well as lymph node cells present a state of heightened antigen reactivity (Kassiotis et al. 2002; Stefanova, Dorfman, and Germain 2002). This pre-activation status of mouse lymph node cells can be lost both by experimental and physiological interruption of T-cell contact with self-peptide MHC ligands, leading to a rapid decline in signalling and response sensitivity to foreign antigens (Stefanova, Dorfman, and Germain 2002).

To study the responsiveness of human tissue cells *ex vivo*, lymph node samples obtained from the pancreas of non-diabetic brain-dead multi-organ donors received at the Islet Isolation Facility of the San Raffaele Hospital, Milan, Italy, were stimulated with 1 µg/mL TGN1412 (Dr. Manuela Battaglia). In Figure 24 single cell suspensions were either kept on ice or at 37°C for 1 h in order to interrupt cell-cell contacts. There was a small but significant proliferative response to TGN1412, which was diminished to approximately half after being kept in suspension at 37°C. This result supports the concept that tissue-resident T cells, particularly LN cells, present a pre-activation state, which allows them to proliferate after TGN1412 stimulation. Importantly, the sensitive state can be lost by suspension culture, namely interruption of cellular interactions.

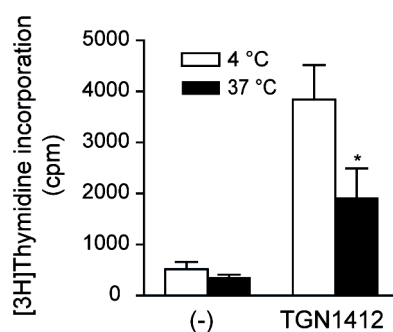


**Figure 24. Human lymph node cells lose TGN1412 reactivity by suspension culture.** Human lymph node (LN) cells were kept on ice or at 37°C (5% CO<sub>2</sub>) for 1 h in suspension (1x10<sup>6</sup> cell/mL), and the proliferative response to TGN1412 (1 µg/mL) was assessed. One of two individual experiments with similar results is shown. Two-way ANOVA: \**P*<.05. Data are mean ± SD of triplicate samples. Data are mean ± SD of triplicate samples. Experiment performed by Dr. Manuela Battaglia.

Memory T cells from circulating PBMC are the cell subset that responds to TGN1412 stimulation *in vitro* after 2-day high-density preculture (Figure 8 and Figure 10). To identify the proliferating cell subset in human LN samples (obtained from the para-iliac region of renal transplant recipients at the Academic Medical Center, Amsterdam, Netherlands; Ineke ten Berge) cells were stained after TGN1412 stimulation with surface markers and the nuclear proliferation marker Ki67 (Figure 25). In accordance to the high-density precultured PBMC results, the main subset proliferating to TGN1412 stimulation were the CD4<sup>+</sup>CD45RO<sup>+</sup> T cells. Again, this sensitive state can be lost by keeping LN cells in suspension, as seen by the reduction of responding cells to 39% after 2h, and 27% after 4h. Of note, keeping LN cells at high-cell density did not improve their reactivity (not shown). Fresh PBMC obtained from the same donor failed to respond to TGN1412 stimulation (Figure 25), in keeping with results shown previously (Figure 4). Taken together, these results support the notion that CD4 memory T cells depend on cell interactions given within tissues to maintain responsiveness to TGN1412.

#### 4.1. Pharmacologic inhibition of the precultured-T-cells response

The RESTORE protocol represents a robust methodology that allows asking questions about the response to soluble TGN1412. Corticosteroid treatment is known to control the cytokine-release-syndrome (CRS) generated by certain drugs, such as OKT3 (Goldman et al. 1989). Perhaps the CRS generated by TGN1412 could also be controlled that way. The cytokine release elicited both by TGN1412 and OKT3 on HDC PBMC was suppressed by Dexamethasone (Dex) with comparable efficiency (Figure 26). Methylprednisolone showed similar results (not shown).

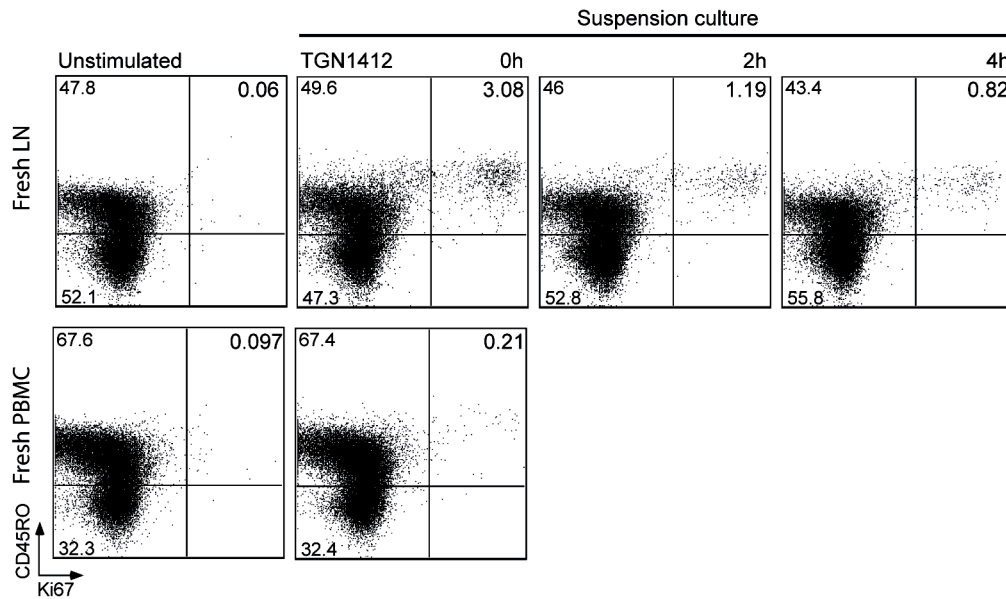


**Figure 25. Human LN cells are reactive to TGN1412 in contrast to PBMC, a state which is lost by suspension culture.** Fresh LN cells were placed in suspension in low cell density ( $1 \times 10^6$  cell/mL), and either stimulated immediately with  $1 \mu\text{g}/\text{mL}$  TGN1412 or kept in suspension culture at  $37^\circ\text{C}$ ,  $5\% \text{CO}_2$ , for 2 or 4 h (top panel). A PBMC sample from the same donor was analyzed in parallel (bottom panel). Cell proliferation was determined after 4 days of stimulation by Ki67 staining. Gated on  $\text{CD4}^+$  cells. One of two individual experiments with similar results is shown.

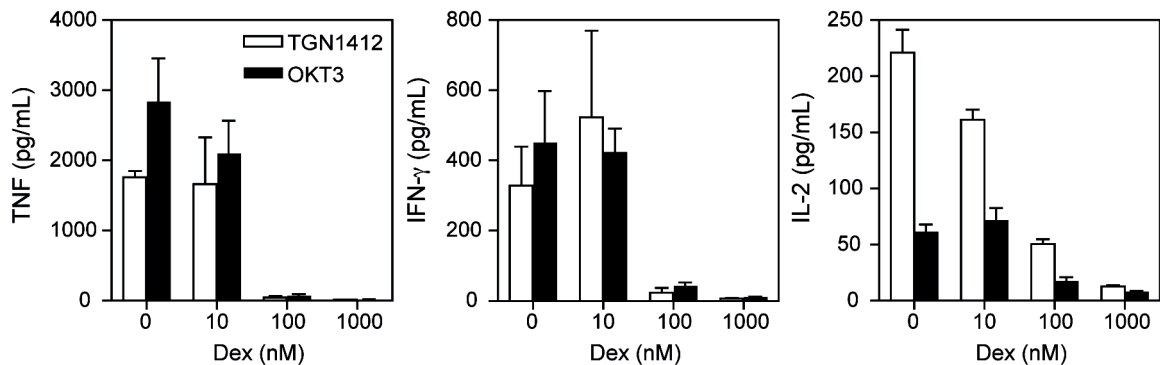


**Figure 26. Corticosteroid suppression of TGN1412-induced cytokine release from precultured PBMC is of comparable efficacy as found with OKT3.** HDC PBMC were stimulated with  $1 \mu\text{g}/\text{mL}$  TGN1412 or OKT3, dexamethasone (Dex) was added at the final concentrations shown. Cytokine release was measured in cell culture supernatants by CBA. Data are mean  $\pm$  SD of triplicate samples.

The fact that preculturing PBMC at high density renders T cells reactive to TGN1412 suggests that the in vitro response to other substances involving the TCR could also become more sensitive. The OKT3 response is of equal magnitude for both fresh and precultured PBMC (Figure 3, Figure 4). The likely explanation for this is that because this high-affinity ligand addresses the TCR complex directly, the need for a pre-primed TCR machinery is

overcome. Nevertheless, it has been shown in mice that “tonic” TCR signals improve signaling intensity to cognate TCR ligands (Stefanova, Dorfman, and Germain 2002). Therefore, for example, signal transduction in fresh PBMC might be less sensitive to pharmacological inhibition than in HDC PBMC. To test this, OKT3 was used in a sub-optimal concentration (0.01  $\mu\text{g}/\text{mL}$ ), and as an inhibitor titrated amounts of the Lck inhibitor PP1, which blocks at the early steps of the TCR signal transduction cascade. High-density precultured PBMC were in fact less sensitive to PP1 inhibition than fresh PBMC (Figure 27).

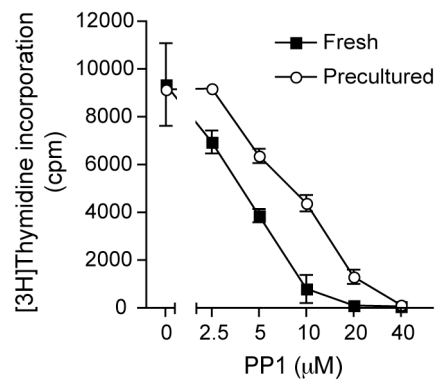


**Figure 27. OKT3-stimulated HDC PBMC are less sensitive to PP1 inhibition than fresh PBMC.** Proliferation of fresh and precultured PBMC stimulated with a suboptimal concentration of OKT3 (0.01  $\mu\text{g}/\text{mL}$ ) in the presence of titrated amounts of PP1. Data are mean  $\pm$  SD of triplicate samples.

An immunosuppressive drug widely used in organ transplantation to prevent rejection is the fungus metabolite cyclosporine A (CsA) (Borel et al. 1994). It is a cyclic nonribosomal peptide of 11 aminoacids that acts exclusively on T cells (Kaminski 2008). It binds to cyclophilin A forming a complex which inhibits TCR-induced calcineurin activity, therefore preventing the dephosphorylation of NFAT and transcription of cytokines such as IL-2 (Schreiber and Crabtree 1992; Koenen et al. 2003). It therefore acts on a signaling molecule downstream of the TCR. This undecapeptide was tested for its ability to inhibit OKT3-induced T cell proliferation of fresh and precultured cells (Figure 28). Both responses were comparable, although a small but statistically significant difference was detected for a higher CsA concentration (125 ng/mL).

Taken together, these results suggest that the use of fresh PBMC for in vitro testing of T-cell directed immunosuppressive substances might, in some cases, be misleading, because circulating T cells are in a non-primed state making them functionally disabled.

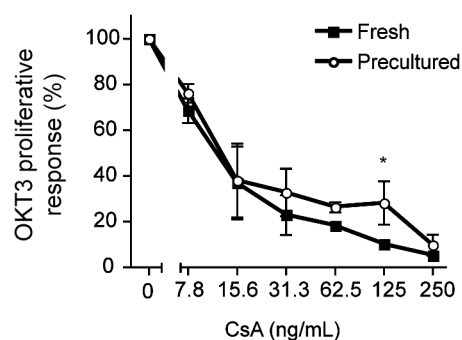


**Figure 28. Cyclosporine A inhibition of the fresh and precultured PBMC response to OKT3.** Proliferation of fresh and precultured PBMC stimulated with a suboptimal concentration of OKT3 (0.01  $\mu\text{g/mL}$ ) in the presence of titrated amounts of CsA was measured. Results shown as percentage of maximum OKT3 response. Paired t test for 125 ng/mL (\* $P < .05$ ) Data are mean  $\pm$  SD of triplicate samples.

#### 4.2. Response to T-cell mitogens

Mitogens are substances that induce a cascade of biochemical events leading to mitosis (Lichtman, Segel, and Lichtman 1983). Widely used mitogens are lectins, which are proteins that specifically bind to membrane glycoproteins of cells. They act as mitogens by crosslinking cell surface receptors (Sharon and Lis 1972; Andersson, Sjöberg, and Möller 1972). Concanavalin A (ConA) is a plant lectin from jack bean capable of binding non-covalently to carbohydrate groups (mannose) located on the surface of T and B lymphocytes, although it selectively activates T cells by promoting an increase in the rate of calcium entry into the cell, resulting in DNA synthesis and cellular proliferation (McCole et al. 1998). Phytohemagglutinin (PHA) is a lectin found in plants, especially legumes, and it induces T-cell proliferation and activation in the same manner as ConA does (Lichtman, Segel, and Lichtman 1983).

Cell proliferation induced by PHA or ConA was greater after the cells were precultured in high density (Figure 29). Even though the results varied greatly (see SD), the difference between fresh and precultured PBMC proliferation was statistically significant. Together, these results suggest that the RESTORE protocol improves the mitogenic T-cell response to lectins.

The CD2 molecule is a surface glycoprotein expressed on virtually all T cells, thymocytes and NK cells (Wang et al. 1999). It binds to LFA-3 (CD58) expressed on APC, promoting intercellular adhesion. This adhesion occurs at the initial stages of cell contacts between T cells and APC before T cell activation, when T cells are roaming the lymph nodes looking at the surface of APCs for cognate peptide:MHC complexes (Wang et al. 1999). LFA-

3 together with anti-CD2 mAbs have a co-stimulatory function in activation of T cells (Hünig et al. 1987). By the use of mAbs that bind the CD2 molecule, it has been found that combinations of mAbs directed to appropriate epitopes of the molecule causes T-cell activation (Moretta et al. 1989; Tiefenthaler and Hunig 1989; Meuer et al. 1984). Since CD2 stimulation depends on the TCR it was therefore hypothesized that precultured T cells might be more sensitive to  $\alpha$ CD2 mAb stimulation. To elucidate this question, a stimulation of fresh and precultured PBMC was performed with an  $\alpha$ CD2 antibody combination (M1, M2 and 3PT). Figure 30 shows that cells that have been made reactive by the RESTORE protocol are more sensitive to  $\alpha$ CD2 antibody stimulation than circulating cells (fresh), shown by increased TNF release.

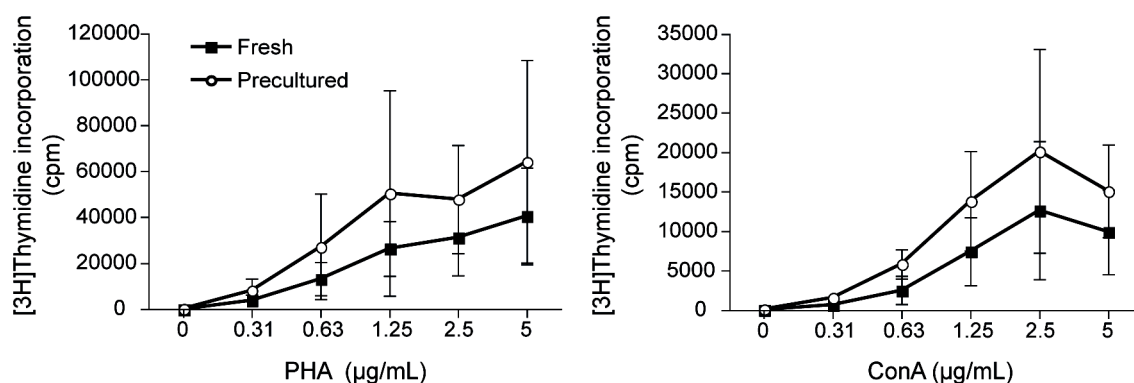


**Figure 29. Mitogenic capacity of PHA and ConA on fresh and precultured PBMC.** Difference between fresh and precultured curves is statistically significant for both PHA and ConA as determined by a Wilcoxon signed rank test ( $P < .05$ ). Data are mean  $\pm$  SD of 5 individual donors for PHA and 4 for ConA.

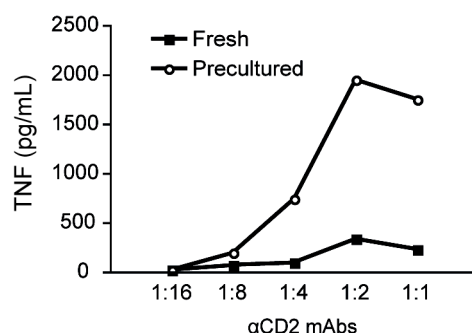


**Figure 30. TNF release upon  $\alpha$ CD2 mAbs stimulation of fresh and precultured PBMC.** mAbs M1, M2 (1  $\mu$ g/mL) and 3PT (0.33  $\mu$ g/mL). Data represents TNF concentration on pooled triplicates of cell culture stimulation supernatants.

### 4.3. Response of precultured PBMC to bacterial antigens

Stimulation of circulating PBMC is widely used to routinely test for recall responses to antigens and to identify antigen-specific memory T cells. However, mouse TCR-transgenic CD4 T cells isolated from lymphoid tissues lose sensitivity to their cognate antigen when kept in suspension, resembling what happens when cells go into the circulation (Stefanova, Dorfman, and Germain 2002). By resetting circulating PBMC to tissue-like conditions with the RESTORE protocol the in vitro response to recall antigens could presumably be improved.

Tetanus/diphtheria toxoid (Td) is a common vaccine that is recommended in most countries, such as the United States and Germany, to be applied to children under a year of age (ACIP 2012; Kroger et al. 2011; STIKO 2011). This vaccine generates memory cells that can give a protective recall response when exposed to the infection or upon in vitro stimulation. Proliferative Td recall response was greatly enhanced by high-density preculture of PBMC (Figure 31).

Pathogenic microbes such as viruses, mycoplasma and bacteria, can produce another kind of antigens or exotoxins called superantigens, which cause excessive and aberrant non-specific T cell activation and can activate up to 20% of the T-cell compartment in vivo, provoking a massive cytokine release, and causing a broad range of health problems. The best characterized are the staphylococcal enterotoxins (SEA, SEB, etc.) and the streptococcal pyrogenic exotoxins that trigger the staphylococcal and streptococcal toxic shock syndromes (Llewelyn and Cohen 2002). When SEB was tested for its mitogenic activity on fresh and precultured PBMC, the latter showed to have increased sensitivity to the superantigen stimulation (Figure 32).

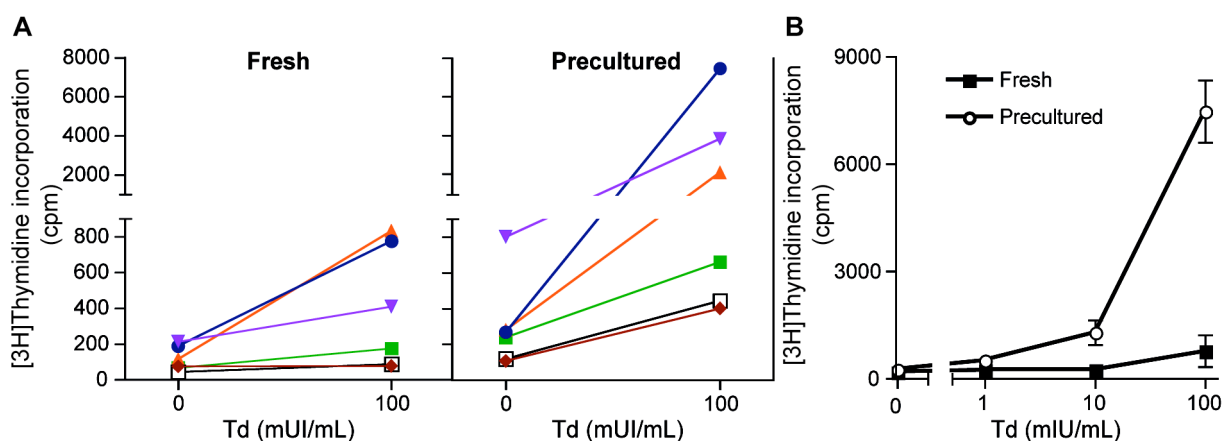


**Figure 31. Proliferative response to Td of fresh and precultured PBMC. A.** Compilation of tetanus/diphtheria toxoid (Td) recall responses of 6 random healthy donors. **B.** Dose response to Td of the stronger responder shown in A (blue line). The difference between fresh and precultured paired values was statistically significant as determined by a Wilcoxon signed rank test ( $P < .05$ ). Data represents mean  $\pm$  SD of triplicate samples.

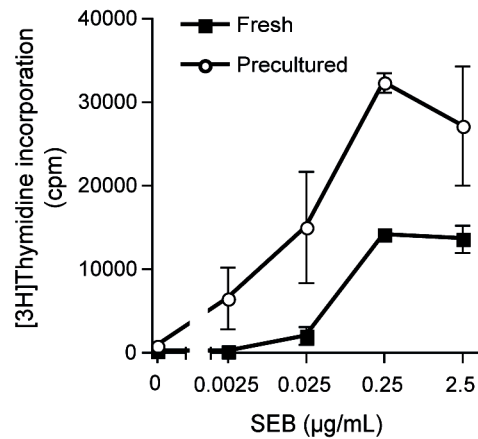


**Figure 32. Proliferative response to SEB of fresh and precultured PBMC.** Data represents mean  $\pm$  SD of triplicate samples.

#### 4.4. Role of the Fc portion of CD28 superagonists on T- cell stimulation

TGN1412 is an IgG4 antibody, i.e. of the isotype for which FcR have lower affinity than for other isotypes, such as IgG1 (Presta and Namenuk 2005). FcR ligation improves the activation capacity of some antibodies like OKT3. Despite this fact, TGN1412 is very active both in vivo and in high-density precultured PBMC. Based on the experience with OKT3, the hypothesis arose that TGN1112, an IgG1 version of TGN1412, should be even more active than the IgG4 counterpart. However, when mitogenic activity was tested on precultured PBMC, TGN1412 showed to be much more active than TGN1112 (Figure 33).

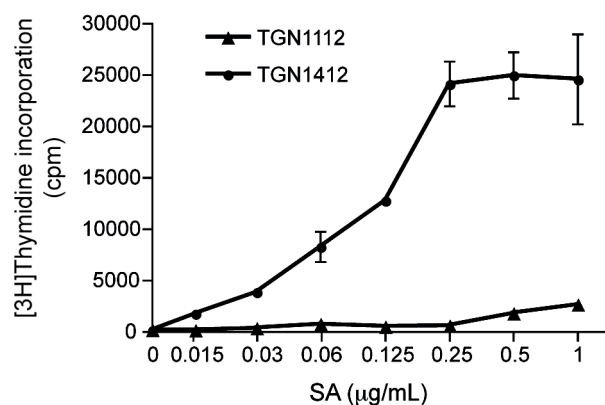


**Figure 33. Mitogenic activity of TGN1412 and TGN1112 on HDC PBMC.** Proliferation of precultured PBMC stimulated with titrated amounts of the superagonists (SA) TGN1112 and TGN1412. Data are mean  $\pm$  SD of triplicate samples.

The difference in the antibody shape between TGN1112 and TGN1412 (IgG1 and IgG4) (Aalberse and Schuurman 2002) might cause steric interferences which might influence their binding and therefore their activation capacity. Ligation of the Fc portion by FcR on other cells might also have an effect on the stimulatory activity. Therefore Fab and Fab2 fragments from TGN1112 and TGN1412 were generated. Surprisingly, Fab2 fragments of both TGN1112 and TGN1412 had a mitogenic effect on HDC PBMC (Figure 34). The monomeric Fab fragments did not induce proliferation, which is most likely due to the fact that the CD28 superagonists need to crosslink two CD28 molecules in order to activate T cells.

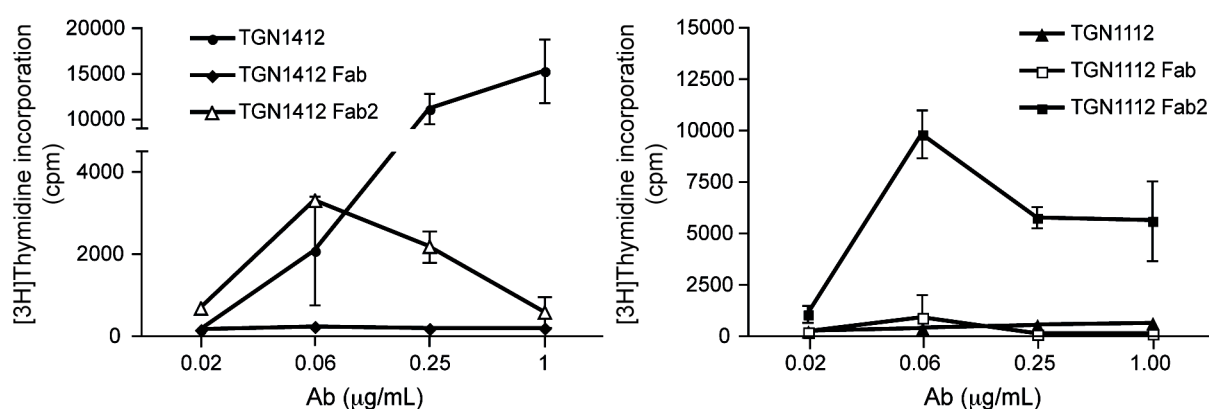


**Figure 34. Mitogenic activity of intact, Fab and Fab2 fragments from TGN1112 and TGN1412 antibodies on precultured PBMC.** Proliferation of precultured PBMC stimulated with titrated amounts of TGN1112, TGN1412 and their Fab and Fab2 fragments. Data are mean  $\pm$  SD of triplicate samples.

A finer titration was performed for intact and Fab2 TGN1112 and TGN1412 on precultured PBMC (Figure 35). Donor dependent variability was observed, but the tendency remained. Both Fab2 fragments presented a concentration-dependent mitogenic activity, while intact TGN1112 did not induce cell proliferation. Of note, the stimulatory effect of intact TGN1412 reached saturation at the highest concentrations, while the Fab2 presented a bell-shaped response. This type of response is explained by a phenomenon termed the Heidelberger-Kendall curve (Heidelberger and Kendall 1929), which will be discussed later.

Fab2 fragments also showed to have the capacity to induce cytokine release on precultured PBMC, as shown in Figure 36 by TNF release. In accordance to the proliferation data, cytokine release response was stronger with TGN1112 Fab2 than with TGN1412 Fab2. Intact TGN1112 antibody does not induce TNF release. This goes to show that TGN1112 is more active without the Fc portion, i.e. as a Fab2 fragment.

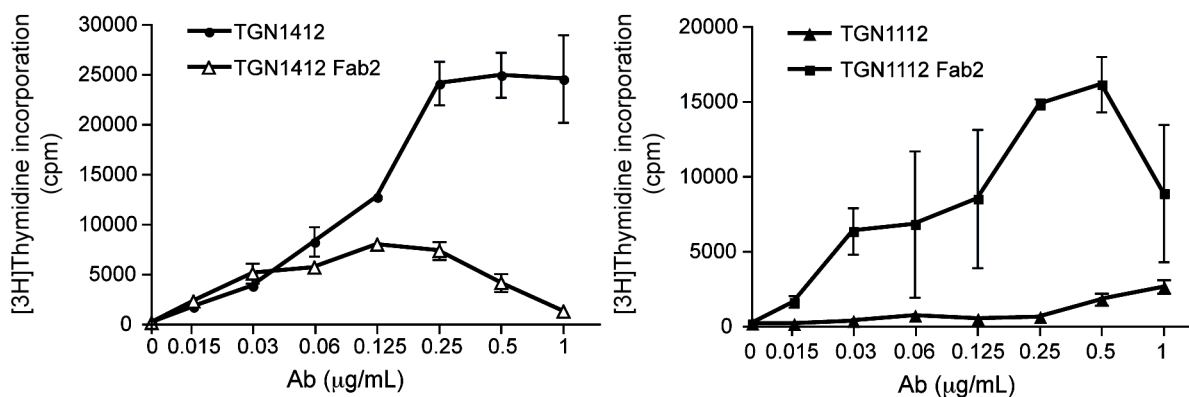


**Figure 35. Mitogenic activity of intact and Fab2 fragments from TGN1112 and TGN1412 antibodies on precultured PBMC.** Proliferation of precultured PBMC stimulated with a fine titration of TGN1112, TGN1412 and their Fab and Fab2 fragments. Data are mean  $\pm$  SD of triplicate samples.

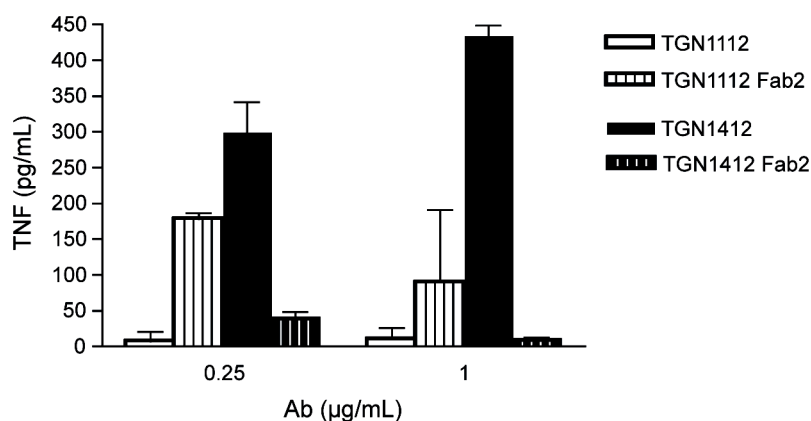


**Figure 36. TNF release by precultured PBMC in response to intact and Fab2 TGN1112 and TGN1412.** TNF release measured by CBA in cell culture supernatants after 24h stimulation. Data are mean  $\pm$  SD of three different blood donors for intact Ab, and of two donors for Fab2.

It is intriguing that TGN1112 does not have stimulatory capacity as its IgG4 counterpart (TGN1412), but it does when the Fc portion is removed. Binding affinity or binding dynamics of the antibodies could influence their stimulatory capacity. Therefore the binding kinetics of intact, Fab and Fab2 fragments of TGN1112 and TGN1412 were compared. First, binding kinetics of TGN1412-FITC was studied at two different temperatures, 4°C and 37°C for fresh and precultured PBMC. In Figure 37 binding of TGN1412-FITC at a suboptimal concentration (0.3 µg/mL) on fresh and precultured PBMC is shown. As expected, TGN1412 binds faster at 37°C than at 4°C, since Ab-Ag interactions are increased at physiological temperature, i.e. by faster movement of the antibodies and of the cells. Based on these results, all subsequent binding assays were performed at 37°C. It can also be seen that binding of TGN1412 reaches saturation after 4 hours of incubation at 37°C. There is no difference in binding kinetics between fresh and precultured cells.

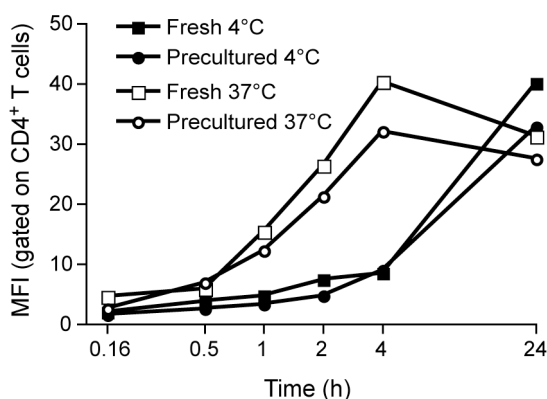


**Figure 37. TGN1412 binding kinetics on fresh and precultured PBMC at 4°C and 37°C.** Fresh and precultured PBMC were stained with 0.3  $\mu\text{g}/\text{mL}$  TGN1412-FITC for the timepoints indicated.

To study the binding kinetics in more detail,  $\text{CD4}^+$  T cells were isolated from freshly obtained PBMC. The experiment was performed in RPMI + 10% FCS. PBMC were placed in the incubator at 37°C, 5%  $\text{CO}_2$ , in the presence or absence of the intact antibodies, Fab or Fab2 fragments, of TGN1112 or TGN1412 for different time points, harvested, washed, and stained with a fluorochrome-conjugated monoclonal antibody directed against the human kappa light chain (Figure 40). This secondary antibody allows proper comparison of the amount of intact antibodies as well as single Fab and Fab2 fragments bound to the cell surface.

It is important to keep in mind that CD28 superagonists bind exclusively to the laterally exposed C'D loop of the extracellular immunoglobulin-like domains of CD28, in contrast to conventional anti-CD28 antibodies, which recognize an epitope close to the binding site for binding to the natural ligands CD80/CD86 (Luhder et al. 2003). Monomeric Fab fragments of TGN1412 and TGN1112 (Figure 38 and Figure 40) achieved binding equilibrium already after 10 minutes of incubation, and saturation was reached at 1  $\mu\text{g}/\text{mL}$  (Figure 38A). The amount of CD28 surface expression remained constant in time. A schematic representation of the possible binding behavior of the Fab fragments is shown in Figure 38B, under saturating concentrations and when binding equilibrium is reached.

Antibodies have two antigen binding sites, so they can potentially bind bivalently to antigens. The lateral binding mode of CD28 superagonists suggests crosslinking of CD28 dimers on the cell surface (Evans et al. 2005). Figure 39 supports the notion that TGN1412 binds bivalently, but this process takes time. During the first 2h of incubation antibodies bind with one arm to CD28, when in excess (Figure 39B). Binding equilibrium is reached after 4 hours of incubation and it is maintained for at least 20 hours (Figure 39C). Of note, the MFI

after 10 minutes is double the value than after 4h with saturating antibody amounts (4  $\mu\text{g}/\text{mL}$ ), which supports the hypothesis of a transition from monovalent to bivalent binding of CD28SA. Binding stability is much higher with bivalent binding, since the interaction of the antigen binding site with their ligand is not a static phenomenon, it opens and closes, so the chance that at least one arm of the antibody is bound is much higher. This translates in higher avidity (in orders of magnitude) of the antibody.

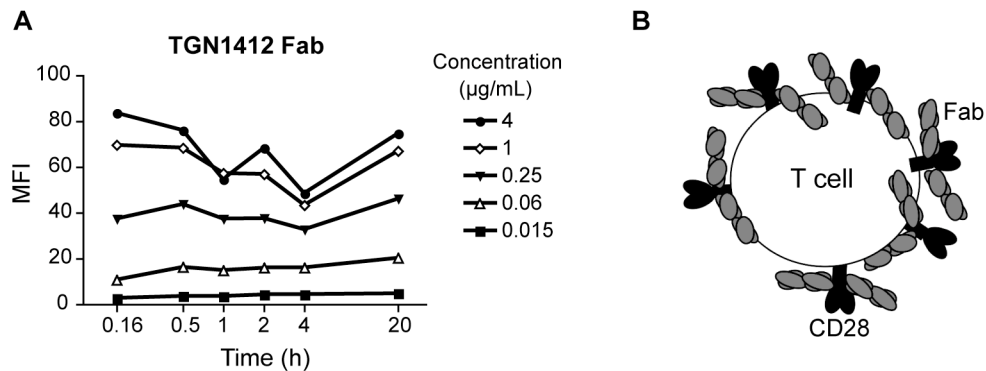


**Figure 38. TGN1412 Fab fragment binding kinetics on isolated  $\text{CD4}^+$  T cells.** **A.** MFI of TGN1412 Fab on isolated  $\text{CD4}^+$  T cells from fresh PBMC. **B.** Schematic representation of TGN1412 Fab fragment binding to CD28 on T cells in saturation when binding equilibrium is reached.

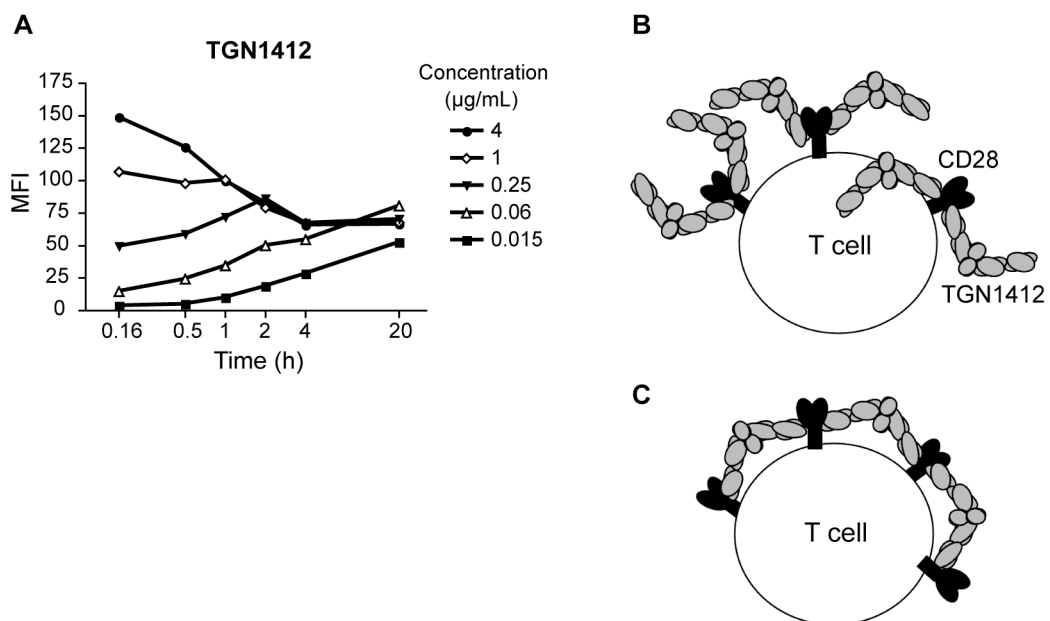


**Figure 39. Intact TGN1412 antibody binding kinetics on isolated  $\text{CD4}^+$  T cells.** **A.** MFI of TGN1412 Fab on isolated  $\text{CD4}^+$  T cells from fresh PBMC. **B.** Schematic representation of TGN1412 binding above saturation to CD28 on T cells after short incubation, and **C.** when binding equilibrium is reached.

Importantly, the binding kinetics of TGN1412, TGN1112 and their Fab2 fragments is nearly identical (Figure 40), so the difference in the stimulatory capacity of these two antibodies must have a different explanation.

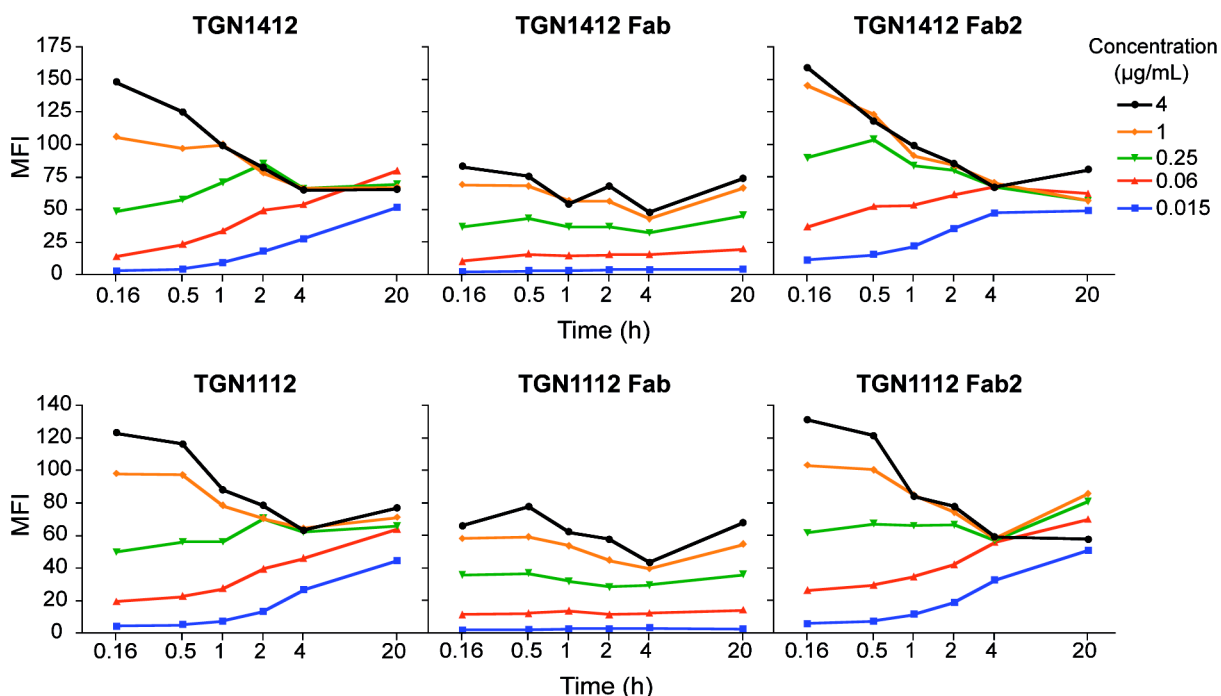


**Figure 40. TGN1112 and TGN1412 intact antibodies, Fab and Fab2 fragments binding kinetics on isolated CD4<sup>+</sup> T cells.** MFI of TGN1112, TGN1412 and their Fab and Fab2 fragments on isolated CD4<sup>+</sup> T cells from fresh PBMC over time.

There does not seem to be any steric interference with binding due to the antibody shape or by the Fc portion. Nevertheless, intact TGN1112 does not activate T cells, but the Fab2 fragment does, so the Fc portion seems to play a role. To determine if the binding kinetics differs in any way in the presence of other Fc expressing cells the experiment shown in Figure 40 was repeated but with freshly isolated intact PBMC (Figure 41), with surprising results. First of all, Fab and Fab2 fragments bind in the same way to CD4<sup>+</sup> T cells in intact PBMC as to isolated CD4<sup>+</sup> T cells. In contrast, T cells incubated with intact antibodies seem to lose surface expression of CD28, especially in the case of TGN1112. Binding equilibrium is reached after around 4h of incubation (Figure 39C), but drops dramatically after 18h.

A plausible explanation for this phenomenon is that the antibody is being ripped-off from the T-cell surface by other cells through Fc-FcR interactions, especially TGN1112 being an IgG1, in which the Fc part is more available than IgG4, and has a higher binding affinity. It has been reported that CTLA-4 can capture its ligands from opposing cells by a process called trans-endocytosis (Qureshi et al. 2011); such a process could also help explain the CD28 + TGN1112 disappearance from the cell surface.

Since Fc receptor affinity is lower for TGN1412, CD28 might be being “less” ripped off from the surface, or perhaps this is due to the fact that the Fc portion of TGN1112 is more available than TGN1412, hence difficult to reach by FcR bearing cells (Aalberse and Schuurman 2002).

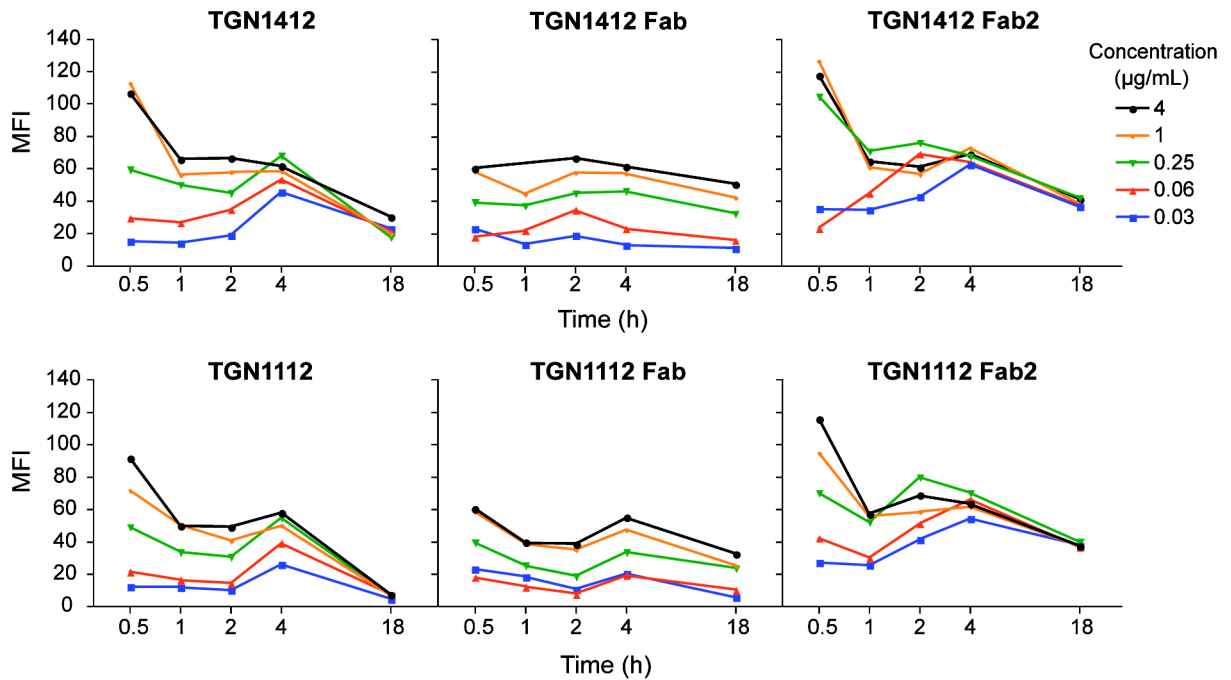


**Figure 41. Binding kinetics of TGN1112 and TGN1412 intact antibodies, Fab and Fab2 fragments on intact PBMC.** MFI of TGN1112, TGN1412 and their Fab and Fab2 fragments on freshly isolated PBMC over time.

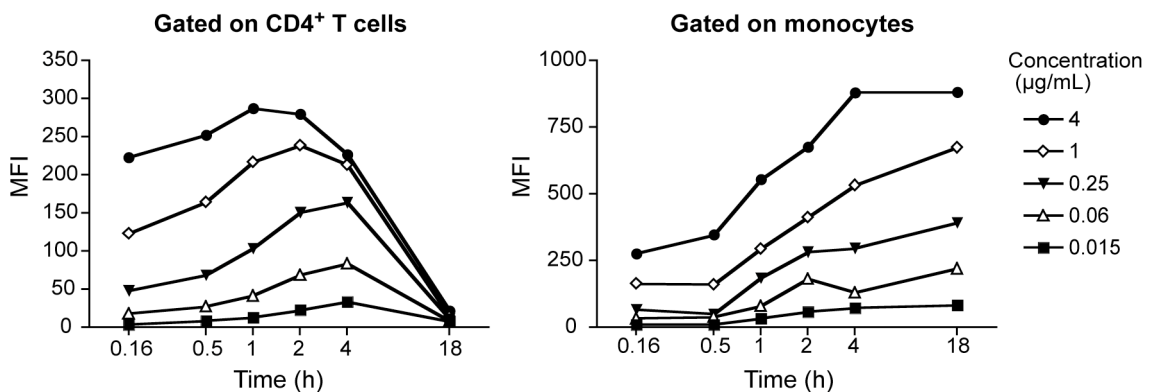


**Figure 42. TGN1112 binding kinetics on CD4<sup>+</sup> T cells and monocytes.** MFI of TGN1112-FITC binding to the CD4<sup>+</sup> T cell surface and increase of FITC signal detected on monocytes. Staining performed on freshly isolated intact PBMC.

Fluorescently labeled antibodies can be traced by FACS analysis. In order to determine whether TGN1112 is indeed ripped-off from the cell surface of T cells, TGN1112-FITC was used to stain the cells. If the FITC signal were detected on other cells, this would

support the theory of trans-endocytosis. After 18h there was no antibody bound to the cell surface of CD4<sup>+</sup> T cells anymore (no CD28 expression) (Figure 42). When gating on monocytes, an increase in FITC signal was detected, proportional to the antibody concentration and to the disappearance from the T cell surface (Figure 42). Since monocytes do not express CD28, this finding leads to the conjecture that monocytes rip-off CD28-TGN1112 complexes from the surface of T cell via Fc-FcR interactions.

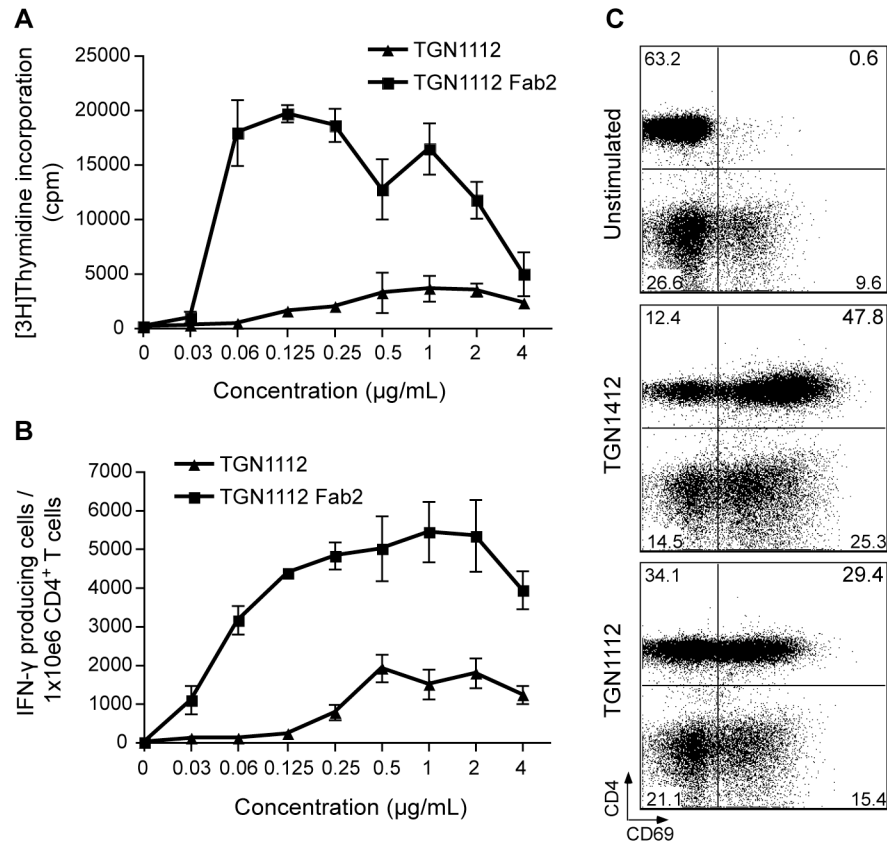


**Figure 43. TGN1112 has low mitogenic activity on precultured PBMC but it induces IFN- $\gamma$  production and CD69 expression in short-term sensitive assays. A.** Proliferation of precultured PBMC stimulated with TGN1112 intact and Fab2, measured from day 2-3 by [3H]Thymidine incorporation. **B.** IFN- $\gamma$  producing cells measured by ELISPOT after 16h stimulation of precultured PBMC. **C.** CD69 expression by CD4<sup>+</sup> T cells in precultured PBMC induced by 16h stimulation with 1  $\mu$ g/mL intact TGN1412 or TGN1112 mAbs. Lymphocyte gate. A, B and C are results from the same donor. Data represents mean  $\pm$  SD of triplicate samples.

This phenomenon might explain why TGN1112 has no mitogenic activity, since this “regulatory” mechanism occurs early enough to prevent cells to get the activation signal for a sufficient time to proliferate. Proliferation is measured from day 2 to 3 of the stimulation, which might be a too late read-out of the effect of TGN1112. To have a more sensitive short-term assay, an IFN- $\gamma$  ELISPOT was performed. Cytokine-producing cells could indeed be detected after 16h stimulation with soluble TGN1112 though to a much lower extent than with

the Fab2 fragments (Figure 43B), which shows that the intact antibody has an initial stimulatory effect that might be being blocked or stopped by ripping the antibody off from the cell surface, as seen in the low counts obtained in the proliferation assay (Figure 43A). TGN1112 Fab2 induced a very strong cytokine release (Figure 43B), supporting the hypothesis of the involvement of the TGN1112 Fc part on the regulation of the response. CD69 expression, an early T-cell activation marker, is also a good read-out for short-term responses. TGN1112 induced CD69 expression on 46% CD4<sup>+</sup> T cells, while TGN1412 induced it on 79% (Figure 43C). Nevertheless, it is clear that TGN1112 has a short-term stimulatory effect on T cells.

The binding experiments were done using RPMI + 10% FCS as medium. Human AB serum contains many more immunoglobulins than FCS, approximately 10 mg/mL (Cassidy, Nordby, and Dodge 1974). These Igs could compete with the antibodies added for FcR binding, so TGN1112 might not be ripped off by FcR-positive cells in a physiological situation.

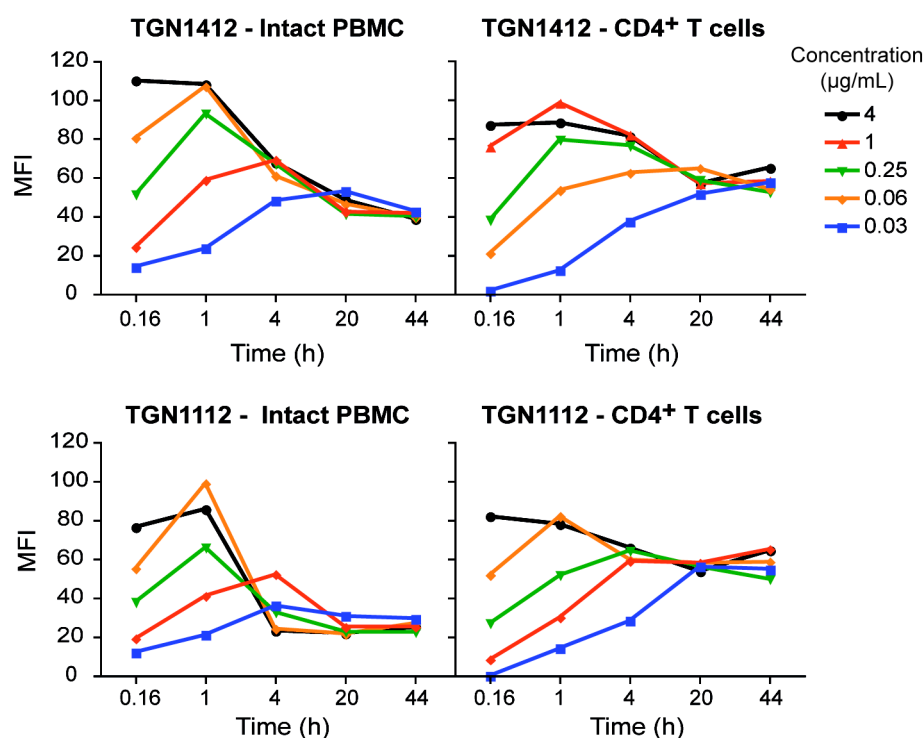


**Figure 44. Binding kinetics of TGN1112 and TGN1412 intact antibodies on PBMC or isolated CD4<sup>+</sup> T cells in the presence of human serum.** MFI of TGN1112 and TGN1412 on freshly isolated PBMC or isolated CD4<sup>+</sup> T cells over time, using AB medium. Gated on CD4<sup>+</sup> cells.

This hypothesis was tested by performing a similar experiment as shown in Figure 40 and Figure 41, but in medium containing 10% human AB serum (AB medium). TGN1412 was

only ripped off to a small degree from the cell surface in the presence of other cells, as it has been shown before in FCS-supplemented medium, where it was more pronounced (Figure 41). The IgG1 version of the anti-CD28 SA, TGN1112, which was completely ripped-off in medium with FCS (Figure 41), was also removed from the T cell surface in intact PBMC in the presence of AB serum but to a lesser extent, while on isolated CD4<sup>+</sup> T cells it was not, instead it reached binding equilibrium as shown in previous experiments. These observations suggest that the limited stimulatory activity of TGN1112 might be indeed due to the fact that the antibody is ripped-off from the T cell surface before it can induce proliferation. This might also occur physiologically, since the phenomenon was observed in the presence of human serum, leaving TGN1412 as the most effective anti-CD28SA to induce T-cell activation and proliferation.

## 5. Discussion

The unexpected and tragic outcome of the CD28 superagonist TGN1412 first-in-man clinical trial in 2006 was not predicted by any of the preclinical studies done with circulating human PBMC (Duff 2006) or animal models including rats (Lin and Hunig 2003), mice (Dennehy et al. 2006), and rhesus (TeGenero 2005) and cynomolgus monkeys (Duff 2006). In contrast, the rat superagonist JJ316 showed to preferentially activate Treg cells (Lin and Hunig 2003), thus favoring the clinical improvement in several autoimmune disease models (Schmidt et al. 2003; Beyersdorf, Hanke, et al. 2005). The need for new methods that would allow to predict this cytokine release syndrome immediately arose.

As introduced previously several approaches have been made to find an explanation on the failure of circulating PBMC to predict the TGN1412-induced cytokine storm and to find in vitro assays that mimic the response observed in vivo (Stebbing et al. 2007; Findlay et al. 2010). These include immobilization of TGN1412 by air-drying or wet-coating the plates, or captured by immobilized anti-Fc antibodies. Eastwood et al. (2010) point out that immobilizing a mAb to a plastic surface is a highly artificial system that is unlikely to simulate a physiological situation. Plastic immobilization does allow predicting in vitro if a drug would activate cells, but titrations are not possible.

Another finding is that TGN1412 can activate T cells in the presence of an endothelial layer (primary umbilical vein endothelial cells or HUVECs), although the results obtained by Stebbings et al. (2007) show a very poor TNF response in the presence of a HUVEC layer after 16-24h TGN1412 stimulation, similar to the one obtained by Findlay et al. (2011), who also report that the profile of released cytokines after 24h TGN1412 stimulation in the presence of endothelial cells did not mirror that in the clinical trial volunteers or the plastic-immobilized TGN1412. Recently, Weissmüller et al. (2012) agreed that the TGN1412 response depends on the interaction with endothelial cells. They showed that this does not depend on interactions between Fc-FcR, finding that supports the observation of Findlay et al. (2011) who show that TGN1412 does not bind to HUVECs; they claim it depends instead on the interaction of the ICOS (CD278) expressed on activated T cells with its ligand (LICOS or CD275). Human endothelial cells constitutively express low levels of LICOS, which is strongly upregulated during an immune response, namely in the presence of pro-inflammatory cytokines such as TNF- $\alpha$ , IFN- $\gamma$  or IL-1 $\beta$  (Moore 1999). Weissmüller et al. (2012) showed T cell cytokine release upon TGN1412 stimulation in the presence of cytokine-preactivated HUVECs (TNF- $\alpha$  + IFN- $\gamma$  for 3 days), a condition that would account for an active immune response, which was not the case in the healthy volunteers previous to

TGN1412 infusion. Therefore although this ICOS-LICOS interaction might occur in tissues boosting an existing immune response, it cannot explain the initial T-cell activation by soluble TGN1412 observed in vivo.

In contrast, we found that by simple preculture of circulating human PBMC under high-cell density conditions for two days T cells became TGN1412 reactive. The response obtained, both mitogenicity and cytokine release, was of comparable magnitude to that obtained with the anti-CD3 mAb OKT3, response that is well studied and characterized. Both of these antibodies induced a similar in vivo response in humans, namely a cytokine release syndrome that can be controlled by corticosteroids (Abramowicz et al. 1989; Chatenoud et al. 1990; Duff 2006). Importantly, the cytokine release profile obtained with the 2-day high-density preculture of PBMC corresponds to the one measured during the TGN1412 first-in-man clinical trial, reported by Suntharalingam et al. (2006). The hypothesis behind these observations is that cells are acquiring tissue like properties by being first exposed to a 10-fold higher cell density than what is used in standard immunological assays. Cells are highly packed together, having therefore many more interactions as they do within tissues. The acquisition of TGN1412 reactivity depends on these cell-cell contacts, which could be due to both adhesion-induced T cell priming, which occurs upon binding to artificial substrates such as immobilized ligands as well as upon interaction with dendritic cells (Randriamampita et al. 2003), and due to "tonic signals" obtained by MHC scanning by the TCR (Stefanova, Dorfman, and Germain 2002). Reactivity of lymph node T cells to TGN1412 stimulation supports this idea. Importantly, performing TGN1412 stimulation of high-density precultured PBMC in the presence of a HUVEC cell monolayer did not improve the response (not shown).

A possible explanation for this re-acquisition of T-cell reactivity to TGN1412 could be the enrichment or depletion of a particular cell subset after the preculture, but this was not the case. HDC cells also did not lose a hypothetical suppressive capacity, because when mixed with fresh cells there was no inhibition of the response. This means that T cells are gaining function or reactivity by the RESTORE protocol.

A previous study showed that release of proinflammatory cytokines in vitro by immobilized TGN1412 stimulation of human PBMC was by CD4 effector memory cells (Eastwood et al. 2010). This finding was confirmed with the RESTORE protocol using soluble TGN1412, where the CD4<sup>+</sup>CD45RO<sup>+</sup>CCR7<sup>-</sup> population released IFN- $\gamma$  and TNF and proliferated upon stimulation. Thus the "cytokine storm" elicited in the human volunteers upon TGN1412 infusion might have been released by the CD4 effector memory cell compartment, which is localized mainly in peripheral tissues such as the gut or the lungs

(Sallusto et al. 1999). Cytokines likely released by tissue resident T cells diffused to the circulation, causing a systemic reaction. Of note, 90% of the body's lymphocytes reside in the lungs and gastrointestinal mucosa, while the blood contains only around 1% (Cerf-Bensussan and Guy-Grand 1991; Smit-McBride et al. 1998). It has also been determined that naive and central memory CD4<sup>+</sup> T-cell subsets have limited potential for cytokine expression, in contrast to the effector memory subset which presents a considerable capability for cytokine production. Importantly, IFN- $\gamma$  expression has been shown to be largely limited to the CD4<sup>+</sup> effector memory T-cells (Sallusto et al. 1999; Amyes, McMichael, and Callan 2005). Of importance, we showed that the cytokine release induced by TGN1412 could be controlled by corticosteroids (namely methylprednisolone and dexamethasone). The use of high doses of these anti-inflammatory agents proved, in animal models, not to interfere with the activation of Treg cells, suggesting that the desired effect of Treg activation could be obtained in humans by co-administration of corticosteroids (Gogishvili et al. 2008).

Phosphorylation of tyrosine residues on intracellular proteins or ITAMs (immunoreceptor tyrosine-based activation motifs) on the cytoplasmic tails of membrane receptors after appropriate ligand binding events leads to the initiation of intracellular signaling cascades and cell activation (Cambier 1995). Previous studies in a mouse model showed that lymph node cells present a constitutively phosphorylated CD3 molecule (p21 of the CD3 $\zeta$  chain), while circulating T cells do not (Stefanova, Dorfman, and Germain 2002). This is probably due to tonic signals through MHC recognition by the TCR in the densely packed tissue environment. It has been shown that CD28SA mitogenic activity depends on tonic signals (Hünig and Dennehy 2005). The RESTORE protocol allowed the recovery of protein phosphorylation associated with the TCR (probably p21 on the CD3 $\zeta$  chain) seen in human lymph node cells, and the formation of cap-like structures was observed as well, where pTyr and CD3 colocalized, supporting the notion of the generation of pre-activated TCR complexes. Activated Lck (Src-family kinase) phosphorylates the CD3 $\zeta$  chain, promoting the recruitment of the Syk/ZAP-70 family of kinases to the TCR complex (van Oers 1999). MHC scanning reportedly leads to phosphorylation of ZAP70 (Stefanova, Dorfman, and Germain 2002), which phosphorylates SLP-76, promoting the recruitment of Vav (a guanine nucleotide exchange factor), adaptor proteins, and an inducible T cell kinase (Itk) (Qi and August 2007). It has been shown that CD28SA are able to amplify tonic signals at the level of the SLP-76/Vav/Itk signalosome, which becomes phosphorylated after CD28 costimulation, and it seems to cooperate in the activation of downstream molecules such as PLC- $\gamma$  (Figure 45) (Hünig and Dennehy 2005). Furthermore, Gogishvili et al. (2008) demonstrated that CD28 ligation can mediate Lck- and Vav1-dependent proliferative signals

independently of PI3K. The fact that inclusion of PP1, which inhibits Lck, into the high-density 2-day preculture actually impeded the sensitization of T cells to TGN1412 supports the findings that lead to the hypothesis that tonic signals received via TCR scanning induce the formation of a pre-activated TCR machinery, rendering T cells more sensitive to stimulation.

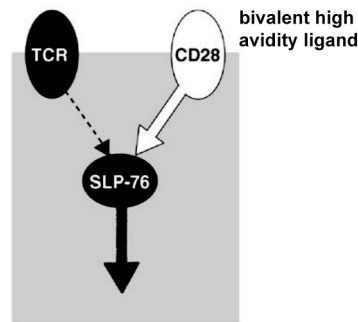


**Figure 45. CD28SA T-cell activation depends on TCR tonic signals.** Schematic representation of CD28SA intracellular signaling (Hünig and Dennehy 2005)\*.

When MHC scanning was blocked with antibodies or Fab fragments against HLA class I and II, T cells failed to acquire full TGN1412 reactivity. The fact that both  $\alpha$ HLA class I and II antibodies would block acquisition of TGN1412 reactivity could be confusing, because most of the cytokine producing cells are CD4<sup>+</sup> T cells, which recognize HLA class II. However, most of the binding interface (75–80%) of the TCR involves contact between the gene-encoded components (complementarity-determining region 1 (CDR1) and region 2 (CDR2)) and the conserved parts of the MHC helices. Ergo, the TCR V-gene repertoire is specific for MHC molecules regardless of the MHC class or allele (Wu et al. 2002; Matsui et al. 1991; Garcia et al. 2009).

As discussed, tonic signals occur in a densely packed cell environment, such as the one in lymph nodes, tissues or in the RESTORE protocol. Hochweller et al. (2010) demonstrated that in the mouse lymph nodes T cells obtain the preactivated state by scanning of DC, a cell type that is scarce in the blood. In the RESTORE system monocytes seem to play an important role, by helping overcome the lack of DC among PBMC. But why does the acquisition of reactivity takes 2 days, when recovery of reactivity in the mouse system on a DC/CD4<sup>+</sup> T cell coculture takes only a few hours? (Hochweller et al. 2010). Monocytes seem to functionally mature after high-density preculture in the presence of accessory cells, as seen by the rapid increase of sensitivity of fresh CD4<sup>+</sup> T cells to

\* Reprinted from Immunology Letters, 100/1, Thomas Hünig, Kevin Dennehy, CD28 superagonists: Mode of action and therapeutic potential, 21-28, 2005, with permission from Elsevier.

TGN1412 stimulation when cocultured with precultured monocytes, so both monocytes and CD4<sup>+</sup> T cells need time to functionally mature so the latter can become TGN1412-reactive. A difference observed between fresh and precultured monocytes was the upregulation of MHC class I in the former, a molecule that is scanned by the TCR.

T cells present an all or nothing effect after preculture in response to TGN1412. For other T cell activating agents the effect of preculture is not absolute which could account for the reason that the impaired T cell responsiveness was not previously appreciated in humans. T cell response inhibition was less pronounced after the PBMC were precultured at high cell density for 2 days, namely T cells from precultured PBMC were less sensitive to PP1 blockade after OKT3 stimulation, and to a lesser extent, to CsA. T cell mitogens showed to be more potent on precultured T cells (PHA, ConA,  $\alpha$ CD2 Abs), and HDC T cells also showed increased sensitivity to the bacterial superantigen SEB. Detection of recall responses to antigens is a very important diagnostic tool, and it is routinely performed in diagnostic laboratories to detect previous or latent infections or vaccination status. High-density preculture of PBMC improved the recall response to tetanus/diphtheria toxoid.

Taken together these results show that the RESTORE protocol might have important implications in preclinical assays on T-cell directed drugs, as well as a simple, cost-effective, and straightforward diagnostic tool. It has already been used to test the immunomodulatory activity of crude extracts derived from marine-sponge associated bacteria containing secondary metabolites (Tabares et al. 2011), as well as on CD8<sup>+</sup> T cell-directed viral antigens (J. Fischer and T. Hünig, unpublished). In both studies the response was higher and more sensitive at low doses of the stimulants after PBMC were precultured at high cell density for 2 days, proving that the method is a more sensitive read-out for immunological stimulants.

This method allowed to reveal, for the first time, the in vitro cytokine release induced by soluble TGN1412. It was demonstrated by others that the antibody concentration used in the clinical trial, which was determined by in silico calculations (0.1 mg per kg body weight) (Duff 2006), achieved 45-80% receptor occupancy (Figure 46A) (Waibler et al. 2008), equivalent to 1  $\mu$ g/mL in vitro, concentration which also showed to be in functional saturation as determined by the RESTORE protocol (Figure 4B, Figure 46B). The threshold for TNF induction by TGN1412 is at < 5% receptor occupancy (0.06  $\mu$ g/mL, Figure 46). In the light of these observations it is clear that the amount of antibody infused in the healthy volunteers during the clinical trial was over-dosed.

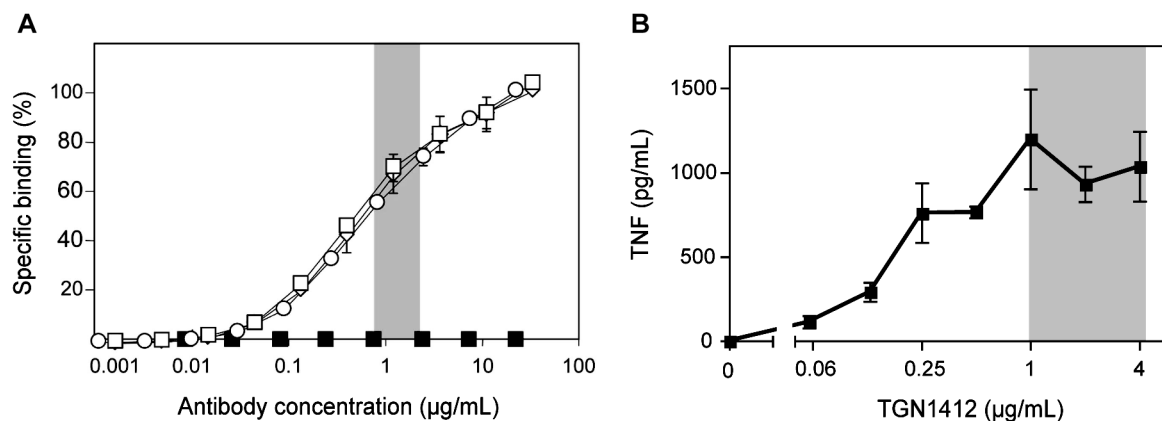


**Figure 46. Receptor occupancy and activation threshold of TGN1412.** Median of the percentage of specific TGN1412 binding to CD3<sup>+</sup> cells (open symbols). Each curve represents a different experiment. Black squares represent negative control ( $\alpha$ CD20 Ab) (Waibler et al. 2008)<sup>†</sup>. **B.** TNF release after TGN1412 stimulation of PBMC, as seen in Figure 4B. The grey bar in both panels represents the theoretical concentration range achieved in the blood of the TGN1412 clinical trial volunteers. Calculations done in **A** yielded 45-80% receptor occupancy of the antibody (Waibler et al. 2008).

The concentration of TGN1412 infused to the volunteers in the first-in-man trial was determined using the “no observed adverse effect level” (NOAEL) approach, based on results obtained in cynomolgus monkeys. This method determines the highest concentration of a substance at which there was no adverse reaction. The tolerated dose in primates was very high (50 mg/kg body weight). This value was then lowered by an adjustment factor and a safety margin, resulting in a dose 500 times lower (Duff 2006), meaning 0.1 mg/kg body weight was administered during the London Trial, which, as mentioned, was in functional saturation and very high level of CD28 occupancy (Waibler et al. 2008).

It is now known that macaque CD4<sup>+</sup> effector memory cells do not express CD28 on the cell surface, which is the subset that responds to TGN1412 stimulation (Eastwood et al. 2010). This explains the failure of the CD28SA to induce cytokine release in the macaque model. NOAEL calculations were made based on these misleading observations. Following the very serious adverse reactions that occurred in the first-in-man clinical trial of TGN1412 in March 2006, the European Medicines Agency (EMA) changed the rules for calculating the entry dose of biologicals in clinical trials (EMA 2007). An Expert Scientific Group on Phase I Clinical Trials was established to review and improve the safety of early clinical trials. In the report 22 recommendations were outlined that covered several aspects regarding safety of preclinical and early clinical development of biologicals. Among these, the “minimal

<sup>†</sup> Reprinted from Journal of Allergy and Clinical Immunology, 122/5, Zoe Waibler, Linda Y. Sender, Christel Kamp, Jan Müller-Berghaus, Bernd Liedert, Christian K. Schneider, Johannes Löwer, Ulrich Kalinke, Toward experimental assessment of receptor occupancy: TGN1412 revisited, 890-892, 2008, with permission from Elsevier.

anticipated biological effect level” (MABEL) approach is suggested for entry dose calculations. It takes into account many parameters that include: the novelty of the agent, its biological potency and its mechanism of action, the degree of species-specificity of the agent, the dose-response curves of biological effects in human and animal cells, dose-response data from in vivo animal studies, pharmacokinetic and pharmacodynamic modeling and the calculation of target occupancy (Duff 2006). If the entry dose would have been calculated using the MABEL approach, the TGN1412 concentration would have been at least 200-fold lower (Hünig 2012). In hindsight, the tragic outcome of the failed TGN1412 London trial may have contributed to increase safety standards for the future development of immunomodulatory drugs.

When the humanized version of the CD28SA was developed by TeGenero, IgG4 was the isotype of choice, due to its poor binding affinity to FcR, which translates in a lower likelihood of attracting cytotoxic effector mechanisms (Duff 2006), ergo antibody-dependent cell-mediated cytotoxicity or complement-dependent cytotoxicity (Hansel et al. 2010). Nevertheless there was an IgG1 version developed as well, TGN1112, isotype that binds FcR with high affinity and this ligation is known to improve the activation capacity of some antibodies (Presta and Namenuk 2005). In contrast to TGN1412 that had such a huge effect in humans, both in vivo and in vitro (RESTORE), TGN1112 did not show to have a mitogenic activity on T cells in vitro. A plausible explanation is that the differences in the antibody shape between IgG1 and IgG4 (Aalberse and Schuurman 2002) of the human CD28SA might have an effect on the binding to CD28 and therefore on T cell activation. As depicted in Figure 47, IgG4 presents a flat shape resembling a boomerang, while IgG1 has the classical shape of an antibody shown in textbooks. TGN1112’s structure might cause steric interference so the antibody cannot crosslink two CD28 molecules on the cell surface, preventing T cell activation.

In this context it is important to keep in mind that “conventional” costimulatory  $\alpha$ CD28 antibodies bind close to the CD80/CD86-binding site to CD28 (at the top of the molecule) in a monovalent fashion (Figure 1). In contrast, CD28SA bind laterally to the C'D loop allowing lattice formation by crosslinking CD28 homodimers (Luhder et al. 2003; Evans et al. 2005; Beyersdorf, Hanke, et al. 2005).

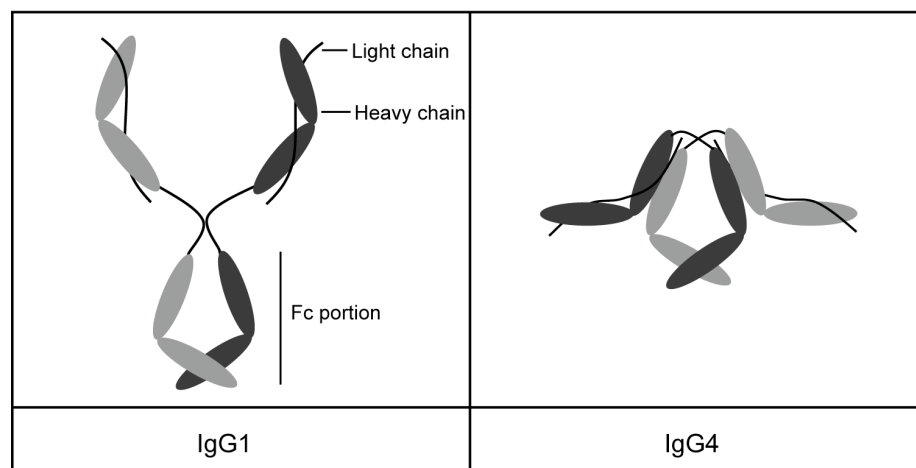


**Figure 47. Model of the structure of IgG1 compared to IgG4.** The structure of IgG1 is in accordance to the classical antibody structure, while IgG4 presents a compact structure (Aalberse and Schuurman 2002)<sup>‡</sup>.

The type of proliferative response seen with Fab2 fragments presented a bell-shaped curve. This kind of behavior has been explained by Heidelberger and Kendall (1929), when they described quantitatively the formation of a precipitate when an antigen-antibody complex formed. When the amount of antigen added was increased, the degree of precipitate followed a bell-shaped curve as shown in Figure 48, where the formation of precipitate depends on the amount of antigen (ligand) and antibody. This type of behavior can be adapted to the context of this work. For the Fab2 fragments it is shown as the percentage of maximum proliferative response achieved (Figure 48), the ligand excess would be equivalent to lower concentrations of Fab2 (antibody) in the presence of T cells expressing CD28 (ligand). Under these conditions there are not enough Fab2 molecules to crosslink sufficient CD28 dimers on the surface of T cells to induce T-cell activation (Figure 48A). When enough Fab2 is added the maximum response is achieved, due to maximum crosslinking (equivalence zone, Figure 48B), but when higher concentrations of antibody are added, the excess does not allow CD28-crosslinking anymore, hence a lower proliferative response was detected (Figure 48C). On the other hand, as expected, monomeric Fab fragments did not induce proliferation or cytokine release, since it is known that CD28SA need to crosslink CD28 dimers in order to activate T cells (Figure 1C) (Luhder et al. 2003; Evans et al. 2005; Beyersdorf, Hanke, et al. 2005). Intact TGN1412 response does not follow this behavior probably because of (although weak) interactions with the Fc part of the antibody with FcR expressed on other cells that might modulate the response to a certain degree by allowing secondary crosslinking.

<sup>‡</sup> Reprinted from *Immunology*, 105/1, Rob C. Aalberse, Janine Schuurman, IgG4 breaking the rules, 9-19, 2002, with permission from John Wiley and Sons.

We considered the possibility that the shape or tertiary structure of TGN1112 as an IgG1 antibody does not allow crosslinking of CD28 molecules. The fact that Fab2 fragments of both TGN1112 and TGN1412 did activate T cells from high-density precultured PBMC could support this hypothesis. But, contrary to the theory of steric interference of TGN1112, the binding kinetics to isolated T cells was comparable to that of TGN1412. After 10 minutes, excess antibody probably did not crosslink, but was bound by one arm of the antibody (as shown in Figure 48C), so the detected antibody on the T cell surface was much higher. With time it reached binding equilibrium, achieving probably maximum level of CD28 crosslinking (Figure 48B). Lower antibody concentrations behaved as shown in Figure 48A, and after 4h it reached crosslinking equilibrium. The fact that initial binding of excess antibody gave double the MFI value than after reaching equilibrium (4h) supports the hypothesis of CD28SA crosslinking of CD28 homodimers (bivalent binding) on the T cell surface after initial monovalent binding of the antibody (Evans et al. 2005).

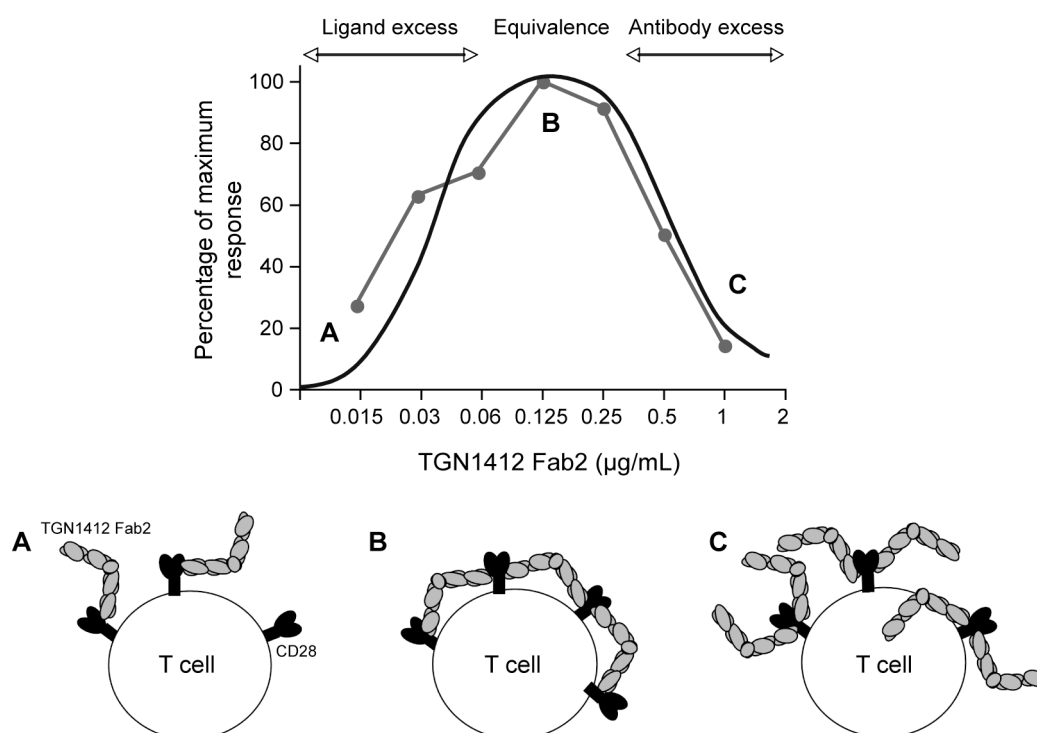


**Figure 48. Representation of the Heidelberger-Kendall curve with TGN1412 Fab2 proliferative response.** The grey line represents the calculated percentage of maximum proliferative response from the experiment shown in Figure 35 and the black line a fitted bell-shaped curve of a classical Heidelberger-Kendall curve. **A.** Area of ligand (CD28) excess. **B.** Equivalence zone, where maximum response is reached due to crosslinking equilibrium. **C.** TGN1412 Fab2 excess.

The difference between TGN1112 and TGN1412 T-cell activation cannot be explained by different binding kinetics. Instead, the Fc portion does seem to play an unexpected

negative role. The binding kinetics on intact PBMC showed a different pattern than on purified T cells. TGN1112 seemed to be being ripped-off from the T-cell surface, a phenomenon seen as well, but to a much lower degree, for TGN1412, and not at all for the Fab or Fab2 fragments of either CD28SA. As discussed, the Fc portion of TGN1112 is much more available than that of TGN1412 (Figure 47), and it also presents higher binding affinity to Fc receptors (Presta and Nameruk 2005). It seems that monocytes and other FcR-positive cells are ripping off CD28-TGN1112 complexes from the T-cell surface by Fc-FcR mediated interactions, even in the presence of human serum which contains high Igs concentrations. Qureshi et al. (2011) reported a similar phenomenon on CTLA-4 positive cells, termed trans-endocytosis, in which the cells ripped-off its ligands (CD80/CD86) from the surface of dendritic cells, which seems to be another regulatory mechanism of CTLA-4 to block CD28 costimulation.

The fact that TGN1112 might be being removed from the T cell surface could account for the lack of stimulatory capacity, since proliferation was measured from day 2-3, and cytokines in the supernatant after 24h of stimulation. Using a shorter and more sensitive read-out (ELISPOT, 16h stimulation) allowed detecting cytokine release (IFN- $\gamma$ ) induced by intact TGN1112, still lower than Fab2 fragments.

In conclusion, the RESTORE protocol is a straightforward, simple and practical method that allows circulating T cells to recover the functional pre-activation state that they have in lymph nodes and tissues (Figure 49). It allows, for the first time, to reproduce in vitro the cytokine storm that TGN1412 elicited during the first-in-man clinical trial in London in 2006. This method also renders T cells more sensitive to stimulation or less sensitive to blockade with different substances, showing the relevance of its use on the testing of novel T cell directed drugs. On a more general note, the RESTORE protocol could improve greatly the predictive value of T cell directed assays in preclinical trials, as well as allowing drug testing on an individualized or personalized level.

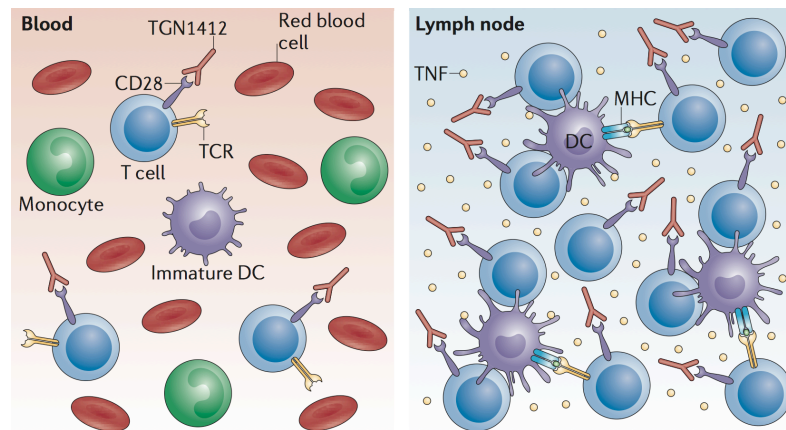


**Figure 49. T-cell response to soluble TGN1412 takes place within the dense environment in tissues.** Circulating lymphocytes are not in contact with DC, so they do not receive tonic signals. Tissues have a highly packed environment where lymphocytes come in close contact with DC, which they scan for cognate antigen via MHC-TCR interactions, receiving tonic signals that renders them more sensitive, and therefore TGN1412 reactive (Hünig 2012)<sup>¶</sup>.

<sup>¶</sup> Reprinted from Nature Reviews Immunology, 12/5, Thomas Hünig, The storm has cleared: lessons from the CD28 superagonist TGN1412 trial, 317-318, 2012, with permission from Nature Publishing Group.

## List of figures

Figure 1. Binding of the superagonistic and conventional $\alpha$ CD28 monoclonal antibodies to CD28. ....	21
Figure 2. Clonal expansion of Treg cells during a normal immune response and by a CD28 superagonist. ....	22
Figure 3. Human PBMC cytokine release response to soluble TGN1412. ....	35
Figure 4. Properties of the RESTORE response to TGN1412. ....	36
Figure 5. Optimization of the RESTORE protocol. ....	37
Figure 6. Cell subset composition of fresh and precultured PBMC. ....	38
Figure 7. TNF release of fresh and precultured PBMC mixed at different ratios during stimulation. ....	38
Figure 8. Intracellular cytokine staining of precultured PBMC. ....	39
Figure 9. TNF release by effector memory T cells from precultured PBMC in response to TGN1412. ....	40
Figure 10. Proliferation of high density precultured PBMC in response to TGN1412 and OKT3 determined by Ki67 staining. ....	40
Figure 11. Cell contact is required for acquisition of TGN1412 reactivity. ....	41
Figure 12. Colocalization of CD3 with tyrosine-phosphorylated proteins in human lymph node sections. ....	42
Figure 13. Colocalization of CD3 with tyrosine-phosphorylated proteins in fresh and high density precultured human PBMC. ....	43
Figure 14. Statistical analysis and colocalization coefficient of CD3 and pTyr in fresh and precultured PBMC. ....	44
Figure 15. Western blot of fresh and precultured PBMC lysates. ....	45
Figure 16. Role of HLA recognition in TGN1412-reactivity acquisition during high-density preculture. ....	46
Figure 17. LcK inhibitor PP1 affects acquisition of TGN1412 reactivity during preculture. ....	47
Figure 18. Depletion of cell subsets from fresh human PBMC. ....	47
Figure 19. Acquisition of TGN1412 reactivity requires the presence of monocytes during high-density preculture. ....	48
Figure 20. CD69 expression by fresh PBMC in response to stimulation with soluble TGN1412 in the presence of HDC PBMC. ....	49

Figure 21. Kinetics of CD69 expression by fresh PBMC in response to TGN1412 stimulation in a HDC co-culture. ....	50
Figure 22. Fresh CD4 <sup>+</sup> T cells acquire TGN1412 reactivity in the presence of monocytes derived from high-density PBMC cultures. ....	51
Figure 23. Monocyte phenotype in fresh and precultured PBMC. ....	51
Figure 24. Human lymph node cells lose TGN1412 reactivity by suspension culture. ....	53
Figure 25. Human LN cells are reactive to TGN1412 in contrast to PBMC, a state which is lost by suspension culture. ....	54
Figure 26. Corticosteroid suppression of TGN1412-induced cytokine release from precultured PBMC is of comparable efficacy as found with OKT3. ....	54
Figure 27. OKT3-stimulated HDC PBMC are less sensitive to PP1 inhibition than fresh PBMC. ....	55
Figure 28. Cyclosporine A inhibition of the fresh and precultured PBMC response to OKT3. ....	56
Figure 29. Mitogenic capacity of PHA and ConA on fresh and precultured PBMC. ....	57
Figure 30. TNF release upon $\alpha$ CD2 mAbs stimulation of fresh and precultured PBMC. ....	57
Figure 31. Proliferative response to Td of fresh and precultured PBMC. ....	58
Figure 32. Proliferative response to SEB of fresh and precultured PBMC. ....	59
Figure 33. Mitogenic activity of TGN1412 and TGN1112 on HDC PBMC. ....	59
Figure 34. Mitogenic activity of intact, Fab and Fab2 fragments from TGN1112 and TGN1412 antibodies on precultured PBMC. ....	60
Figure 35. Mitogenic activity of intact and Fab2 fragments from TGN1112 and TGN1412 antibodies on precultured PBMC. ....	61
Figure 36. TNF release by precultured PBMC in response to intact and Fab2 TGN1112 and TGN1412. ....	61
Figure 37. TGN1412 binding kinetics on fresh and precultured PBMC at 4°C and 37°C. ....	62
Figure 38. TGN1412 Fab fragment binding kinetics on isolated CD4 <sup>+</sup> T cells. ....	63
Figure 39. Intact TGN1412 antibody binding kinetics on isolated CD4 <sup>+</sup> T cells. ....	63
Figure 40. TGN1112 and TGN1412 intact antibodies, Fab and Fab2 fragments binding kinetics on isolated CD4 <sup>+</sup> T cells. ....	64
Figure 41. Binding kinetics of TGN1112 and TGN1412 intact antibodies, Fab and Fab2 fragments on intact PBMC. ....	65
Figure 42. TGN1112 binding kinetics on CD4 <sup>+</sup> T cells and monocytes. ....	65
Figure 43. TGN1112 has low mitogenic activity on precultured PBMC but it induces IFN- $\gamma$ production and CD69 expression in short-term sensitive assays. ....	66

Figure 44. Binding kinetics of TGN1112 and TGN1412 intact antibodies on PBMC or isolated CD4 <sup>+</sup> T cells in the presence of human serum. ....	67
Figure 45. CD28SA T-cell activation depends on TCR tonic signals.....	72
Figure 46. Receptor occupancy and activation threshold of TGN1412. ....	74
Figure 47. Model of the structure of IgG1 compared to IgG4. ....	76
Figure 48. Representation of the Heidelberger-Kendall curve with TGN1412 Fab2 proliferative response. ....	77
Figure 49. T-cell response to soluble TGN1412 takes place within the dense environment in tissues. ....	79

## Annex

### Materials

#### Chemicals and reagents

Chemical / reagent	Manufacturer
10X Permeabilization Buffer	eBioscience
$\beta$ -mercaptoethanol	Invitrogen
Agarose	AppliChem
Amplifying solution	Perkin Elmer
Anti-FITC microbeads	Miltenyi Biotec
Anti-PE microbeads	Miltenyi Biotec
BD FACSRinse Solution	BD Biosciences
Brefeldin A	Sigma
Bovine Serum Albumin (BSA)	Roth
CD14 microbeads human	Miltenyi Biotec
Dexamethasone	Sigma
Dimethylsulfoxide (DMSO)	AppliChem
DNase (Benzonase)	Merck KGaA
Ethanol	AppliChem
Fixation / Permeabilization Concentrate	eBioscience
Fixation / Permeabilization Diluent	eBioscience
Perm/Wash	eBioscience
Perm/Wash	BD
Gigasept Instru AF	Schülke & Mayr
Goat anti-mouse IgG microbeads	Miltenyi Biotec
HEPES	AppliChem
Isopropanol	Roth
Lymphocyte separation medium	PAA
NBT/BCIP Liquid Substrate System	Sigma
Non-essential amino acids	Invitrogen
Paraformaldehyde	Sigma
SDS	Roth
Sodium azide ( $\text{NaN}_3$ )	Roth
Sodium pyruvate	Invitrogen
TEMED	AppliChem
Triton X-100	Roth
Trypan blue	Sigma
Tween-20	AppliChem

### Enzymes and inhibitors

Name	Abbreviation	Manufacturer
Sodium orthovanadate	Na-O-Vanadate	Roth
Sodium fluoride	NaF	Sigma-Aldrich
Dithiothreitol	DTT	Roche
Phenylmethanesulphonylfluoride	PMSF	Roche
Protease inhibitor tablet / Complete mini	-	Roche
Cyclosporin A	CsA	Calbiochem
PP1 analog	PP1	Calbiochem

### Commercial kits

Kits	Manufacturer
CD4 <sup>+</sup> T Cell Isolation Kit II	Miltenyi Biotec
Human IL-10 Flex Set	BD Biosciences
Human IL-2 Flex Set	BD Biosciences
Human INF- $\gamma$ Flex Set	BD Biosciences
Human TNF Flex Set	BD Biosciences
Human Soluble Protein Master Buffer Kit	BD Biosciences
Monocyte Isolation Kit II	Miltenyi Biotec

### Magnetic beads for cell isolation or depletion

Beads	Manufacturer
Anti-PE microbeads	Miltenyi Biotec
Anti-FITC microbeads	Miltenyi Biotec

### Radioactive materials

Name	Isotope	Manufacturer
[3H]-thymidine	Tritium	Hartmann Analytic GmbH

## Antibodies and secondary reagents

### Primary and secondary antibodies

Antigen	Clone	Conjugation	Isotype	Manufacturer
HLA-DR,DP,DQ	Tü39	Purified	mIgG2a, κ	Kind gift of Prof. Rammansee, Tübingen, Germany
HLA-ABC	W6/32	Purified	mIgG2a, κ	
Anti-Phosphotyrosine	4G10	FITC	Mouse IgG2b, κ	Millipore
h CCR7	3D12	FITC	Rat IgG2a, κ	BD
h CCR7	3D12	PE	Rat IgG2a, κ	BD
h CCR7	3D12	Alexa647	Rat IgG2a, κ	BD
h CD14	MfP9	FITC	Mouse IgG2b, κ	BD
h CD14	M5E2	PE	Mouse IgG2a, κ	BD
h CD154	TRAP1	FITC	Mouse IgG1, κ	BD
h CD19	HIB19	FITC	Mouse IgG1, κ	BD
h CD19	HIB19	PE	Mouse IgG1, κ	BD
h CD247	K25-407.69	Alexa647	Mouse IgG2a, κ	BD
h CD25	M-A251	FITC	Mouse IgG1, κ	BD
h CD25	M-A251	PE	Mouse IgG1, κ	BD
h CD28	CD28.2	Alexa488	Mouse IgG1, κ	Biolegend
h CD28	CD28.2	PECy5	Mouse IgG1, κ	BD
h CD3	UCHT1	Alexa647	Mouse IgG1, κ	BD
h CD4	RPA-T4	PECy5	Mouse IgG1, κ	BD
h CD4	RPA-T4	PECy5	Mouse IgG1, κ	Biolegend
h CD4	M-T477	FITC	Mouse IgG2a, κ	BD
h CD45	H130	Alexa647	Mouse IgG1, κ	Biolegend
h CD45RO	UCHL1	FITC	Mouse IgG2a, κ	BD
h CD45RO	UCHL1	APC	Mouse IgG2a, κ	BD
h CD45RO	UCHL1	APC	Mouse IgG2a, κ	Biolegend
h CD56	B159	PE	Mouse IgG1, κ	BD

<b>Antigen</b>	<b>Clone</b>	<b>Conjugation</b>	<b>Isotype</b>	<b>Manufacturer</b>
h CD69	FN50	PE	Mouse IgG1, k	BD
h CD69	FN50	PE	Mouse IgG1, k	Biolegend
h CD8	RPA-T8	FITC	Mouse IgG1, k	BD
h CD8	RPA-T8	PE	Mouse IgG1, k	BD
h CD80	L307.4	FITC	Mouse IgG1, k	BD
h CD83	HB15e	PE	Mouse IgG1, k	BD
h CD86	2331 (FUN-1)	PECy5	Mouse IgG1, k	BD
h CD95	DX2	FITC	Mouse IgG1, k	BD
h Foxp3	259D/C7	Alexa488	Mouse IgG1	BD
h HLA-ABC	G46-2.6	FITC	Mouse IgG1, k	BD
h HLA-DR	G46-6	FITC	Mouse IgG2a, k	BD
H HLA-DQ	Tu169	FITC	Mouse IgG2a, k	BD
h IL-2	MQ1-17H12	PE	Rat IgG2a, k	BD
h INF- $\gamma$	4S.B3	PE	Mouse IgG1, k	BD
h kappa Ig	G20-193	PE	Mouse IgG1, k	BD
h Ki67	B56	PE	Mouse IgG1, k	BD
h Ki67	Ki-67	PE	Mouse IgG1, k	Biolegend
h TCR $\gamma\delta$	B1	PE	Mouse IgG1, k	BD
h TNF	MAB11	PE	Mouse IgG1, k	BD
h TNF-a	MAB11	FITC	Mouse IgG1, k	Biolegend
m IgG (H+L)	Polyclonal	PE	Donkey IgG Fab2 fragment	Dianova
m IgG1, k Isotype control	MOPC-21	PE	Mouse IgG1, k	Biolegend

h: human    m: mouse

### Antibodies for ELISPOT

<b>Antibody</b>	<b>Format</b>	<b>Manufacturer</b>
Human IFN- $\gamma$ ELISpot pair	Capture antibody: purified anti-human IFN $\gamma$	BD Biosciences
	Detection antibody: biotinylated anti-human IFN $\gamma$	BD Biosciences

Antibody	Format	Manufacturer
Human IL-2 ELISpot pair	Capture antibody: purified anti-human IL-2	BD Biosciences
	Detection antibody: biotinylated anti-human IL-2	BD Biosciences
Human TNF ELISpot pair	Capture antibody: purified anti-human TNF	BD Biosciences
	Detection antibody: biotinylated anti-human TNF	BD Biosciences

### Antibodies for Western Blot

Antigen	Clone	Conjugate	Isotype	Manufacturer
CD3- $\zeta$	6B10.2	Purified	Mouse IgG2a, k	Santa Cruz
Phosphotyrosine	4G10	Purified	Mouse IgG2b, k	Millipore

### Secondary reagents

Reagent	Conjugation	Manufacturer
Streptavidin	HRP	BD Biosciences
Streptavidin	AP	Southern Biotech

### Cell stimulation-related reagents

Name	Manufacturer
Brefeldin A	Sigma
CD2 antibodies (M1, M2, 3PT)	Kind gift from De Jutta Schröder-Braunstein, Heidelberg, Germany
Human Serum Type AB from Male AB	Sigma
Lectin from <i>Phaseolus vulgaris</i> Phytohemagglutinin PHA-P	Sigma
Methylprednisolone (Urbason)	Sanofi Aventis
Muromonab-CD3 (OKT3)	Janssen-Cilag
Tetanus diphtheria toxoid (Td) (Td-Impfstoff Mérieux)	Sanofi Pasteur MSD
TGN1412 (TAB08)	Theramab GmbH
Tuberculin purified protein derivate (PPD)	Statens Serum Institut

**Buffers, media and solutions****BSS (balanced salt solution) / 0.2% BSA (bovine serum albumin) (BSS/BSA)**

BSS I		1100 mL
BSS II		1100 mL
BSA		20.0 g
ddH <sub>2</sub> O	ad	10.0 L

**BSS I**

Glucose		100 g
KH <sub>2</sub> PO <sub>4</sub>		6.0 g
Na <sub>2</sub> HPO <sub>4</sub> ·2H <sub>2</sub> O		23.8 g
Phenol red		1.0 g
ddH <sub>2</sub> O	ad	10.0 L

**BSS II**

CaCl <sub>2</sub> ·2H <sub>2</sub> O		18.6 g
KCl		40.0 g
NaCl		800 g
MgCl <sub>2</sub> ·6H <sub>2</sub> O		20.0 g
MgSO <sub>4</sub> ·7H <sub>2</sub> O		20.0 g
ddH <sub>2</sub> O	ad	10.0 L

**Citrate buffer**

Citric acid	0.1 M
Sodium citrate	0.1 M

Adjust pH to 6.0

**FACS buffer**

BSA	0.1%
Sodium azide	0.01%

In PBS

**Freezing medium**

Heat-inactivated human AB serum	50%
AB medium (w/o human AB serum)	40%
DMSO	10%

Sterile filter. Freezing medium is good for two weeks if stored at 4°C.

**Lysis buffer**

Tris.Cl pH 8.0	50 mM
NaCl	150 mM
Triton X-100	1%
Protease and phosphatase inhibitors:	
Complete mini	4%
Na-O-Vanadate	1 mM
NaF	1 mM
DTT	1 mM
PMSF	0.1 mM

In ddH<sub>2</sub>O

**PBS (Phosphate buffered saline)**

NaCl	80.0 g
KCl	2.0 g
KH <sub>2</sub> PO <sub>4</sub>	2.0 g
Na <sub>2</sub> HPO <sub>4</sub>	11.5 g
ddH <sub>2</sub> O	ad 10.0 L

Adjust pH to 7.4

**RPMI + 10% AB serum (AB medium)**

RPMI + 2 mM L-Glutamine		500 mL
Penicillin / Streptomycin (100 U/mL)	ca	1.2 mL
Non-essential amino acids (100X MEM)		5.0 mL
Na-Pyruvate (100 mM)		5.0 mL
β-Mercaptoethanol (50 mM)		500 μL
HEPES (1 M)		5.0 mL
10% heat inactivated human AB serum (or autologous)		50 mL

**Versene**

KCl		1.0 g
KH <sub>2</sub> PO <sub>4</sub>		1.0 g
NaHPO <sub>4</sub>		2.84 g
NaCl		41.0 g
Versene		1.0 g
ddH <sub>2</sub> O	ad	5.0 L

**Human cells**

Cell type	Source	Location
Human PBMC	Venous blood	Institute of Transfusion Medicine and Hemotherapy, University Clinic Würzburg, Germany
Human lymph nodes	Para-iliac region of renal transplant recipients	Renal Transplant Unit, Department of Medicine, Academic Medical Center, Amsterdam, The Netherlands
	Pancreas of non-diabetic brain-dead multi-organ donors	Islet Isolation Facility, San Raffaele Hospital, Milan, Italy

**Equipment and supplies**

Equipment / Supplies	Manufacturer	Specifications
10 µL tips	Roth	
1000 µL blue tips	Roth	
200 µL yellow tips	Roth	
24 well plates	Greiner Bio-One	Flat bottom cell culture
48 well plates	Greiner Bio-One	Flat bottom cell culture
96 well plates	Greiner Bio-One	Flat bottom cell culture
96 well plates	Greiner Bio-One	U bottom suspension culture
Cell strainer	BD Falcon	70 µm Nylon
Centrifuge	Eppendorf	Eppendorf centrifuge 5804 R
Centrifuge	Heraus	Heraus Megafuge 1.0R
Cryotubes	Nunc	Cryotube Vials 1.8 mL
Cuvette	Bio-Rad	
Dispenser tips	Brand	1.25 mL, 2.5 mL

<b>Equipment / Supplies</b>	<b>Manufacturer</b>	<b>Specifications</b>
Confocal microscope	Zeiss	Laser Scan Microscope, LSM510 Meta, equipped with an inverted Zeiss Axiovert 200M stand
ELISPOT plates	Millipore	MultiScreen Filter plates (white)
ELISPOT reader	C.T.L.	ImmunoSpot S5 Versa Analyzer
FACS tubes	BD Biosciences	REF 352052
	Hartenstein	RE03
Centrifuge tubes	Greiner Bio-One	15, 50 mL polypropylene
Flow cytometer	BD Biosciences	FACSCalibur
Flow cytometer	BD Biosciences	LSR II
Freezing container	Nalgene	"Mr Frosty", 18 vials
Harvester	Perkin Elmer LAS GmbH	
Humidified incubator	Thermo Scientific	HERA Cell 150
Laminar flow hood	Antair	Antair ZKB hood
	Hera Cell	Hera safe hood
Leucosep tubes	Greiner Bio-One	50 mL
Liquid scintillation counter	Perkin Elmer LAS GmbH	MicroBeta Liquid Scintillation Counter
MACS separation columns	Miltenyi Biotec	25 LS and LD
Refrigerator	Liebherr	Glassline
Transwell plate	Corning Incorporated (COSTAR)	6.5 mm diameter inserts 8.0 µm pore size
Western blot membrane	Roth	Roti-PVDF membrane

### **Software**

<b>Software</b>	<b>Application</b>	<b>Reference</b>
Adobe Illustrator CS2 v.12.0.0	Figure preparation	Adobe
CELLQuest v3.3	FACS data acquisition on FACSCalibur flow cytometer	BD Biosciences
EndNote X5	Reference management	Thomson Reuters
FACSDiva Software v6.1.3	FACS data acquisition on LSR II flow cytometer	BD Biosciences
FCAP Array software v2.0	CBA results analysis	SoftFlow Inc, www.fcaparray.com
FlowJo v9.5.2	FACS data analysis	TreeStar, Inc
Graphpad Prism v5 for Macintosh	Graphs and statistical analysis	www.graphpad.com

---

<b>Software</b>	<b>Application</b>	<b>Reference</b>
ImageJ	Colocalization coefficient analysis of confocal microscopy images	<a href="http://rsbweb.nih.gov/ij/">rsbweb.nih.gov/ij/</a>
Image Reader LAS-3000 v2.0	Dark Box image acquisition	Fujifilm
ImmunoSpot reader systems	Read ELISPOT plates	C.T.L.
ImmunoSpot software v4.0	Analyze ELISPOT images	C.T.L.
Microbeta Windows Workstation v2	Liquid scintillation counting	Perkin Elmer LAS GmbH
Microsoft Office 2011 for MAC	Data management, manuscript preparation	Microsoft

---

## List of abbreviations and acronyms

°C	Degrees Celsius
AP	Alkaline Phosphatase
AP-1	Activator Protein 1
-APC	Allophycocyanin
APC	Antigen-Presenting Cell
B-CLL	B-cell Chronic Lymphocytic Leukemia
BCR	B-cell receptor
BSA	Bovine Serum Albumin
BSS	Balanced Salt Solution
BTLA	B- and T-Lymphocyte Attenuator
CBA	Cytometric Bead Array
CD	Cluster of Differentiation
CDR	Complementarity-Determining Region
CFSE	Carboxyfluorescein diacetate, Succinimidyl Ester
CLL	Chronic Lymphocytic Leukemia
cpm	Counts per Minute
CRS	Cytokine Release Syndrome
CTLA-4	Cytotoxic T-Lymphocyte Antigen 4 or CD152
ddH <sub>2</sub> O	Double distilled water
DNase	Deoxyribonuclease
ELISpot	Enzyme-Linked Immunospot Assay
EMA	European Medicines Agency
Fab	Fragment antigen binding
FACS	Fluorescence-Activated Cell Sorter/-ing
Fc	Fragment Crystallizable
FcR	Fc receptor
FCS	Fetal Calf Serum
FITC	Fluorescein Isothiocyanate
FoxP3	Forkhead box P3
g	Grams
GMP	Good Manufacturing Practice

Grb2	Growth factor Receptor-bound protein 2
GvHD	Graft-versus-Host Disease
h	Hours
HLA	Human Leukocyte Antigen
HRP	Horseradish Peroxidase
IFN- $\gamma$	Interferon gamma
Ig	Immunoglobulin
IL	Interleukin
IL-#R	IL-# Receptor
IP	Immunoprecipitation
ITAM	Immunoreceptor Tyrosine-based Activating Motif
kD	Kilodalton
L	Liter
Lck	Lymphocyte-specific protein tyrosine kinase
LFA-1,3	Lymphocyte Function-associated Antigen 1 or 3
LN	Lymph Nodes
LRS-C	Leukoreduction System Chambers
mA	Milliampere
MABEL	Minimum Anticipated Biological Effect Level
MFI	Mean Fluorescence Intensity
min.	Minutes
mL	Milliliter
mRNA	Messenger Ribonucleic Acid
NFAT	Nuclear Factor of Activated T cells
NF $\kappa$ B	Nuclear Factor kappa-light-chain-enhancer of activated B cells
NOAEL	No Observed Adverse Effect Level
O/N	Overnight
OKT3	Muronomab – Orthoclone OKT3
PBMC	Peripheral Blood Mononuclear Cells
PBS	Phosphate Buffered Saline
PD-1	Programed-Death receptor 1
PE	Phycoerythrin
PECy5	Phycoerythrin-Cy5

pg	Picograms
PI3K	Phosphatidylinositol 3 kinase
PKC- $\theta$	Protein Kinase C theta
PPD	Tuberculin Purified Protein Derivate
RT	Room Temperature
SD	Standard Deviation
SDS-PAGE	Sodium Dodecyl Sulfate-Polyacrylamide Gel Electrophoresis
sec.	Seconds
SMAC	Supramolecular Activation Cluster
Td	Tetanus Diphtheria toxoid
TNF	Tumor Necrosis Factor
TNFRII	Tumor Necrosis Factor Receptor II
V	Volts
x g	Relative centrifugal force (RCF, g-force)
ZAP-70	Zeta-chain Associated Protein kinase of 70 kD
$\alpha$	Alfa
$\mu$	Micro

## References

- Aalberse, R. C., and J. Schuurman. 2002. IgG4 breaking the rules. *Immunology* 105 (1):9-19.
- Abramowicz, D., L. Schandene, M. Goldman, A. Crusiaux, P. Vereerstraeten, L. De Pauw, J. Wybran, P. Kinnaert, E. Dupont, and C. Toussaint. 1989. Release of tumor necrosis factor, interleukin-2, and gamma-interferon in serum after injection of OKT3 monoclonal antibody in kidney transplant recipients. *Transplantation* 47 (4):606-8.
- ACIP. *Immunization Action Coalition*, January 2012 [cited 22 May 2012]. Available from <http://www.immunize.org/adultrules>.
- Amyes, E., A. J. McMichael, and M. F. Callan. 2005. Human CD4+ T cells are predominantly distributed among six phenotypically and functionally distinct subsets. *J Immunol* 175 (9):5765-73.
- Andersson, Jan, Olof Sjöberg, and Göran Möller. 1972. Mitogens as Probes for Immunocyte Activation and Cellular Cooperation. *Immunological Reviews* 11 (1):131-177.
- Arduin, Laurence, Claude Boyer, Anne Gillet, Jeannine Trucy, Anne-Marie Bernard, Jacques Nunes, Jérôme Delon, Alain Trautmann, Hai-Tao He, Bernard Malissen, and Marie Malissen. 1999. Crippling of CD3- $\zeta$  ITAMs Does Not Impair T Cell Receptor Signaling. *Immunity* 10 (4):409-420.
- Beaudette-Zlatanova, B. C., B. Whalen, D. Zipris, H. Yagita, J. Rozing, H. Groen, C. D. Benjamin, T. Hunig, H. A. Drexhage, M. J. Ansari, J. Leif, J. P. Mordes, D. L. Greiner, M. H. Sayegh, and A. A. Rossini. 2006. Costimulation and autoimmune diabetes in BB rats. *American Journal of Transplantation* 6 (5):894-902.
- Bevan, M. J. 2011. Memory T cells as an occupying force. *Eur J Immunol* 41 (5):1192-5.
- Beyersdorf, N., K. Balbach, T. Hunig, and T. Kerkau. 2006. Large-scale expansion of rat CD4+ CD25+ T(reg) cells in the absence of T-cell receptor stimulation. *Immunology* 119 (4):441-50.
- Beyersdorf, N., S. Gaupp, K. Balbach, J. Schmidt, K. V. Toyka, C. H. Lin, T. Hanke, T. Hunig, T. Kerkau, and R. Gold. 2005. Selective targeting of regulatory T cells with CD28 superagonists allows effective therapy of experimental autoimmune encephalomyelitis. *J Exp Med* 202 (3):445-55.
- Beyersdorf, N., T. Hanke, T. Kerkau, and T. Hunig. 2005. Superagonistic anti-CD28 antibodies: potent activators of regulatory T cells for the therapy of autoimmune diseases. *Ann Rheum Dis* 64 Suppl 4:iv91-5.
- Bingham, C. O. 2012. *Rheumatoid arthritis treatment*. The Johns Hopkins Arthritis Center 2012 [cited 30 June 2012]. Available from [http://www.hopkins-arthritis.org/arthritis-info/rheumatoid-arthritis/rheum\\_treat.html](http://www.hopkins-arthritis.org/arthritis-info/rheumatoid-arthritis/rheum_treat.html).
- Bischof, A, T Hara, C-H Lin, AD Beyers, and T Hünig. 2000. Autonomous induction of proliferation, JNK and NFkB activation in primary resting T-cells by mobilized CD28. *Eur J Immunol* 30:876-882.

- Boomer, J. S., and J. M. Green. 2010. An enigmatic tail of CD28 signaling. *Cold Spring Harb Perspect Biol* 2 (8):a002436.
- Borel, J. F., Camille Feurer, H. U. Gubler, and H. Stähelin. 1994. Biological effects of cyclosporin A: A new antilymphocytic agent. *Inflammation Research* 43 (3):179-186.
- Cambier, J. C. 1995. Antigen and Fc receptor signaling. The awesome power of the immunoreceptor tyrosine-based activation motif (ITAM). *J Immunol* 155 (7):3281-5.
- Cassidy, J. T., G. L. Nordby, and H. J. Dodge. 1974. Biologic variation of human serum immunoglobulin concentrations: sex-age specific effects. *J Chronic Dis* 27 (11-12):507-16.
- Cerf-Bensussan, N., and D. Guy-Grand. 1991. Intestinal intraepithelial lymphocytes. *Gastroenterol Clin North Am* 20 (3):549-76.
- Chatenoud, L., C. Ferran, C. Legendre, I. Thouard, S. Merite, A. Reuter, Y. Gevaert, H. Kreis, P. Franchimont, and J. F. Bach. 1990. In vivo cell activation following OKT3 administration. Systemic cytokine release and modulation by corticosteroids. *Transplantation* 49 (4):697-702.
- Chen, J., L. Xie, S. Toyama, T. Hunig, S. Takahara, X. K. Li, and L. Zhong. 2011. The effects of Foxp3-expressing regulatory T cells expanded with CD28 superagonist antibody in DSS-induced mice colitis. *Int Immunopharmacol* 11 (5):610-7.
- Clevers, H., B. Alarcon, T. Wileman, and C. Terhorst. 1988. The T cell receptor/CD3 complex: a dynamic protein ensemble. *Annu Rev Immunol* 6:629-62.
- Collins, A. V., D. W. Brodie, R. J. Gilbert, A. Iaboni, R. Manso-Sancho, B. Walse, D. I. Stuart, P. A. van der Merwe, and S. J. Davis. 2002. The interaction properties of costimulatory molecules revisited. *Immunity* 17 (2):201-10.
- Dariavach, P., M. G. Mattei, P. Golstein, and M. P. Lefranc. 1988. Human Ig superfamily CTLA-4 gene: chromosomal localization and identity of protein sequence between murine and human CTLA-4 cytoplasmic domains. *Eur J Immunol* 18 (12):1901-5.
- Davidson, A., and B. Diamond. 2001. Autoimmune diseases. *N Engl J Med* 345 (5):340-50.
- Dennehy, K. M., F. Elias, S. Y. Na, K. D. Fischer, T. Hunig, and F. Luhder. 2007. Mitogenic CD28 Signals Require the Exchange Factor Vav1 to Enhance TCR Signaling at the SLP-76-Vav-Itk Signalosome. *J Immunol* 178 (3):1363-71.
- Dennehy, K. M., F. Elias, G. Zeder-Lutz, X. Ding, D. Altschuh, F. Luhder, and T. Hunig. 2006. Cutting edge: monovalency of CD28 maintains the antigen dependence of T cell costimulatory responses. *J Immunol* 176 (10):5725-9.
- Dennehy, K. M., A. Kerstan, A. Bischof, J. H. Park, S. Y. Na, and T. Hunig. 2003. Mitogenic signals through CD28 activate the protein kinase Ctheta-NF-kappaB pathway in primary peripheral T cells. *Int Immunol* 15 (5):655-63.
- Duff, G.W. (chairman). 2006. *Expert Scientific Group on Phase One Clinical Trials Final Report*. Norwich, UK: Stationary Office.

- Dugdale, D.C., and D. Zieve. *Autoimmune disorders*. MedLinePlus, 29.05.2011 2011 [cited 29.06.2012. Available from <http://www.nlm.nih.gov/medlineplus/ency/article/000816.htm>.
- Eastwood, D., L. Findlay, S. Poole, C. Bird, M. Wadhwa, M. Moore, C. Burns, R. Thorpe, and R. Stebbings. 2010. Monoclonal antibody TGN1412 trial failure explained by species differences in CD28 expression on CD4+ effector memory T-cells. *Br J Pharmacol* 161 (3):512-26.
- Ehrenstein, M. R., J. G. Evans, A. Singh, S. Moore, G. Warnes, D. A. Isenberg, and C. Mauri. 2004. Compromised function of regulatory T cells in rheumatoid arthritis and reversal by anti-TNF alpha therapy. *Journal of Experimental Medicine* 200 (3):277-285.
- Elflein, K., M. Rodriguez-Palmero, T. Kerkau, and T. Hunig. 2003. Rapid recovery from T lymphopenia by CD28 superagonist therapy. *Blood* 102 (5):1764-70.
- EMA. *Guidelines on strategies to identify and mitigate risks for first-in-human clinical trials with investigational medicinal products*. European Medicines Agency, Committee for Medicinal Products for Human Use (CHMP) 2007 [cited 14.06.2012. Available from [http://www.emea.europa.eu/docs/en\\_GB/document\\_library/Scientific\\_guideline/2009/09/WC500002988.pdf](http://www.emea.europa.eu/docs/en_GB/document_library/Scientific_guideline/2009/09/WC500002988.pdf).
- Evans, E. J., R. M. Esnouf, R. Manso-Sancho, R. J. Gilbert, J. R. James, C. Yu, J. A. Fennelly, C. Vowles, T. Hanke, B. Walse, T. Hunig, P. Sorensen, D. I. Stuart, and S. J. Davis. 2005. Crystal structure of a soluble CD28-Fab complex. *Nat Immunol* 6 (3):271-9.
- Findlay, L., D. Eastwood, R. Stebbings, G. Sharp, Y. Mistry, C. Ball, J. Hood, R. Thorpe, and S. Poole. 2010. Improved in vitro methods to predict the in vivo toxicity in man of therapeutic monoclonal antibodies including TGN1412. *J Immunol Methods* 352 (1-2):1-12.
- Findlay, L., G. Sharp, B. Fox, C. Ball, C. J. Robinson, C. Bird, R. Stebbings, D. Eastwood, M. Wadhwa, S. Poole, R. Thorpe, and S. J. Thorpe. 2011. Endothelial cells co-stimulate peripheral blood mononuclear cell responses to monoclonal antibody TGN1412 in culture. *Cytokine* 55 (1):141-151.
- Fontenot, J. D., and A. Y. Rudensky. 2005. A well adapted regulatory contrivance: regulatory T cell development and the forkhead family transcription factor Foxp3. *Nat Immunol* 6 (4):331-7.
- Fox, D. A. 2012. Tregs to the Rescue. *Arthritis & Rheumatism* (Accepted article).
- Furtado, G. C., M. A. Curotto de Lafaille, N. Kutchukhidze, and J. J. Lafaille. 2002. Interleukin 2 signaling is required for CD4(+) regulatory T cell function. *J Exp Med* 196 (6):851-7.
- Garcia, K. C., J. J. Adams, D. Feng, and L. K. Ely. 2009. The molecular basis of TCR germline bias for MHC is surprisingly simple. *Nat Immunol* 10 (2):143-7.
- Gaston, R. S., M. H. Deierhoi, T. Patterson, E. Prasthofer, B. A. Julian, W. H. Barber, D. A. Laskow, A. G. Diethelm, and J. J. Curtis. 1991. OKT3 first-dose reaction: association with T cell subsets and cytokine release. *Kidney Int* 39 (1):141-8.
- Gmunder, H., and W. Lesslauer. 1984. A 45-kDa human T-cell membrane glycoprotein functions in the regulation of cell proliferative responses. *Eur J Biochem* 142 (1):153-60.

- Gogishvili, T., F. Elias, J. L. Emery, K. McPherson, K. Okkenhaug, T. Hünig, and K. M. Dennehy. 2008. Proliferative signals mediated by CD28 superagonists require the exchange factor Vav1 but not phosphoinositide 3-kinase in primary peripheral T cells. *Eur J Immunol* 38 (9):2528-33.
- Gogishvili, T., D. Langenhorst, F. Luhder, F. Elias, K. Elflein, K. M. Dennehy, R. Gold, and T. Hunig. 2009. Rapid regulatory T-cell response prevents cytokine storm in CD28 superagonist treated mice. *PLoS One* 4 (2):e4643.
- Goldman, M., D. Abramowicz, L. De Pauw, M. L. Alegre, I. Widera, P. Vereerstraeten, and Kinnaert. 1989. OKT3-induced cytokine release attenuation by high-dose methylprednisolone. *Lancet* 2 (8666):802-3.
- Goldstein, G. 1987. Monoclonal-Antibody Specificity - Orthoclone Okt3 T-Cell Blocker. *Nephron* 46:5-11.
- Gross, J. A., T. Stjohn, and J. P. Allison. 1990. The Murine Homolog of the Lymphocyte-T Antigen-Cd28 - Molecular-Cloning and Cell-Surface Expression. *Journal of Immunology* 144 (8):3201-3210.
- Guilliams, M., T. Bosschaerts, M. Herin, T. Hunig, P. Loi, V. Flamand, P. De Baetselier, and A. Beschin. 2008. Experimental expansion of the regulatory T cell population increases resistance to African trypanosomiasis. *J Infect Dis* 198 (5):781-91.
- Hanke, T. 2006. Lessons from TGN1412. *Lancet* 368 (9547):1569-70; author reply 1570.
- Hansel, T. T., H. Kropshofer, T. Singer, J. A. Mitchell, and A. J. George. 2010. The safety and side effects of monoclonal antibodies. *Nat Rev Drug Discov* 9 (4):325-38.
- Hansen, J. A., P. J. Martin, and R. C. Nowinski. 1980. Monoclonal-Antibodies Identifying a Novel T-Cell Antigen and Ia Antigens of Human-Lymphocytes. *Immunogenetics* 10 (3):247-260.
- Hara, T., S. M. Fu, and J. A. Hansen. 1985. Human T-Cell Activation .2. A New Activation Pathway Used by a Major T-Cell Population Via a Disulfide-Bonded Dimer of a 44-Kilodalton Polypeptide (9.3 Antigen). *Journal of Experimental Medicine* 161 (6):1513-1524.
- Heidelberger, M., and F. E. Kendall. 1929. A Quantitative Study of the Precipitin Reaction between Type Iii Pneumococcus Polysaccharide and Purified Homologous Antibody. *J Exp Med* 50 (6):809-23.
- Hochweller, K., G. H. Wabnitz, Y. Samstag, J. Suffner, G. J. Hammerling, and N. Garbi. 2010. Dendritic cells control T cell tonic signaling required for responsiveness to foreign antigen. *Proc Natl Acad Sci U S A* 107 (13):5931-6.
- Hoffmann, P., R. Eder, L. A. Kunz-Schughart, R. Andreesen, and M. Edinger. 2004. Large-scale in vitro expansion of polyclonal human CD4(+)CD25high regulatory T cells. *Blood* 104 (3):895-903.
- Hori, S., T. Nomura, and S. Sakaguchi. 2003. Control of regulatory T cell development by the transcription factor Foxp3. *Science* 299 (5609):1057-61.

- Hünig, T. 2012. The storm has cleared: lessons from the CD28 superagonist TGN1412 trial. *Nature Reviews Immunology* 12 (5):317-318.
- Hünig, T., and K. Dennehy. 2005. CD28 superagonists: mode of action and therapeutic potential. *Immunol Lett* 100 (1):21-8.
- Hünig, T., G. Tiefenthaler, K. H. Meyer zum Buschenfelde, and S. C. Meuer. 1987. Alternative pathway activation of T cells by binding of CD2 to its cell-surface ligand. *Nature* 326 (6110):298-301.
- Hünig, Thomas. 2007. Manipulation of Regulatory T-Cell Number and Function with CD28-Specific Monoclonal Antibodies. In *Adv Immunol*, edited by K. F. A. T. H. F. M. J. W. U. Frederick W. Alt and R. U. Emil: Academic Press.
- Hutloff, A., A. M. Dittrich, K. C. Beier, B. Eljaschewitsch, R. Kraft, I. Anagnostopoulos, and R. A. Kroczek. 1999. ICOS is an inducible T-cell co-stimulator structurally and functionally related to CD28. *Nature* 397 (6716):263-266.
- Irving, Bryan A., and Arthur Weiss. 1991. The cytoplasmic domain of the T cell receptor  $\zeta$  chain is sufficient to couple to receptor-associated signal transduction pathways. *Cell* 64 (5):891-901.
- Kaminski, Henry J. 2008. Treatment of Myasthenia Gravis. In *Myasthenia Gravis and Related Disorders*, edited by H. J. Kaminski: Humana Press.
- Kassiotis, G., S. Garcia, E. Simpson, and B. Stockinger. 2002. Impairment of immunological memory in the absence of MHC despite survival of memory T cells. *Nat Immunol* 3 (3):244-50.
- Kersh, E. N., A. S. Shaw, and P. M. Allen. 1998. Fidelity of T cell activation through multistep T cell receptor zeta phosphorylation. *Science* 281 (5376):572-575.
- Kerstan, A., and T. Hunig. 2004. Cutting edge: distinct TCR- and CD28-derived signals regulate CD95L, Bcl-xL, and the survival of primary T cells. *J Immunol* 172 (3):1341-5.
- Kitazawa, Y., M. Fujino, X. K. Li, L. Xie, N. Ichimaru, M. Okumi, N. Nonomura, A. Tsujimura, Y. Isaka, H. Kimura, T. Hunig, and S. Takahara. 2009. Superagonist CD28 antibody preferentially expanded Foxp3-expressing nTreg cells and prevented graft-versus-host diseases. *Cell Transplant* 18 (5):627-37.
- Kitazawa, Y., M. Fujino, T. Sakai, H. Azuma, H. Kimura, Y. Isaka, S. Takahara, T. Hunig, R. Abe, and X. K. Li. 2008. Foxp3-expressing regulatory T cells expanded with CD28 superagonist antibody can prevent rat cardiac allograft rejection. *Journal of Heart and Lung Transplantation* 27 (4):362-371.
- Koenen, H. J., E. C. Michielsen, J. Verstappen, E. Fasse, and I. Joosten. 2003. Superior T-cell suppression by rapamycin and FK506 over rapamycin and cyclosporine A because of abrogated cytotoxic T-lymphocyte induction, impaired memory responses, and persistent apoptosis. *Transplantation* 75 (9):1581-90.
- Krämer, S., A. Schimpl, and T. Hunig. 1995. Immunopathology of interleukin (IL) 2-deficient mice: thymus dependence and suppression by thymus-dependent cells with an intact IL-2 gene. *J Exp Med* 182 (6):1769-76.

- Kroger, AT., CV. Sumaya, LK. Pickering, and WL. Atkinson. 2011. General Recommendations on Immunization, Recommendations of the Advisory Committee on Immunization Practices (ACIP). *Morbidity and Mortality Weekly Report* 60 (2).
- Kuhns, M. S., and M. M. Davis. 2012. TCR Signaling Emerges from the Sum of Many Parts. *Front Immunol* 3:159.
- Landegren, U., J. Andersson, and H. Wigzell. 1984. Mechanism of T lymphocyte activation by OKT3 antibodies. A general model for T cell induction. *Eur J Immunol* 14 (4):325-8.
- Leipe, J., A. Skapenko, P. E. Lipsky, and H. Schulze-Koops. 2005. Regulatory T cells in rheumatoid arthritis. *Arthritis Res Ther* 7 (3):93.
- Levin, S. E., C. Zhang, T. A. Kadlecsek, K. M. Shokat, and A. Weiss. 2008. Inhibition of ZAP-70 kinase activity via an analog-sensitive allele blocks T cell receptor and CD28 superagonist signaling. *J Biol Chem* 283 (22):15419-30.
- Lichtman, A. H., G. B. Segel, and M. A. Lichtman. 1983. The role of calcium in lymphocyte proliferation. (An interpretive review). *Blood* 61 (3):413-22.
- Lin, C. H., and T. Hunig. 2003. Efficient expansion of regulatory T cells in vitro and in vivo with a CD28 superagonist. *Eur J Immunol* 33 (3):626-38.
- Lindley, S., C. M. Dayan, A. Bishop, B. O. Roep, M. Peakman, and T. I. M. Tree. 2005. Defective suppressor function in CD4(+)CD25(+) T-cells from patients with type 1 diabetes. *Diabetes* 54 (1):92-99.
- Llewelyn, Martin, and Jon Cohen. 2002. Superantigens: microbial agents that corrupt immunity. *The Lancet Infectious Diseases* 2 (3):156-162.
- Luhder, F., Y. Huang, K. M. Dennehy, C. Guntermann, I. Muller, E. Winkler, T. Kerkau, S. Ikemizu, S. J. Davis, T. Hanke, and T. Hunig. 2003. Topological requirements and signaling properties of T cell-activating, anti-CD28 antibody superagonists. *J Exp Med* 197 (8):955-66.
- Lum, L. G., N. Orcutt-Thordarson, M. C. Seigneuret, and J. A. Hansen. 1982. In vitro regulation of immunoglobulin synthesis by T-cell subpopulations defined by a new human T-cell antigen (9.3). *Cell Immunol* 72 (1):122-9.
- Luster, A. D. 2002. The role of chemokines in linking innate and adaptive immunity. *Curr Opin Immunol* 14 (1):129-35.
- Mackall, C. L., C. V. Bare, L. A. Granger, S. O. Sharrow, J. A. Titus, and R. E. Gress. 1996. Thymic-independent T cell regeneration occurs via antigen-driven expansion of peripheral T cells resulting in a repertoire that is limited in diversity and prone to skewing. *J Immunol* 156 (12):4609-16.
- Malek, T. R., and A. L. Bayer. 2004. Tolerance, not immunity, crucially depends on IL-2. *Nature Reviews Immunology* 4 (9):665-74.
- Maloy, K. J., and F. Powrie. 2005. Fueling regulation: IL-2 keeps CD4+ Treg cells fit. *Nat Immunol* 6 (11):1071-2.

- Matsui, K., J. J. Boniface, P. A. Reay, H. Schild, B. Fazekas de St Groth, and M. M. Davis. 1991. Low affinity interaction of peptide-MHC complexes with T cell receptors. *Science* 254 (5039):1788-91.
- McCole, D. F., M. L. Doherty, A. W. Baird, W. C. Davis, K. McGill, and P. R. Torgerson. 1998. Concanavalin A-stimulated proliferation of T cell subset-depleted lymphocyte populations isolated from *Fasciola hepatica*-infected cattle. *Veterinary Immunology and Immunopathology* 66 (3-4):289-300.
- Meuer, S. C., R. E. Hussey, M. Fabbi, D. Fox, O. Acuto, K. A. Fitzgerald, J. C. Hodgdon, J. P. Protentis, S. F. Schlossman, and E. L. Reinherz. 1984. An alternative pathway of T-cell activation: a functional role for the 50 kd T11 sheep erythrocyte receptor protein. *Cell* 36 (4):897-906.
- Miyasato, K., Y. Takabatake, J. Kaimori, T. Kimura, H. Kitamura, H. Kawachi, X. K. Li, T. Hunig, S. Takahara, H. Rakugi, and Y. Isaka. 2011. CD28 superagonist-induced regulatory T cell expansion ameliorates mesangioproliferative glomerulonephritis in rats. *Clin Exp Nephrol* 15 (1):50-7.
- Monks, C. R., B. A. Freiberg, H. Kupfer, N. Sciaky, and A. Kupfer. 1998. Three-dimensional segregation of supramolecular activation clusters in T cells. *Nature* 395 (6697):82-6.
- Moore, T. L. 1999. Immunopathogenesis of juvenile rheumatoid arthritis. *Curr Opin Rheumatol* 11 (5):377-83.
- Moretta, A., E. Ciccone, G. Pantaleo, G. Tambussi, C. Bottino, G. Melioli, M. C. Mingari, and L. Moretta. 1989. Surface molecules involved in the activation and regulation of T or natural killer lymphocytes in humans. *Immunol Rev* 111:145-75.
- Najafian, N., and M. H. Sayegh. 2000. CTLA4-Ig: a novel immunosuppressive agent. *Expert Opinion on Investigational Drugs* 9 (9):2147-2157.
- Nogid, A., and D. Q. Pham. 2006. Role of abatacept in the management of rheumatoid arthritis. *Clin Ther* 28 (11):1764-78.
- Pang, D. J., J. F. Neves, N. Sumaria, and D. J. Pennington. 2012. Understanding the complexity of gammadelta T-cell subsets in mouse and human. *Immunology* 136 (3):283-90.
- Papiernik, M., M. L. de Moraes, C. Pontoux, F. Vasseur, and C. Penit. 1998. Regulatory CD4 T cells: expression of IL-2R alpha chain, resistance to clonal deletion and IL-2 dependency. *Int Immunol* 10 (4):371-8.
- Presta, LG., and AK. Namenuk. 2005. Non-human primate Fc receptors and methods of use, edited by U. S. Patent. USA: Genentech, Inc.
- Qi, Q., and A. August. 2007. Keeping the (kinase) party going: SLP-76 and ITK dance to the beat. *Sci STKE* 2007 (396):pe39.
- Qureshi, O. S., Y. Zheng, K. Nakamura, K. Attridge, C. Manzotti, E. M. Schmidt, J. Baker, L. E. Jeffery, S. Kaur, Z. Briggs, T. Z. Hou, C. E. Futter, G. Anderson, L. S. Walker, and D. M. Sansom. 2011. Trans-endocytosis of CD80 and CD86: a molecular basis for the cell-extrinsic function of CTLA-4. *Science* 332 (6029):600-3.

- Randriamampita, C., G. Boulla, P. Revy, F. Lemaitre, and A. Trautmann. 2003. T cell adhesion lowers the threshold for antigen detection. *Eur J Immunol* 33 (5):1215-23.
- Reichert, J. M. 2012. Marketed therapeutic antibodies compendium. *MAbs* 4 (3).
- Rinnooy Kan, E. A., S. D. Wright, K. Welte, and C. Y. Wang. 1986. Fc receptors on monocytes cause OKT3-treated lymphocytes to internalize T3 and to secrete IL-2. *Cell Immunol* 98 (1):181-7.
- Rodriguez-Palmero, M., A. Franch, M. Castell, C. Pelegri, F. J. Perez-Cano, C. Kleinschnitz, G. Stoll, T. Hunig, and C. Castellote. 2006. Effective treatment of adjuvant arthritis with a stimulatory CD28-specific monoclonal antibody. *Journal of Rheumatology* 33 (1):110-118.
- Rodriguez-Palmero, M., T. Hara, A. Thumbs, and T. Hunig. 1999. Triggering of T cell proliferation through CD28 induces GATA-3 and promotes T helper type 2 differentiation in vitro and in vivo. *Eur J Immunol* 29 (12):3914-24.
- Römer, P. S., S. Berr, E. Avota, S. Y. Na, M. Battaglia, I. ten Berge, H. Einsele, and T. Hunig. 2011. Preculture of PBMCs at high cell density increases sensitivity of T-cell responses, revealing cytokine release by CD28 superagonist TGN1412. *Blood* 118 (26):6772-82.
- Sakaguchi, S. 2000. Animal models of autoimmunity and their relevance to human diseases. *Curr Opin Immunol* 12 (6):684-690.
- — —. 2004. Naturally arising CD4<sup>+</sup> regulatory t cells for immunologic self-tolerance and negative control of immune responses. *Annu Rev Immunol* 22:531-62.
- Sakaguchi, S., R. Setoguchi, H. Yagi, and T. Nomura. 2006. Naturally arising Foxp3-expressing CD25<sup>+</sup>CD4<sup>+</sup> regulatory T cells in self-tolerance and autoimmune disease. *Curr Top Microbiol Immunol* 305:51-66.
- Sallusto, F., J. Geginat, and A. Lanzavecchia. 2004. Central memory and effector memory T cell subsets: function, generation, and maintenance. *Annu Rev Immunol* 22:745-63.
- Sallusto, F., D. Lenig, R. Forster, M. Lipp, and A. Lanzavecchia. 1999. Two subsets of memory T lymphocytes with distinct homing potentials and effector functions. *Nature* 401 (6754):708-12.
- Salomon, B., D. J. Lenschow, L. Rhee, N. Ashourian, B. Singh, A. Sharpe, and J. A. Bluestone. 2000. B7/CD28 costimulation is essential for the homeostasis of the CD4<sup>(+)</sup>CD25<sup>(+)</sup> immunoregulatory T cells that control autoimmune diabetes. *Immunity* 12 (4):431-440.
- Sanchez-Lockhart, M., M. Kim, and J. Miller. 2011. Cutting edge: A role for inside-out signaling in TCR regulation of CD28 ligand binding. *J Immunol* 187 (11):5515-9.
- Sansom, D. M., and L. S. Walker. 2006. The role of CD28 and cytotoxic T-lymphocyte antigen-4 (CTLA-4) in regulatory T-cell biology. *Immunol Rev* 212:131-48.
- Scheinfeld, N. 2004. A comprehensive review and evaluation of the side effects of the tumor necrosis factor alpha blockers etanercept, infliximab and adalimumab. *J Dermatolog Treat* 15 (5):280-94.

- Schimpl, A., I. Berberich, B. Kneitz, S. Kramer, B. Santner-Nanan, S. Wagner, M. Wolf, and T. Hunig. 2002. IL-2 and autoimmune disease. *Cytokine Growth Factor Rev* 13 (4-5):369-78.
- Schmidt, J., K. Elflein, M. Stienekemeier, M. Rodriguez-Palmero, C. Schneider, K. V. Toyka, R. Gold, and T. Hunig. 2003. Treatment and prevention of experimental autoimmune neuritis with superagonistic CD28-specific monoclonal antibodies. *J Neuroimmunol* 140 (1-2):143-52.
- Schreiber, Stuart L., and Gerald R. Crabtree. 1992. The mechanism of action of cyclosporin A and FK506. *Immunology Today* 13 (4):136-142.
- Setoguchi, R., S. Hori, T. Takahashi, and S. Sakaguchi. 2005. Homeostatic maintenance of natural Foxp3(+) CD25(+) CD4(+) regulatory T cells by interleukin (IL)-2 and induction of autoimmune disease by IL-2 neutralization. *J Exp Med* 201 (5):723-35.
- Sharon, Nathan, and Halina Lis. 1972. Lectins: Cell-Agglutinating and Sugar-Specific Proteins. *Science* 177 (4053):949-959.
- Sharpe, A. H. 2009. Mechanisms of costimulation. *Immunological Reviews* 229:5-11.
- Sharpe, A. H., and G. J. Freeman. 2002. The B7-CD28 superfamily. *Nature Reviews Immunology* 2 (2):116-126.
- Shi, Q., Y. Niu, H. Cao, X. Zhou, S. Jiang, Z. Liu, and H. Fan. 2012. CD28 superagonist antibody treatment attenuated obliterative bronchiolitis in rat allo-orthotopic tracheal transplantation by preferentially expanding Foxp3-expressing regulatory T cells. *Transplant Proc* 44 (4):1060-6.
- Smit-McBride, Z., J. J. Mattapallil, M. McChesney, D. Ferrick, and S. Dandekar. 1998. Gastrointestinal T lymphocytes retain high potential for cytokine responses but have severe CD4(+) T-cell depletion at all stages of simian immunodeficiency virus infection compared to peripheral lymphocytes. *J Virol* 72 (8):6646-56.
- Smith-Garvin, J. E., G. A. Koretzky, and M. S. Jordan. 2009. T cell activation. *Annu Rev Immunol* 27:591-619.
- Sprent, J., and C. D. Surh. 2002. T cell memory. *Annu Rev Immunol* 20:551-79.
- Stankova, J., D. W. Hoskin, and J. C. Roder. 1989. Murine Anti-Cd3 Monoclonal-Antibody Induces Potent Cytolytic Activity in Both T-Cell and Nk-Cell Populations. *Cell Immunol* 121 (1):13-29.
- Stebbing, R., L. Findlay, C. Edwards, D. Eastwood, C. Bird, D. North, Y. Mistry, P. Dilger, E. Liefoghe, I. Cludts, B. Fox, G. Tarrant, J. Robinson, T. Meager, C. Dolman, S. J. Thorpe, A. Bristow, M. Wadhwa, R. Thorpe, and S. Poole. 2007. "Cytokine storm" in the phase I trial of monoclonal antibody TGN1412: better understanding the causes to improve preclinical testing of immunotherapeutics. *J Immunol* 179 (5):3325-31.
- Stefanova, I., J. R. Dorfman, and R. N. Germain. 2002. Self-recognition promotes the foreign antigen sensitivity of naive T lymphocytes. *Nature* 420 (6914):429-34.
- STIKO. *Vaccination Schedule* 2011 [cited 25.05.2012. Available from [www.stiko.de](http://www.stiko.de)].

- Suntharalingam, G., M. R. Perry, S. Ward, S. J. Brett, A. Castello-Cortes, M. D. Brunner, and N. Panoskaltis. 2006. Cytokine storm in a phase 1 trial of the anti-CD28 monoclonal antibody TGN1412. *N Engl J Med* 355 (10):1018-28.
- Tabares, P., S. M. Pimentel-Elardo, T. Schirmeister, T. Hunig, and U. Hentschel. 2011. Anti-protease and immunomodulatory activities of bacteria associated with Caribbean sponges. *Mar Biotechnol (NY)* 13 (5):883-92.
- Tacke, M., G. J. Clark, M. J. Dallman, and T. Hunig. 1995. Cellular distribution and costimulatory function of rat CD28. Regulated expression during thymocyte maturation and induction of cyclosporin A sensitivity of costimulated T cell responses by phorbol ester. *J Immunol* 154 (10):5121-7.
- Tacke, M., G. Hanke, T. Hanke, and T. Hunig. 1997. CD28-mediated induction of proliferation in resting T cells in vitro and in vivo without engagement of the T cell receptor: evidence for functionally distinct forms of CD28. *Eur J Immunol* 27 (1):239-47.
- Takahashi, T., T. Tagami, S. Yamazaki, T. Uede, J. Shimizu, N. Sakaguchi, T. W. Mak, and S. Sakaguchi. 2000. Immunologic self-tolerance maintained by CD25(+)CD4(+) regulatory T cells constitutively expressing cytotoxic T lymphocyte-associated antigen 4. *J Exp Med* 192 (2):303-10.
- Tang, Q., K. J. Henriksen, M. Bi, E. B. Finger, G. Szot, J. Ye, E. L. Masteller, H. McDevitt, M. Bonyhadi, and J. A. Bluestone. 2004. In vitro-expanded antigen-specific regulatory T cells suppress autoimmune diabetes. *J Exp Med* 199 (11):1455-65.
- TeGenero. 2012. *TGN1412 humanized agonistic anti-CD28 monoclonal antibody (1.1)* 2005 [cited June 11 2012]. Available from <http://www.circare.org/foia5/tgn1412investigatorbrochure.pdf>.
- Tezuka, K., T. Tsuji, D. Hirano, T. Tamatani, K. Sakamaki, Y. Kobayashi, and M. Kamada. 2000. Identification and characterization of rat AILIM/ICOS, a novel T-cell costimulatory molecule, related to the CD28/CTLA4 family. *Biochem Biophys Res Commun* 276 (1):335-45.
- Tiefenthaler, G., and T. Hunig. 1989. The role of CD2/LFA-3 interaction in antigen- and mitogen-induced activation of human T cells. *Int Immunol* 1 (2):169-75.
- Urakami, H., D. V. Ostanin, T. Hunig, and M. B. Grisham. 2006. Combination of donor-specific blood transfusion with anti-CD28 antibody synergizes to prolong graft survival in rat liver transplantation. *Transplant Proc* 38 (10):3244-6.
- Valencia, X., G. Stephens, R. Goldbach-Mansky, M. Wilson, E. M. Shevach, and P. E. Lipsky. 2006. TNF downmodulates the function of human CD4+CD25hi T-regulatory cells. *Blood* 108 (1):253-61.
- van Oers, N. S. 1999. T cell receptor-mediated signs and signals governing T cell development. *Semin Immunol* 11 (4):227-37.
- Viglietta, V., C. Baecher-Allan, H. L. Weiner, and D. A. Hafler. 2004. Loss of functional suppression by CD4(+)CD25(+) regulatory T cells in patients with multiple sclerosis. *Journal of Experimental Medicine* 199 (7):971-979.

- Waibler, Z., L. Y. Sender, C. Kamp, J. Muller-Berghaus, B. Liedert, C. K. Schneider, J. Lower, and U. Kalinke. 2008. Toward experimental assessment of receptor occupancy: TGN1412 revisited. *J Allergy Clin Immunol* 122 (5):890-2.
- Wang, Jia-huai, Alex Smolyar, Kemin Tan, Jin-huan Liu, Mikyung Kim, Zhen-yu J. Sun, Gerhard Wagner, and Ellis L. Reinherz. 1999. Structure of a Heterophilic Adhesion Complex between the Human CD2 and CD58 (LFA-3) Counterreceptors. *Cell* 97 (6):791-803.
- Watanabe, N., M. Gavrieli, J. R. Sedy, J. F. Yang, F. Fallarino, S. K. Loftin, M. A. Hurchla, N. Zimmerman, J. Sim, X. X. Zang, T. L. Murphy, J. H. Russell, J. P. Allison, and K. M. Murphy. 2003. BTLA is a lymphocyte inhibitory receptor with similarities to CTLA-4 and PD-1. *Nature Immunology* 4 (7):670-679.
- Weissmüller, S., L.Y. Semmler, U. Kalinke, S. Christians, J. Müller-Berghaus, and Z. Waibler. 2012. ICOS-LICOS interaction is critically involved in TGN1412-mediated T-cell activation. *Blood* 119 (26):6268-6277.
- Wikipedia. 2012. Wikipedia, The Free Encyclopedia., 26 April 2012 [cited 7 May 2012]. Available from <http://en.wikipedia.org/>.
- Wolf, M., A. Schimpl, and T. Hunig. 2001. Control of T cell hyperactivation in IL-2-deficient mice by CD4(+)CD25(-) and CD4(+)CD25(+) T cells: evidence for two distinct regulatory mechanisms. *Eur J Immunol* 31 (6):1637-45.
- Wu, L. C., D. S. Tuot, D. S. Lyons, K. C. Garcia, and M. M. Davis. 2002. Two-step binding mechanism for T-cell receptor recognition of peptide MHC. *Nature* 418 (6897):552-6.
- Zaiss, M. M., B. Frey, A. Hess, J. Zwerina, J. Luther, F. Nimmerjahn, K. Engelke, G. Kollias, T. Hunig, G. Schett, and J. P. David. 2010. Regulatory T cells protect from local and systemic bone destruction in arthritis. *J Immunol* 184 (12):7238-46.

## **Publications**

Paula S. Römer, Susanne Berr, Elita Avota, Shin-Young Na, Manuela Battaglia, Ineke ten Berge, Hermann Einsele and Thomas Hünig. 2011. Preculture of PBMCs at high cell density increases sensitivity of T-cell responses, revealing cytokine release by CD28 superagonist TGN1412. *Blood* 118 (26):6777-82.